AD 273 514

BULLETIN No. 30

SHOCK, VIBRATION AND ASSOCIATED ENVIRONMENTS

PART II

JANUARY 1962

OFFICE OF
THE SECRETARY OF DEFENSE
Research and Engineering

Washington, D. C.

BULLETIN No. 30

SHOCK, VIBRATION AND ASSOCIATED ENVIRONMENTS PART II

JANUARY 1962

OFFICE OF THE SECRETARY OF DEFENSE

Research and Engineering

The 30th Symposium on Shock, Vibration, and Associated Environments was held at the Statler-Hilton Hotel, Detroit, Michigan on October 10-12, 1961. The Department of the Army was host.

Washington. D. C.

INTERSERVICE TECHNICAL GROUP FOR SHOCK, VIBRATION, AND ASSOCIATED ENVIRONMENTS

ARMY MEMBERS

Mr. David Askin
Frankford Arsenal
Philadelphia, Pennsylvania

Dr. W. B. Brierly
Quartermaster Research and
Engineering Command
Natick,

Dr. Joseph S. diRende
Scientific Director
U.S. Army Transportation
Research Command
Fort Eustis, Virginia

Mr. Joseph Kaufman
Office of the Chief of Ordnance
U.S. Army
Pentagon Annex No. 2
Washington 25, D. C.

Mr. Frederick J. Lindner
Packaging Development Branch
U.S. Army Engineer Research and
Development Laboratories
Fort Belvoir, Virginia

Mr. Joseph J. Oliveri
Engineering Science Department
U.S. Army Signal Research and
Development Laboratories
Fort Monmouth, New Jersey

NAVY MEMBERS

Mr. J. M. Crowley
Code 439
Office of Naval Research
Washington 25, D. C.

Mr. E. R. Mullen
U.S. Naval Air Development Center
Johnsville, Pennsylvania

Mr. R. H. Oliver
Code 423
Bureau of Ships
Washington 25, D. C.

Mr. Harry Rich
David Taylor Model Basin
Washington 7, D. C.

Mr. Theodore Soo-Hoo
Office of the Chief of Naval Operations
Pentagon
Washington 25, D. C.

Mr. George Stathopoulos
U.S. Naval Ordnance Laboratory
White Oak
Silver Spring, Maryland

AIR FORCE MEMBERS

Mr. E. A. Catenaro
Rome Air Development Center
Attn: RCSSM
Griffiss Air Force Base, New York

Mr. C. Golueke
Wright Air Development Division
Attn: WWFEVD
Wright-Patterson Air Force Base
Ohio

Mr. D. C. Kennard
Wright Air Development Division
Attn: WWFEV
Wright-Patterson Air Force Base
Ohio

Mr. H. A. McGrath
Wright Air Development Division
Attn: WWRMD
Wright-Patterson Air Force Base
Ohio

Mr. Howard W. Wolko
Air Force Office of Scientific Research
Tempo D Building
Washington 25, D. C.

Dr. George A. Young
Air Force Special Weapons Center
Kirtland Air Force Base
New Mexico

DEFENSE ATOMIC SUPPORT AGENCY MEMBER

Mr. John Lewis
Defense Atomic Support Agency
Pentagon
Washington 25, D. C.

NATIONAL AERONAUTICS AND SPACE ADMINISTRATION MEMBER

Mr. John C. New
Code 320
National Aeronautics and Space
Administration
Goddard Space Flight Center
Greenbelt, Maryland

OFFICE OF DIRECTOR OF DEFENSE RESEARCH AND ENGINEERING MEMBER

Mr. G. B. Wareham
Equipment and Supplies Division
Washington 25, D. C.

CONTENTS

FOREWORD

In recent years many engineers concerned with dynamic motion environments have been exposed, in one way or another, to the term "mechanical impedance." Dependent upon his available time and inclination he may have looked in usual texts and literature and determined that mechanical impedance is the "analog" of electrical impedance. He may also have seen other terms, e.g., "mobility" or "admittance" which appear to be very similar. However, as judged by collective remarks of shock and vibration engineers, what he probably has not seen is an explanation of how this quantity can be useful to him in his day-to-day problems. It was just this situation which prompted the scheduling of a session of arranged and invited papers for the 30th Symposium on Shock, Vibration, and Associated Environments. The intent was to present the concepts of mechanical impedance in "tutorial" fashion, to describe some applications, and to encourage discussion of the subject. The technical content of the session and the invited papers were arranged by R. O. Belsheim of the U.S. Naval Research Laboratory.

The papers reprinted here contain the material presented at the Symposium together with the discussion which followed the presentations and an additional paper, not presented at the meeting, on the same subject.

January 1962

Section 2
MECHANICAL IMPEDANCE

INTRODUCTORY REMARKS

R. O. Belsheim
U. S. Naval Research Laboratory

These papers have been arranged to present, in a "tutorial" sense, the concept, determination, and application of what may be referred to as mechanical impedance procedures. Some historical and introductory material is presented to prepare the way for the papers.

During the last decade or so, a marked change in the speed with which operational engi..eering events occur has greatly increased the scope and number of problems to be solved by the structural dynamicist, test engineer, designer, and others. This increase is caused by the need for greater performance reliability, but with reduced weight of structures, and with more complex and indeterminate motional environments. To meet this need dynamic analysis, design, and testing must be done more exactly, i.e., with less "factor of ignorance" margin. In a historical sense, the electrical engineers faced a similar situation some sixty years ago, with respect to circuit analyses. Their solution was to develop methods, techniques, and theorems which permit consideration of complex circuits by use of a quantitative parameter called impedance [1, 2];* this parameter is the ratio of sinusoidal voltage and sinusoidal current. Because many circuits are linear, this ratio is independent of amplitude and is a function of sinusoidal frequency only. However, because voltage and current are not in phase with each other, their ratio, Z, can be expressed as a complex number with a magnitude and a phase angle, or, alternatively, with real and imaginary parts. Over the years development and evaluation of a great many circuit theorems, design rules, etc., has almost eliminated the classical method of solving linear circuit problems by use of the pertinent differential equations.

Workers in the field of acoustics, particularly in areas where electromechanical devices are important, have also used similar concepts for some 30 to 40 years [3, 4]. Because energy is often converted from electrical to mechanical forms (or vice versa) extensive study of electrical-mechanical analogs [5] has proved useful and impedance of mixed units, e.g., output force to input current, is used.

The field of control by servomechanisms, which has mushroomed during the last 20 to 30 years, also uses similar parameters to facilitate analysis of control systems [6, 7]. Because these systems are specially designed it has been possible to develop specialized (and simple) techniques, since certain restrictions are imposed in the design stages.

MEANING OF MECHANICAL IMPEDANCE

With regard to linear and elastic structures or mechanical systems, the literature during the past 25 years contains a number of

*Numbers in brackets refer to references at end.

papers which discuss and/or utilize mechanical impedance concepts. * Of the earlier papers one should mention the works of Carter [8], Firestone [9], Biot [10], Duncan [11], and Manley [12], all of which were concerned with systems subjected to free or forced vibration. Much of the early work utilized the analogy between the equations governing mechanical systems and electrical circuits and did not really deal with impedance quantities as a unique parameter. This brings up a misconception which some engineers may have, i.e., that impedance is something new and unique which has become available suddenly. Of course this is not the case; mechanical impedance can be an extremely useful "tool" for solving problems in structural dynamics but, as with any tool it should be used with proper regard for its limitations and in conjunction with other methods and techniques. Its unique quality is that it permits a convenient yet precise description of the dynamic characteristics of a structure, either at a point or between two points; this description is equally meaningful regardless of the complexity of the structure, and allows "equivalent black box" manipulations.

Although impedance is a parameter derived from ratios of sinusoidal quantities, a structure properly described by its impedance may be analyzed for response to sinusoidal, random, or transient excitations [11, 13-17].

The limitations on use of impedance may be grouped to include: (a) the assumption that the system treated is linear and elastic, (b) the requirement that the desired impedance quantity be determined (analytically or experimentally) in a reasonable time, yet with sufficient precision [18], and (c) the necessity for extensive computations which may require electronic computation [19]. None of these limitations are really precise so, as with electrical network theory, the supporting theorems, rules, and procedures must be developed and proved over a period of time. Because the mechanical-electrical analogy is applicable, a considerable fund of such theorems is already available, although each should be reconsidered in terms of the aforementioned limitations on mechanical impedance. Also, even though it may be convenient to solve mechanical problems by using an analog, it is desirable to present mechanical impedance in its own language, so that the required limitations are correctly understood and applied.

DEFINITION OF MECHANICAL IMPEDANCE

Mechanical impedance has been defined loosely as the complex ratio of sinusoidal force to sinusoidal velocity. More precisely, if the sinusoidal force F and the resulting sinusoidal velocity V are given by

$$F = F_o \cos(\omega t + \theta) \tag{1}$$

$$V = V_o \cos \omega t , \tag{2}$$

the impedance Z by definition is

$$Z = \frac{|F_o|}{|V_o|} \angle \theta , \tag{3}$$

where θ, the phase angle between the force and velocity, is a function of the frequency ω. This is not a convenient form for the impedance expression. If we use complex notation (where Eqs. (1) and (2) are the real parts only) then

$$F = F_o e^{i(\omega t + \theta)} \tag{4}$$

$$V = V_o e^{i\omega t} \tag{5}$$

and

$$Z = \frac{F_o}{V_o} e^{+i\theta} = Z_o e^{+i\theta} , \tag{6}$$

where the impedance Z is now a complex function of the exciting frequency and is expressed in polar form. The modulus or absolute value Z_o is the ratio of the force magnitude to the velocity magnitude. The argument $i\theta$ gives the phase relationship between the two quantities, with force leading velocity.

It is often convenient to express the impedance in terms of the real and imaginary parts:

$$Z = Z_R + iZ_I . \tag{7}$$

Note that

$$Z = Z_R + iZ_I = \sqrt{Z_R^2 + Z_I^2}\, e^{i \tan^{-1}(Z_I/Z_R)} , \tag{8}$$

$$Z_o = \sqrt{Z_R^2 + Z_I^2} , \tag{9}$$

* It should be emphasized that, although mechanical impedance is defined as the complex ratio of sinusoidal force to sinusoidal velocity, five other ratios between sinusoidal force and sinusoidal displacement, velocity, and acceleration are equally useful and used. The word impedance is often used loosely to refer to all six ratios. It is sometimes convenient to do this in this paper.

and

$$\theta = + \tan^{-1}\left(\frac{Z_I}{Z_R}\right). \qquad (10)$$

The real part Z_R is often called the resistive part of the impedance and the imaginary part Z_I the reactive.

Two types of mechanical impedance can be considered: driving-point impedance and transfer impedance. If the velocity is obtained at the point of application of the exciting force, and in the same direction as the force, the resulting ratio is called driving-point impedance. If the velocity is obtained at some other point of interest on the structure, or in a direction unlike that of the driving force, the ratio is referred to as transfer impedance. The impedance is usually expressed as Z_{jk} where the second subscript k refers to the point and direction of application of the exciting force and the first subscript j, to the point and direction where the velocity is measured. For driving-point impedance $j = k$, and the driving-point impedance is often expressed with the single subscript Z_j.

Impedance can be thought of as a measure of the resistance of the system to motion. If the system is inherently difficult to move, stiff and/or massive, its impedance will be high. Conversely, if the system is easy to move, light and/or flexible, its impedance will be low. However, since impedance is a frequency-dependent quantity, these generalizations are most reliable for low frequencies. In general a plot of impedance versus frequency will show large fluctuations in impedance magnitude, with a number of peaks and valleys. With driving-point impedance the valleys, points of low-impedance, indicate ease of motion and correspond to a resonant condition in the structure. Similarly the peaks, points of high impedance, correspond to antiresonant conditions. With transfer impedance, these observations are sometimes valid.

TERMINOLOGY AND UNITS

As mentioned earlier, six ratios between applied sinusoidal force and resultant sinusoidal displacement, velocity, and acceleration may be used to express the same information. Because certain usages are more convenient with one or the other of these six ratios, examples of most of these may be found in the literature [9, 11, 12, 16, 20-27]. Unfortunately, the terminology has not yet become standardized, since individual researchers have generated individual terminology. This is even illustrated in the other papers in this group, where both "mobility" and "admittance" are used to mean the complex ratio of velocity to force. The American Standards Association recently has published recommended terminology [28], which should improve this confusing situation. Table 1 lists the ASA-recommended terminology, along with some alternative terms which have been used for the same parameters.

This table also shows the relationships between some of the parameters; the relationships which are not shown (e.g., between mechanical impedance and mobility), might appear to be simple inversions, but this is not generally true. For most cases, except for very simple ones such as a pure mass system, the inversion is complex, in that it requires inverting a matrix expression [29]. Because of this, and also because measurement or analytical procedures influence the choice of parameter, there will undoubtedly continue to be different parameters in use by different investigators. However, Table 1 shows that, for the three parameters in which force is always in the numerator (or, conversely, in the denominator), simple relationships exist. Indeed, a single plot on a log-log graph can display all three parameters. Various "standard" graph forms have been proposed, such as that shown in Fig. 1, as suggested by D. V. Wright [30] for use in work of the Structural Impedance Panel, Ship Noise Committee of the Bureau of Ships. This form also standardizes on the British (in-lb-sec) system of units although others have used the cgs (centimeter-gram-second) and the mks (meter-kilogram-second) systems. While terminology and units are technically uninteresting, a wide divergence in usage can be very time-consuming for others trying to use the data.

While the preceding discussion has been concerned with linear force and motion, pure rotational impedances, where force becomes torque and linear motion becomes angular motion, or "mixed" impedances, where one linear quantity and one rotational quantity are used, may be used also. Of course, the complexity increases when more degrees of freedom are considered.

SUMMARIZING REMARKS

By this time, it must be clear to the reader that mechanical impedance is definitely not a panacea for the relief of overworked engineers, but is instead an additional tool which requires

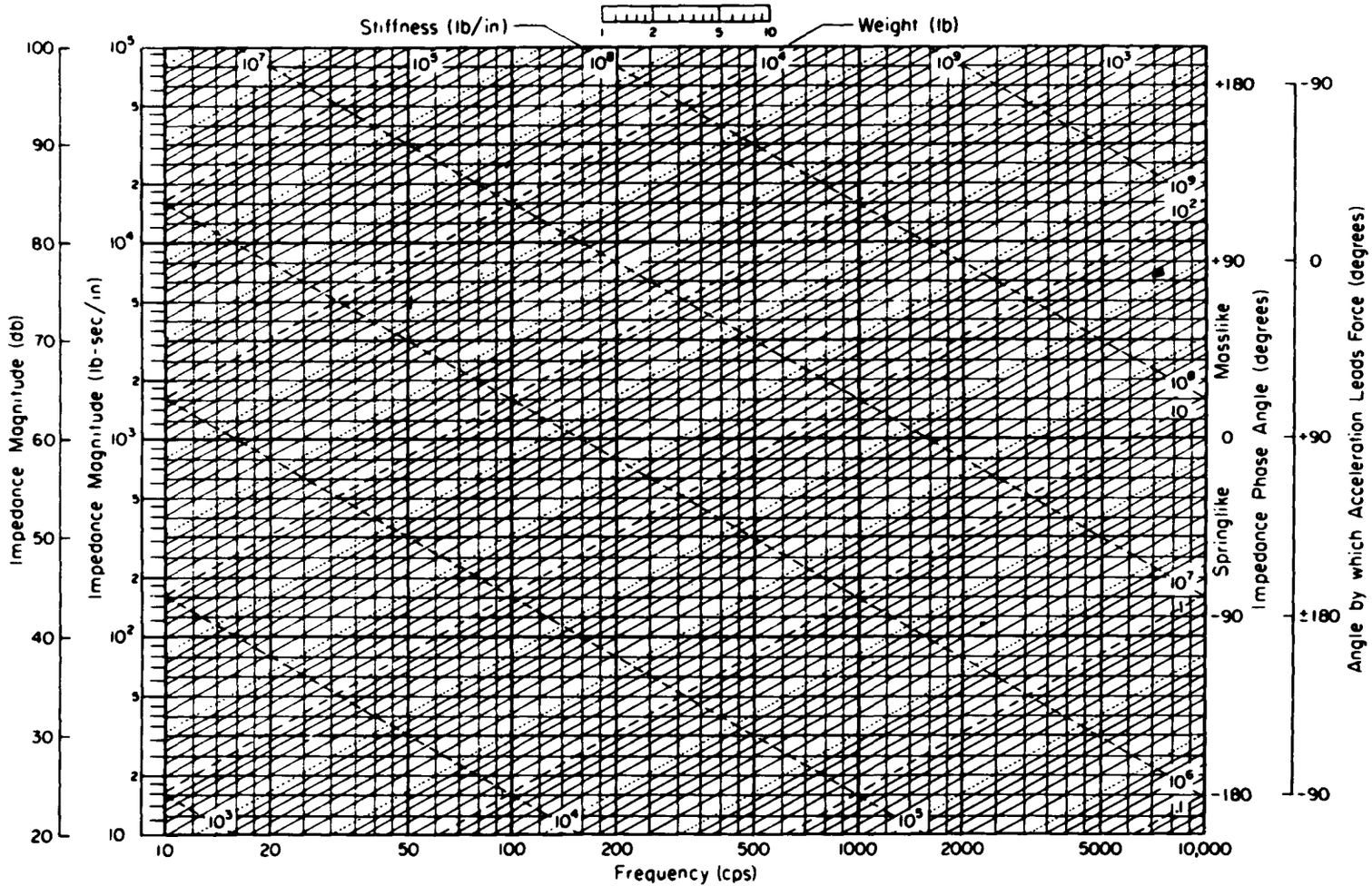

Fig. 1 - Sample graph showing Magnitude on F/a and F/d Scales and Phase Angle on Degree Scales [30]

TABLE 1
Factors* Relating Impedance Parameters, as Defined by American Standards Association [28]

	Symbol	Definition	d/F	V/F	a/F	F/a	F/V	F/d	Alternative Names
Dynamic Stiffness	K	F/d				$x = (i\omega)^2$	$x = i\omega$	$x = 1$	Dynamic Modulus; Mechanical Impedance
Mechanical Impedance	Z	F/V				$x = i\omega$	$x = 1$	$x = 1/i\omega$	Immobility
Effective Mass	M	F/a				$x = 1$	$x = 1/i\omega$	$x = 1/(i\omega)^2$	Apparent Mass
???		a/F	$x = 1(i\omega)^2$	$x = 1/i\omega$	$x = 1$				
Mobility	Y	V/F	$x = 1/i\omega$	$x = 1$	$x = i\omega$				Mechanical Admittance
Dynamic Flexibility	A	d/F	$x = 1$	$x = i\omega$	$x = (i\omega)^2$				Mechanical Admittance

*Sample from line 2 and column 4: $(F/V) = (i\omega) \times (F/a)$.

proper usage to yield good engineering results. The other four papers in this session were prepared by competent engineers to present (1) the fundamentals needed for analytical determination and understanding of impedance parameters, (2) the fundamentals needed for measurement of impedance, (3) a review of practical problems which have used impedance in obtaining solutions, and (4) a detailed procedure for obtaining rational design information through use of impedance information. In the writer's opinion, this set of papers will have accomplished its purpose if it whets the interest of the reader sufficiently so that he (or she) will consult other referenced works and consider where this tool can be of use. Although incomplete, the references and bibliographies herein contain much additional information. No attempt has been made to include laboratory reports on particular projects; during the last several years, there have been a considerable number of these.

REFERENCES

[1] E. A. Guillemin, "Introductory Circuit Theory," John Wiley and Sons, Inc., New York, 1953.

[2] M. B. Reed, "Electrical Network Synthesis," Prentice Hall, Inc., New York, 1955, Chapter 2.

[3] L. L. Beranek, "Acoustics," McGraw-Hill Book Co., New York, 1954, Chapter 3.

[4] W. P. Mason, "Regular Combination of Acoustic Elements," Bell System Technical Journal, V. 6, 1927, p. 258.

[5] H. F. Olson, "Dynamic Analogies," D. Van Nostrand, New York, 1943.

[6] J. G. Truxal, "Automatic Feedback Control System Synthesis," McGraw-Hill Book Co., Inc., New York, 1955.

[7] H. M. Jemes, N. B. Nichols, and R. S. Phillips, "Theory of Servomechanisms," McGraw-Hill Book Co., New York, 1947, Chapter 6.

[8] B. C. Carter, "The Vibration of Airscrew Blades with Particular Reference to Their Response to Harmonic Torque Impulses in the Drive," Reports and Memoranda of the Aeronautical Research Committee, No. 1758, July 6, 1936; also "The Mounting of Aero Engines: Transverse and Whirling Vibrations of Some Idealized Systems

Analyzed by Applying the Method of Admittances as Extended by Duncan," Aeronautical Research Council, London Report Memo 1988, July 1941.

[9] F. A. Firestone, "Mobility Method of Computing the Vibration of Linear Mechanical and Acoustical Systems Mobility-Electrical Analysis," J. Appl. Physics, 9:373-387 (1938).

[10] M. A. Biot, "Coupled Oscillations of Aircraft Engine and Propeller Systems," J. Aeronaut. Sci. 7:376-382 (1940).

[11] W. J. Duncan, "The Admittance Method for Obtaining the Natural Frequencies of Systems," Phil. Mag. 32 401-409 (1941); also "Free and Forced Oscillations of Continuous Beams: Treatment by the Admittance Method," Phil. Mag. 34:49-63, January 1943; also "Mechanical Admittances and their Applications to Oscillation Problems," Ministry of Supply, Aeronautical Research Council Reports and Memoranda, Monograph R&M No. 2000, 1947.

[12] R. G. Manley, "The Mechanical Impedance of Damped Vibrating Systems," J. Roy. Aeronaut. Soc. 45:342-348 (1941); also "Electro-Mechanical Analogy in Oscillation Theory," J. Roy. Aeronaut. Soc. 47:22-28 (1943).

[13] F. A. Firestone, "The Mobility and Classical Impedance Analyses," American Institute of Physics Handbook, McGraw-Hill, New York, N. Y., 1957, pp. 3-140-3-177.

[14] T. V. Korman, and M. A. Biot, "Mathematical Methods in Engineering," New York, McGraw-Hill, pp. 365-409, 1940.

[15] C. R. Freberg, and E. N. Kemler, "Mobility," Chapter IX in "Elements of Mechanical Vibration," New York, John Wiley and Sons, 1949.

[16] E. L. Hixson, and A. F. Wittenborn, "The Measurement of Mechanical Impedance and its Applications," University of Texas, Defense Research Laboratory, October 1957.

[17] "Colloquium on Mechanical Impedance Methods for Mechanical Vibrations," edited by R. Plunkett, American Society of Mechanical Engineers, New York, 1958.

[18] R. O. Beisheim, "The Need for Precision in Measuring Mechanical Impedance," presented at National Meeting, Instrument Society of America, Los Angeles, Calif., 11-15 September 1961.

[19] V. H. Neubert, "Computer Methods for Dynamic Structural Response," presented at 2nd Conference on Electronic Computation, Pittsburgh, Pa., 9-11 September 1960.

[20] W. J. Duncan, "Notes on Biot's Dynamic Modulus," J. Roy. Aeronaut. Soc. 45:225-227 (1941).

[21] H. B. Stewart, "Vibration Theory Combining Dynamic Stiffness and Mobility Methods," J. Aeronaut. Sci. 12:349-355 (1945).

[22] R. T. McGoldrick, "Method of Mechanical Impedance and the Electrical Analogy," David Taylor Model Basin, Report R-226, September 1947.

[23] D. C. Johnson, "Application of Admittance Methods to Small Oscillations," Engineering 171:650-652 (1951).

[24] R. Plunkett, "Experimental Measurement of Mechanical Impedance or Mobility," J. Appl. Mechanics 21:250-256 (1954).

[25] W. R. Runyan, and R. E. Anderson, "Mechanical Impedance Measurements of Soils," J. Acoust. Soc. Am. 28:73-79 (1956).

[26] C. T. Molloy, "Use of Four Pole Parameters in Vibration Calculations," J. Acoustical Society of America, V. 29, p. 842 (1957).

[27] J. H. Argyris, "On the Analysis of Complex Elastic Structures," Appl. Mechanics Reviews, 11, 1958, pp. 331-338.

[28] American Standard Acoustical Terminology (Including Mechanical Shock and Vibration), American Standards Association, New York, 1960; also Proposed American Standard on Nomenclature and Symbols for Specifying the Mechanical Impedance of Structures, 1960.

[29] R. A. Frazer, W. J. Duncan, and A. R. Collar, "Elementary Matrices and Some Applications to Dynamics and Differential Equations," McMillan Co., New York, 1947.

[30] Bureau of Ships letter to SSN Noise Advisory Committee Structural Impedance Panel, 13 July 1961.

BIBLIOGRAPHY

J. Miles, "Applications and Limitations of Mechanical-Electrical Analogies, New and Old," J. Acoust. Soc. Am. 14:183-192 (1943).

E. N. Kemler, and C. R. Freberg, "Electrical Methods in Teaching and Application of Vibration Theory," J. Eng. Educ. 34:274-281 (1943).

R. E. D. Bishop, "Analysis and Synthesis of Vibrating Systems," J. Roy. Aeronaut. Soc. 58:703-719 (1954).

P. F. Chenea, "On Application of Impedance Method to Continuous Systems," J. Appl. Mechanics 20:233-236 (1953), Discussion, 20:571-574 (1953).

T. S. Korn, and F. Kirschner, "Measures De L'Impédance D'Entree Du Sol Dans Le But D'Isolement Des Vibrations," Acoustica 4:671-676 (1954).

W. J. Duncan, "Factorization of a Class of Determinates and Applications to Dynamical Chains," Phil. Mag. 36:615:622 (1945).

J. Morris, and J. W. Head, "The 'Escalator' Process for the Solution of LaGrangian Frequency Equations," Phil. Mag. 35:735:759 (1944).

R. E. D. Bishop, "Analysis of Vibrating Systems," Proc. Inst. Mech. Engrs. 169:1031-1050 (1955).

D. C. Apps, "Quieter Automotive Vehicles," Noise Control, March 1955.

A. M. Wiggins, "Mechanical Impedance Bridge," J. Acoust. Soc. Am. 15:50-53 (1943)

E. W. Ayers, E. Aspinall, and J. Y. Morton, "An Impedance Measuring Set for Electrical, Acoustical, and Mechanical Impedances," Acoustica 6:11-16 (1956).

H. G. Yates, "Prediction and Measurement of Vibration in Marine Geared-Shaft Systems," Proc. Inst. Mech. Engrs. 169:611-642 (1955).

N. O. Myklestad, "The Concept of Complex Damping," J. Appl. Mech. 19:284-286 (1952).

R. Plunkett, "Semi-Graphical Method for Plotting Vibration Response Curves" Proceedings of the Second U. S. National Congress of Applied Mechanics, pp. 121-126, 1954.

R. M. Foster, "A Reactance Theorem," Bell System Tech. J., April 1924, pp. 259-267.

R. E. Blake, "The Need to Control the Output Impedance of Vibration and Shock Machines," Shock and Vibration Bulletin No. 23, Office of the Secretary of Defense, June 1956.

G. J. O'Hara, "Effect upon Shock Spectra of the Dynamic Reaction of Structures," NRL Report 5236, Dec. 1958; also published in Proceedings of the Society for Experimental Stress Analysis 1961.

A. O. Sykes, "The Evaluation of Mounts Isolating Nonrigid Machines from Nonrigid Foundations," Shock and Vibration Instrumentation, American Society of Mechanical Engineers, 1956.

* * *

ANALYTICAL DETERMINATION OF MECHANICAL IMPEDANCE

Robert Plunkett
University of Minnesota
Minneapolis, Minnesota

This paper discusses the impedance, dynamic stiffness, effective mass, mobility, and receptance of simple lumped elements and shows how they may be combined to find the impedance of systems of moderate complexity. It also indicates methods for finding the impedance of simple, uniform, continuous systems and lists references dealing with more complex structures.

INTRODUCTION

Impedance methods cannot replace other types of vibration analysis but may supplement them to solve certain kinds of problems more easily. In its simplest form, the impedance concept applies only to steady-state, sinusoidal vibrations of linear structures, those in which the vibration level at any given frequency is directly proportional to the applied force. The key to the viewpoint introduced by the impedance concept is that it concentrates on the vibration response of one point of a structure as a function of frequency, whereas the usual types of analysis determine the way in which the whole structure responds and let frequency be a secondary parameter.

The major advantage one derives from this new viewpoint is the ability to find the effect on vibratory response of interconnecting systems of known characteristics or of modifying some of the elements of a given system. In the standard methods of analysis, if any part of the system is changed in any way, the complete analysis must be repeated and each time we find the behavior of the whole structure; using impedance methods, we must make a separate analysis for the response of each point of a complex structure but a change in one of the elements requires a new analysis only for that element.

This paper discusses some of the methods used for finding the impedance of various kinds of structures but does not have space to give all the details or many examples. A recent symposium [1] includes 12 papers, many of which demonstrate specific methods for finding impedances and also gives an extensive bibliography of other specific cases. Another recent set of magazine articles [2] goes into the analysis of some simple systems in great detail with numerical examples. One of the current texts [3] shows the way in which impedance methods fit into the whole field of vibration analysis and gives extensive tables of mode shapes and frequencies useful in this approach.

SIMPLE ELEMENTS

The easiest place to start is with the classic building blocks of linear vibration theory—spring, viscous damper, and mass—connected into a damped single-degree-of-freedom system (Fig. 1a).

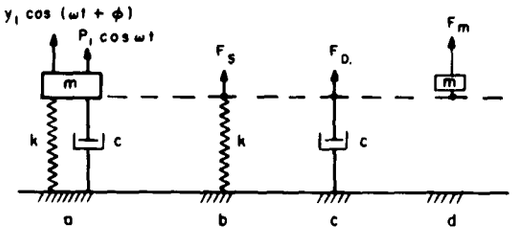

Figure 1

From Fig. 1a we see that all three elements have the same steady-state amplitude of vibration, $y_1 \cos(\omega t + \phi)$, and that $P_1 \cos \omega t$ is the total force applied to all three of them; it will be remembered that we are planning to consider only a steady-state sinusoidal vibration of constant amplitude and to ignore any transients.

The governing equation of kinematic constraint is that each of the elements has the same motion. The equation of dynamic constraint is:

$$P_1 \cos \omega t = F_s + F_D + F_m . \quad (1)$$

The next step is to find the F's in terms of y. By definition,

$$F_s = ky - ky_1 \cos (\omega t + \phi). \quad (2)$$

Likewise,

$$F_D = cv = c\dot{y} = -c\omega y_1 \sin (\omega t + \phi) \quad (3)$$

and

$$F_m = ma = m\ddot{y} = -m\omega^2 y_1 \cos (\omega t + \phi) . \quad (4)$$

Now we may expand Eqs. (2), (3), and (4) by the trigonometric identities:

$$\sin (A+B) = \sin A \cos B + \cos A \sin B$$

and

$$\cos (A+B) = \cos A \cos B - \sin A \sin B ,$$

and substitute into Eq. (1) to get

$$\begin{aligned} P_1 \cos \omega t = {} & (k \cos \phi - c \sin \phi \\ & - m\omega^2 \cos \phi) y_1 \cos \omega t \\ & + (-k \sin \phi - c \cos \phi \\ & + m\omega^2 \sin \phi) y_1 \sin \omega t . \end{aligned} \quad (5)$$

When $\sin \omega t = 1$, then $\cos \omega t = 0$, so that

$$(-k \sin \phi - c\omega \cos \phi + m\omega^2 \sin \phi) = 0 ,$$

or,

$$\tan \phi = \frac{c\omega}{m\omega^2 - k} . \quad (6)$$

Since

$$\sin^2 \phi = \frac{\tan^2 \phi}{1 + \tan^2 \phi} \quad \text{and} \quad \cos^2 \phi = \frac{1}{1 + \tan^2 \phi},$$

$$P_1 \cos \omega t = \sqrt{(k - m\omega^2)^2 + c^2\omega^2}\ y_1 \cos (\omega t + \phi) , \quad (7)$$

after a certain amount of algebraic manipulation.

Of necessity, Eqs. (6) and (7) are exactly those one finds in any text in mechanical vibrations for the steady-state response and phase angle of a single-degree-of-freedom system.

The most difficult and time-consuming part of this development has been the algebraic manipulation. The labor can be reduced by using phasors which rely on Euler's formula,

$$e^{j\phi} = \cos \phi + j \sin \phi , \quad (8)$$

where $j^2 = -1$. If we now let the sinusoidal force be

$$P = P_1 e^{j\omega t} ,$$

y becomes

$$y = \bar{y} e^{j\omega t} = y_1 e^{j\phi} e^{j\omega t} = y_o e^{j(\omega t + \phi)} ,$$

where $\bar{y}$ is a complex number, including the phase angle and y_1 is a real number, the modulus or absolute value of $\bar{y}$ If these are now substituted into the above relationships,

$$F_s = ky = k\bar{y} e^{j\omega t} , \quad (2a)$$

$$F_D = cv = c\dot{y} = jc\bar{y}\omega e^{j\omega t} , \text{ and} \quad (3a)$$

$$F_m = ma = m\ddot{y} = -m\bar{y}\omega^2 e^{j\omega t} . \quad (4a)$$

If these are substituted into Eq. (1),

$$P_1 e^{j\omega t} = (k + jc\omega - m\omega^2)\ \bar{y} e^{j\omega t} . \quad (5a)$$

The tangent of the phase angle is the negative of the ratio of the real to imaginary parts of the coefficient,

$$\tan = \frac{c\omega}{m\omega^2 - k} , \quad (6a)$$

and the absolute value is the square root of the sum of the squares, or

$$P_1 = \left[(k - m\omega^2)^2 + c^2\omega^2\right]^{1/2} y_1 , \quad (7a)$$

at a great saving in algebra.

It is also convenient to nondimensionalize Eqs. (6) and (7) by letting

$$\begin{aligned} \omega_n^2 &= k/m \\ \beta &= \omega/\omega_n \\ c_c &= 2\sqrt{km} = 2m\omega_n = 2k/\omega_n = 2Z_o \quad (9) \\ \zeta &= c/c_c \\ y_o &= P_1/k . \end{aligned}$$

Then,

$$\tan \phi = \frac{2\zeta\beta}{1 - \beta^2} \quad (6b)$$

and

$$y_1 = y_o \left[(1 - \beta^2)^2 + (2\rho\beta)^2 \right]^{-\frac{1}{2}} . \qquad (7b)$$

It will be seen that both ϕ and y_1/y_o are functions of β only, if ρ is considered as a parameter, the dimensionless damping. We may thus make two plots—ϕ versus β and y_1/y_o versus β—with ρ as a parameter and have the response curves for all single-degree-of-freedom systems.

PRESENTATION OF RESULTS

Very often for engineering work, however, we are interested in actual frequencies and the numerical values of spring, mass, and damping; in this case, we must multiply β by ω_n (or f_n) and ρ by c_c to get dimensional values. It has recently become customary to plot log y_1/y_o and ϕ versus log β so that dimensional values may be found by relabeling the graphs without changing the shape of the curves; Fig. 2 shows nondimensional curves and the results for f_n = 10 cps.

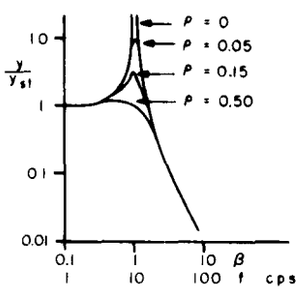

Figure 2

The development just presented and Fig. 2 give the result for vibration displacement. Although it was customary for many years to consider mainly vibration displacement, it is not the only quantity of interest since vibration velocity controls both stress and noise [4] and vibration acceleration is controlled by unbalance [5]. It is easy to get one from another since if

$$\left.\begin{aligned} y &= y_1 e^{j\omega t} \\ v &= \dot{y} = j\omega y \\ a &= \ddot{y} = j\omega v = -\omega^2 y \end{aligned}\right\} . \qquad (10)$$

We may rewrite Eq. (7b) either as

$$v = v_o \frac{\beta}{\left[(1 - \beta^2)^2 + (2\rho\beta)^2 \right]^{\frac{1}{2}}} = v_o \left[\left(\frac{1}{\beta} - \beta \right)^2 + 2\rho \right]^{-\frac{1}{2}} \qquad (7c)$$

or

$$a = a_o \left[\left(\frac{1}{\beta^2} - 1 \right)^2 + \frac{2\rho}{\beta} \right]^{-\frac{1}{2}} . \qquad (7d)$$

While any of the forms (7b), (c), or (d), are equally useful, the author prefers (7c) because it is symmetrical in β and $1/\beta$ and it has some other technical advantages. Therefore this paper will henceforth present all developments and results in terms of velocity as in Fig. 3 which is a replot of Fig. 2.

Heretofore, all results have been given in terms of reference displacement y_o, velocity

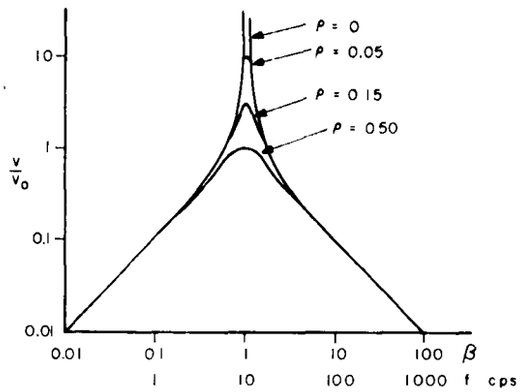

Figure 3

v_o, or acceleration a_o; as was pointed out before, dimensionless charts are not directly useful for engineering applications where we usually want to know how much vibration we get per unit force. The impedance is the quantitative measure of how well a vibratory system resists a force; it is the force per unit velocity. Thus for this system,

$$Z = \frac{P_1}{v} = \frac{P_1}{v_o} \left[\left(\frac{1}{\beta} - \beta \right)^2 + 2\rho \right]^{\frac{1}{2}} \qquad (11)$$

$$\frac{P_1}{v_o} = \frac{P_1}{\omega_n y_o} = \sqrt{km} = Z_o \quad \text{[Eq. (9)]}. \qquad (12)$$

Borrowing still further from circuit theory, $1/2\rho$ is often known as the quality factor Q. Thus, finally the impedance for a single-degree-of-freedom system is

$$Z = Z_o\left[\left(\frac{1}{\beta} - \beta\right)^2 + \frac{1}{Q}\right]. \qquad (13)$$

The mobility is a measure of how mobile the system is, how easily it moves, or the ratio of velocity to force

$$M = \frac{v}{P} = Z^{-1} = M_o\left[\left(\frac{1}{\beta} - \beta\right)^2 + \frac{1}{Q}\right]^{-1}. \qquad (14)$$

Other ratios which have been used are: receptance [3], ratio of displacement to force; dynamic stiffness [6], ratio of force to displacement; effective mass, ratio of force to acceleration; and acceleration mobility [5], ratio of acceleration to force. Figure 4 is a plot of the mobility of a single-degree-of-freedom system with a natural frequency of 10 cps, a Q of 10 or ρ of 0.05 and a mass which weighs 10 pounds. Figure 5 is a plot of the impedance of the same system.

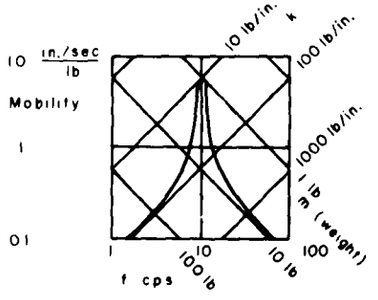

Figure 4

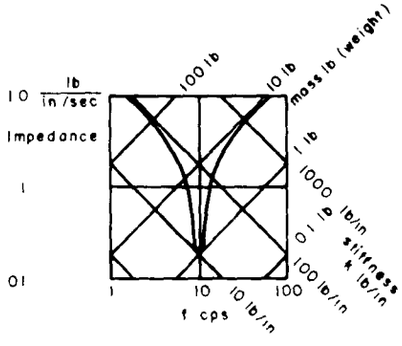

Figure 5

CHAINS OF SIMPLE ELEMENTS

We have defined impedance as the ratio (complex) of force to velocity, or

$$Z = \frac{F}{v}. \qquad (15)$$

Referring to Fig. 1 and Eq. (1), we see that all the elements of a single-degree-of-freedom system have the same velocity and the total force is the sum of the forces. Thus if we divide Eq. (1) by the common velocity,

$$\frac{P_1}{v} = \frac{F_s}{v} + \frac{F_D}{v} + \frac{F_m}{v},$$

or

$$Z_1 = Z_s + Z_D + Z_m. \qquad (16)$$

Equation (16) says that the impedance of this system is the sum of the impedances of the elements because the velocity is common. In Fig. 6 the force on the mass and the spring are the same and the velocity of the end point of the spring is the sum of that due to the mass and that due to the spring, or

$$\frac{v_1}{P} = \frac{v_s}{P} + \frac{v_m}{P}$$

and

$$M_1 = M_s + M_m. \qquad (17)$$

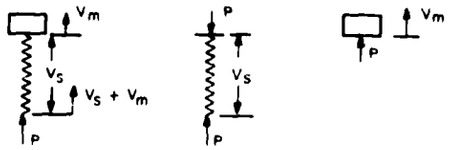

Figure 6

Whether we add impedances or mobilities depends on whether the forces add and the velocity is the same (mechanical parallel) or the velocities add and the force is the same (mechanical series). It is possible to construct the impedance of a lumped system by successively adding the elementary components.

Let us consider the case of torsional vibration of a shaft with disks distributed along it, Fig. 7. We may start from the left end and build up the impedances until we get to the right end.

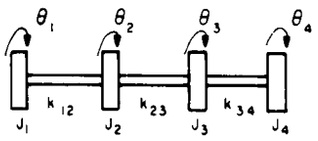

Figure 7

Let Z_1 be the impedance of the disk J_1 which is, by definition, the ratio of the applied torque to the resulting vibratory angular velocity; then,

$$Z_{1R} = j\omega J_1 . \tag{18}$$

The vibratory velocity of J_2 is the vibratory velocity of the left end of k_{12}, which is the right end of Z_1, plus the increase in vibratory velocity across k_{12},

$$V_2 = V_1 + V_{12} . \tag{19}$$

However, the torque applied to the right end of k_{12} is the torque applied to the right end of J_1, or

$$\frac{V_2}{T_{12}} = \frac{V_1}{T_{12}} + \frac{V_{12}}{T_{12}}$$

$$M_{2L} = M_{1R} + M_{12} . \tag{20}$$

But,

$$M_{1R} = \frac{1}{Z_{12}}$$

$$M_{12} = \frac{j\omega}{k_{12}} .$$

Thus,

$$M_{2L} = \frac{j\omega}{k_{12}} + \frac{1}{j\omega J_1} . \tag{21}$$

Now,

$$Z_{2L} = \frac{1}{M_{2L}} = \frac{1}{\frac{j\omega}{k_{12}} + \frac{1}{j\omega J_1}} . \tag{22}$$

The velocity of J_2 is the same as that of the right end of k_{12} and the torque applied to the right end of J_2 is the sum of that applied to k_{12} and that applied to J_2, or

$$\frac{T_{2R}}{v_2} = \frac{T_2}{v_2} + \frac{T_{12}}{v_2} .$$

Thus,

$$Z_{2R} = Z_2 + Z_{2L}$$

$$= j\omega J_2 + \frac{1}{\frac{j\omega}{k_{12}} + \frac{1}{j\omega J_1}} . \tag{23}$$

We may proceed as above to the left side of J_3,

$$M_{3L} = \frac{j\omega}{k_{23}} + M_{2R}$$

$$= \frac{j\omega}{k_{23}} + \frac{1}{j\omega J_2 + \frac{1}{\frac{j\omega}{k_{12}} + \frac{1}{j\omega J_1}}}$$

$$Z_{3L} = \frac{1}{\frac{j\omega}{k_{23}} + \frac{1}{j\omega J_2 + \frac{1}{\frac{j\omega}{k_{12}} + \frac{1}{j\omega J_1}}}} . \tag{24}$$

and to the right side of J_3,

$$Z_{3R} = j\omega J_3 + Z_{3L}$$

$$= j\omega J_3 + \frac{1}{\frac{j\omega}{k_{23}} + \frac{1}{j\omega J_2 + \frac{1}{\frac{j\omega}{k_{12}} + \frac{1}{j\omega J_1}}}} . \tag{25}$$

The pattern is now obvious, and we may write for the impedance, looking at the right end of J_4,

$$Z_{4R} = j\omega J_4 + \frac{1}{\frac{j\omega}{k_{34}} + \frac{1}{j\omega J_3 + \frac{1}{\frac{j\omega}{k_{23}} + \frac{1}{j\omega J_2 + \frac{1}{\frac{j\omega}{k_{12}} + \frac{1}{j\omega J_1}}}}}} . \tag{26}$$

The approach is obviously the same as that of the Holzer method, except that frequency is carried as a parameter instead of being evaluated numerically. The use one makes of the final expression depends on the application and relative magnitude of the terms; one might use the theorems of continued fractions [7] to find the characteristic equation containing the four natural frequencies (one of them is zero) or one may use various approximations to find the impedance over a limited frequency range.

The development just presented shows that impedance and mobility are equally important in our analysis. Which we use, depends on

whether we are joining elements so that they see the same velocity and add forces, or see the same force and add velocities. In the first case, we speak of mechanical parallel and add impedances (Fig. 8a); in the second, we speak of mechanical series and add mobilities (Fig. 8b).

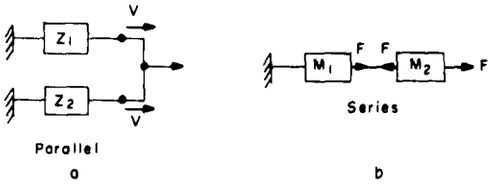

Figure 8

COMBINING SUBSYSTEMS

It was stated in the Introduction that impedance methods differ from previous, more classical methods in focussing attention on the vibration response of one point as a function of frequency. It is this aspect of the approach that is used for combining subsystems. This may be illustrated by considering the classical case of the damped dynamic vibration absorber attached to a single-degree-of-freedom system [8] (Fig. 9). This system may be considered in two parts (Fig. 10).

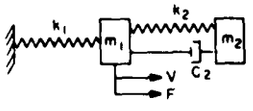

Figure 9

Figure 10

The governing equations are clearly,

$$v = v_1 = v_2 ,$$

and

$$F = F_1 + F_2 .$$

Thus,

$$\frac{F}{v} = \frac{F_1}{v} + \frac{F_2}{v} = \frac{F_1}{v_1} + \frac{F_2}{v_2} ,$$

or

$$Z = Z_1 + Z_2 , \tag{27}$$

since the velocity is the same for both pieces and the forces add (mechanical parallel, Fig. 8a). We have already seen that

$$Z_1 = j\left(\omega m_1 - \frac{k_1}{\omega}\right) . \tag{28}$$

And it is not difficult to show that

$$Z_2 = \frac{j\omega m_2 k_2 - \omega^2 c_2 m_2}{\left(k_2 - \omega^2 m_2\right) + j\omega c_2} . \tag{29}$$

If Eqs. (28) and (29) are substituted into Eq. (27),

$$Z = j\frac{k_1}{\omega}\left[\frac{\omega^2 m_1}{k_1} - 1 + \left(\frac{\omega^2 m_1}{k_1}\right)\left(\frac{m_2}{m_1}\right)\frac{1 + \frac{j\omega c_2}{k_2}}{1 - \omega^2\frac{m_2}{k_2} + \frac{j\omega c_2}{k_2}}\right] . \tag{30}$$

This development may be compared with that used in the classic approach [8]. One might point out some conclusions that may be more obvious in this formulation than in the usual one. If there is no absorber, Z_1 becomes zero at $\omega^2 = k_1/m_1$ and amplitude becomes excessive; from Eq. (30) we see that Z can never be zero unless c_2 is, in which case there are two frequencies of resonance, one lower than either $\sqrt{k_1/m_1}$ or $\sqrt{k_2/m_2}$ and one higher than either. The larger the mass ratio, m_2/m_1, the more these two new resonant frequencies differ from the old ones. Such a device is used for a system driven at a constant frequency to increase the impedance and reduce the response at that frequency; this means that Z_2 should be as large as possible at the frequency it is desired to suppress. It is clear from Eq. (29) that this frequency is very close to $\sqrt{k_2/m_2}$ and that the maximum value of Z_2 decreases as c_2 increases; c_2 is useful only to control amplitude at the two new resonances and not at $\sqrt{k_2/m_2}$. If these conclusions were made quantitative, they would confirm the major results of previous investigations. What is more interesting, these conclusions are not confined to vibration absorbers used on single-degree-of-freedom systems. The major point of interest is that Eqs. (27) and (29) still hold, but Eq. (28) no longer gives the impedance of the primary system. If we can find some expression for Z_1,

analytic or measured, we may adjust k_2/m_2, $\omega c_2/k_2$ and m_2 for adequate control at any desired frequency.

MULTIMASS SYSTEMS

Up to this point, we have discussed the vibration response of one point of a system when it is excited by a sinusoidal force of the same character as the motion acting at the same point. In the case of a rotation (Fig. 7), the force must be a torque about the same axis; in the case of linear motion, the force must be in the same vectorial direction as the motion. To state it more rigorously, the force must be that generalized force corresponding to the generalized coordinate of the Lagrangian. When we deal with cases where more than one point, or motions at one point in more than one direction, are involved, we must use somewhat more complicated expressions. Suppose we are concerned with a system of many masses, springs, and dampers and that the reactions or constraints are fully defined. Then, if the system be linear, the vibration response to any one sinusoidal vibratory force is sinusoidal, of the same frequency and proportional to the force. The amplitude of any one point is, in general, different from that of any other so that we may write

$$v_1 = M_{11} F_1$$

$$v_2 = M_{21} F_1$$

$$v_3 = M_{31} F_1, \text{ etc.}$$

In these equations, M_{11}, M_{21}, M_{31}, and the like, are complex numbers giving the ratio of the vibration velocity at points 1, 2, 3, etc., to the vibratory force at point 1. Referring to our previous discussion, they are functions of frequency, and may be called mobilities; M_{11} is called a driving point, or input mobility and M_{21} or M_{31} are called transfer mobilities. If we now have a force operating on point 2 alone and none on point 1, we may write

$$v_1 = M_{12} F_2$$

$$v_2 = M_{22} F_2$$

$$v_3 = M_{32} F_2, \text{ etc.}$$

Now, if both forces act at the same time and with the same frequency, the vibration amplitudes will be sum of those due to each force separately:

$$\begin{aligned} v_1 &= M_{11} F_1 + M_{12} F_2 \\ v_2 &= M_{21} F_1 + M_{22} F_2 \\ v_3 &= M_{31} F_1 + M_{32} F_2 . \end{aligned} \tag{31}$$

In expressions of this type, Mij is the velocity response of point i due to a unit vibratory force at point j with all other forces except the stated reactions or constraints being zero; it may be shown that for all such passive mechanical systems, $Mij = Mji$ (dynamic reciprocity) [9, 10]. When we start defining the more general form of impedance, we find the situation somewhat more difficult. Since the vibration velocities are caused by the vibratory forces, we may not use more independently defined velocities than forces. Thus in the equations similar to Eqs. (31), we must have as many equations for force as we have given velocities,

$$\begin{aligned} F_1 &= Z_{11} v_1 + Z_{12} v_2 \\ F_2 &= Z_{21} v_1 + Z_{22} v_2 , \end{aligned} \tag{32}$$

if there are only two forces. In this case, Zij is the force at point i due to a unit velocity of point j when all other velocities corresponding to forces being considered are held zero; that is, all other forces must be replaced by rigid constraints. Under these conditions, it may be shown that reciprocity still holds, $Zij = Zji$; however, it may no longer be said that the impedances, Z, are the reciprocals of the mobilities M. Instead, one must say that the square matrix of impedances is the inverse of the corresponding square matrix of the mobilities [11]. It should be noted that, in general, the values of the Z's will depend on how many forces are being considered, whereas the values of the M's do not. As for simpler systems, the impedance or stiffness formulation must be used for some analyses [6, 12] and mobility or receptance formulation for others [3, 13].

Starting with these formulations, we may set up general expressions for the Mobilities or Impedances in terms of the resonant frequencies and mode shapes. While these procedures have been known to be valid since the time of Fourier [9], it has been only since the development of high-speed digital computers that they have become practical [14, 15]. Since these methods (Given or Jacobi) are now readily available, we will assume that all of the normal modes and frequencies of an undamped multimass system are known. It may be shown that the mobilities can be expanded as a series

of partial fractions whose poles are the natural frequencies [10]; for example,

$$M_{11} = \frac{a_1}{\frac{\omega_1}{\omega} - \frac{\omega}{\omega_1}} + \frac{a_2}{\frac{\omega_2}{\omega} - \frac{\omega}{\omega_2}} + \frac{a_3}{\frac{\omega_3}{\omega} - \frac{\omega}{\omega_3}} + \cdots\cdots + \frac{a_n}{\frac{\omega_n}{\omega} - \frac{\omega}{\omega_n}}, \quad (33)$$

where n is the number of masses, natural frequencies, and mode shapes. The a's may be found from the mode shape [14]; the easiest approach is by matrix multiplication, an operation well suited to digital calculators. If Eq. (33) is converted into one fraction, the denominator is the product of the individual denominators and the numerator is a polynomial of degree $n-1$ in ω^2, or

$$M_{11} = \frac{M_{110}}{\omega} \frac{\left(1 - \frac{\omega^2}{\omega_I^2}\right)\left(1 - \frac{\omega^2}{\omega_{II}^2}\right)\cdots}{\left(1 - \frac{\omega^2}{\omega_1^2}\right)\left(1 - \frac{\omega^2}{\omega_2^2}\right)\cdots\left(1 - \frac{\omega^2}{\omega_n^2}\right)}, \quad (34)$$

where ω_I, ω_{II}, and the like, are the antiresonant frequencies of the point. This type of expression is known as Foster's Theorem [16]. In this case, the denominator is the same for all points and depends only on the resonant frequencies of the system; the constant and the numerator are different for all points since the antiresonant frequencies are point and not system parameters.

The impedance functions of Eqs. (32) may be expressed in a similar way, except that now the zeros are system parameters and the poles are the point parameters. One of the more useful aspects of Foster's theorem is that the mobility or impedance may be expressed quite accurately over a limited frequency range by using only the resonant or antiresonant frequencies that fall within the range [6]. Figure 11 is a schematic representation of mobility or impedance over such a limited range [2, 5, 14].

CONTINUOUS SYSTEMS

Foster's theorem or the expansion in normal modes, Eq. (33), lets us express the mobility or impedance of continuous systems in terms of a finite number of frequencies. In fact, when we are talking of real systems, this is what we always do; all real systems have an infinite number of natural frequencies so that only finite expression is only on approximation. We may also solve such systems by approximating them with lumped springs and masses and solving the reduced physical problem.

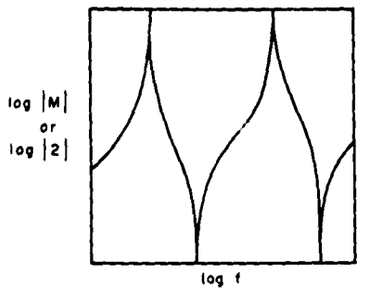

Figure 11

The arithmetical labor of this approach is reduced by matrix formulation [17, 18] and by extensive tables of the mode shapes and frequencies of simple shapes [3]. Impedance methods may also be useful for analyzing nonlinear vibration problems where most of the system is linear and the nonlinearity involves only a few elements [19].

DAMPING

The phase and amplitude effects of damping are discussed at some length in several of the papers of Ref. 1, notably Refs. 12 and 16, and these precise formulations are often useful in servomechanism or feedback problems. For most vibration problems, small damping is most easily handled by assuming an amplification factor for each mode shape as in Figs. 4 and 5. It can be shown that this will also control the antiresonances in a similar fashion [20].

If the damping is not linear but still small, it may be handled as Jacobsen's equivalent viscous damping in the manner described in most vibration texts. (Also on damping, "Analysis of Dynamic Systems Using the Mechanical Impedance Concept," W. C. Sperry, Noise Control, 7, 2, March-April 1961, pp. 13-21.)

REFERENCES

[1] R. Plunkett, Ed., "Mechanical Impedance Methods for Mechanical Vibrations," ASME, New York City, 1958.

[2] R. P. Thorn and A. H. Church, "Simplified Vibration Analysis by Mobility and Impedance Methods," Penton Publ. Co., Cleveland, Ohio, 1959-60, 80 pp.

[3] R. E. D. Bishop and D. C. Johnson, "Mechanics of Vibration," Cambridge Press, 1960.

[4] H. G. Yates, "Vibration Analysis in Marine Geared Turbines," Trans. North-East Coast Inst. of Engineers and Shipbuilders, Vol. 65, 1949.

[5] A. H. Church and R. Plunkett, "Balancing Flexible Rotors," Trans. ASME, Vol. 83, 1961.

[6] M. A. Biot, "Coupled Oscillations of Aircraft Engine Propeller Systems," J. Aero. Sci., January 1940.

[7] See any book on intermediate algebra, e.g., "Textbook of Algebra," G. Chrystal, Part II, Dover, 1961, Chapter XXXII.

[8] J. P. Den Hartog, "Mechanical Vibrations," McGraw-Hill, New York, 4th ed., 1956, sec. 3.3.

[9] Lord Rayleigh, "Theory of Sound," Dover, New York, 1945.

[10] E. A. Guillemin, "Introductory Circuit Theory," John Wiley, New York, 1953.

[11] L. A. Pipes, "Applied Mathematics for Engineers and Physicists," McGraw-Hill, New York, 1946, VIII-10.

[12] D. V. Wright, "Impedance Analysis of Distributed Mechanical Systems," pp. 19-42 of Ref. 1.

[13] R. Plunkett, "Calculation of Optimum Concentrated Damping," J. Appl. Mech., 25, 2, pp. 219-224, June 1958.

[14] V. Neubert and W. H. Egell, "Dynamic Behavior of a Foundation-Like Structure," pp. 77-86 of Ref. 1.

[15] S. H. Crandall, "Engineering Analysis," McGraw-Hill, New York, 1956.

[16] S. H. Crandall, "Impedance Analysis of Lumped Systems," pp. 5-18, Ref. 1.

[17] J. H. Argyris, "Analysis of Complex Elastic Structures," Appl. Mech. Rev., 11, 331-338, 1958.

[18] R. Plunkett and M. E. Gurtin, "Use of Excess Constraints in Structural Analysis," Jour. Mech. Eng. Sci., IME, 2, 2, 1960, pp. 101-4.

[19] P. R. Paslay and M. E. Gurtin, "Vibration Response of a Linear Undamped System Resting on a Nonlinear Spring," J. Appl. Mech., 27, E, 2, pp. 272-74.

[20] R. Plunkett, "Plotting Vibration Response Curves," Proc. 2nd Nat. Cong. Appl. Mech., ASME, 1954, pp. 121-126.

DISCUSSION

A question was asked about the electrical analogy.

Dr. Plunkett: I was afraid somebody was going to ask that question. The answer is yes and no. I do not like to think of this tool in terms of an analogy. Because if you are going to try and set up an analogy you can set it up in a number of different ways depending on the application. From my standpoint, I find it easier to think of it in terms of its primitive definition, in terms of a ratio between a sinusoidal force and the resulting sinusoidal motion. Now it depends, if you are going to call it admittance, it depends on whether you call your analogy between motion and voltage, or between motion and current. You can set up your analogy either way and this then determines whether you call it admittance or not, which is why I personally dislike the use of the word admittance. I think it is unfortunate that we have used the word impedance, that's bad enough. Does that successfully evade your question?

Mr. Saunders (General Electric): One thing I would like to mention. I think Dr. Plunkett has done a great and very interesting task on this. One thing he has neglected to

mention and that is the application of matrix methods. Now, if you have a very large and complex system, it's very easy to use the matrix method; in fact, you let the computing machine do all the work for you. When you have the matrix method, if you have to break into it as Dr. Plunkett mentioned, why you can actually store the matrix in the machine, you can actually start from there and put your new system on, or add anything else on to it. Actually the machine will do most of your work for you. One of the other things I would like to mention also is about the Myklestaad method. Now if you have, say, a non-uniform beam like a missile, you can actually determine your transfer impedances by using the Myklestadd procedure very easily, and simply. Therefore, by using a computer and using some of these other tools you can actually reduce your work down to a bare minimum. Let the machine do all the work for you.

Dr. Plunkett: I can only agree with what he says, and I can only reiterate what I said earlier—that impedance methods do not replace any other method that is useful in vibration—and you can make use of any of them for certain applications.

Mr. Stern (General Electric): As you probably know, many times when items are being evaluated to meet a particular test their failure rates can be rather excessive due to the specs calling for a rather rigid fixture. Whereas, in the actual application, the supporting structures are usually quite soft, and even for the same input, you usually don't get the same severity of damage. I wondered how you felt about the possibility of having impedances, fixture impedances called down in specifications? Particularly on missile equipment or satellite equipment where weight is important.

Dr. Plunkett: Well, I think you may be asking the wrong person this because Dr. Belsheim is the authority. Let me say it though because he may not want to. The people at the U. S. Naval Research Laboratory in recent years have demonstrated quite conclusively that this lack of appreciation of the influence of support impedance on shock level, in particular, has led to shock specifications being considerably more severe than they ought to be. I am not sure he would want to be quoted on a particular number. My personal impression is that they are at least five times too high, but that is not an official opinion, fortunately. I would think that one of the places where we could get most mileage out of this kind of approach is by making sure that our specification does indeed match the environments to which we think that we are trying to subject the equipment. Very often, we have gotten in exactly that kind of a trap. This is the converse problem of course of the isolator effectiveness, where isolators turn out not to be effective because they are not supported properly. Likewise, if we make a measurement and then don't support things properly, why we will get a lower vibration or shock environment than we expected. If, on the other hand, our machines are carefully specified to be extremely rigid, our environment will turn out to be much higher than we thought. The only answer I can give to that is I'm also in favor of motherhood and against sin. . .firmly. . .oh! I'm an anti-Communist too.

* * *

INSTRUMENTS AND METHODS FOR MEASURING MECHANICAL IMPEDANCE

R. R. Bouche
Endevco Corporation
Pasadena, California

After mentioning some of the various methods used for experimentally measuring mechanical impedance, this paper describes the performance characteristics that affect the accuracy of recently developed mechanical impedance heads. The results of calibrations and evaluation tests performed on an impedance head are described. Tests on a simple structure are made to illustrate the suitability of the head for making impedance measurements.

INTRODUCTION

Various methods have been employed for the experimental determination of the mechanical impedance of structures.

An indirect method [1] employs an electrodynamic vibration exciter equipped with both a driving coil and velocity sensing coil. The transfer electrical impedance of the coils is measured with known mechanical impedances attached to the exciter and with the structure of unknown impedance attached. The mechanical impedance of the structure is computed from equations relating it to the measured electrical impedances. Other indirect methods for measuring mechanical impedance include (a) measuring the terminal electrical impedance of a variable reluctance transducer under blocked and free conditions and (b) measuring the change in response of two identical reeds of known mechanical impedance when one is connected to the structure of unknown impedance. These methods and others are briefly discussed by Coleman [2].

A transient method also has been used for measuring mechanical impedance [3]. A transient force is applied and the resulting motion of the structure is measured with an accelerometer. The impedance is determined from "the ratio of the Fourier spectra of the force and response histories."

The most direct technique to determine mechanical impedance is to utilize force and motion measuring transducers. Recently a number of experimentists [2-10] have employed this technique on structures. Since this technique is quite widely accepted, the remainder of this paper is devoted to a calibration and evaluation of an impedance head and its use in measuring the impedance of a simple structure. A mechanical impedance head is a transducer with built-in force and motion measuring devices. Although one type of impedance head is herein described in detail, the calibration procedures and discussion of accuracies are applicable to all transducers and their use in making mechanical impedance measurements.

DESCRIPTION OF IMPEDANCE HEAD

Mechanical impedance is defined as the ratio of the force exciting a structure to the resulting velocity. The motion transducer in the impedance head may be a displacement, velocity, or acceleration transducer. Plotting the apparent stiffness (ratio of force to displacement) or apparent weight (ratio of force to acceleration) on suitable graph paper provides directly the magnitude of the mechanical impedance when the excitation is sinusoidal. Sinusoidal excitation also makes it possible to utilize a variety of instruments for accurately measuring the phase angle of the impedance.

Most impedance measurements are made in the frequency range from 10 cps to 5000 cps. In order to have wide application, the impedance head transducers should be flat (free of

frequency distortion) and have zero phase angle between the force and motion transducers throughout this frequency range. If the phase angle is not zero, the data may be corrected, if the phase shift is known and the excitation sinusoidal. The transducers must also be amplitude linear in order to measure a wide range of impedances. Mechanical impedance measurements usually are made at forces ranging from less than 1 pound up to about 100 pounds, and accelerations up to several hundred times the acceleration of gravity. Even very heavy structures can be measured in the low force ranges since the frequencies of primary interest are those above which the structure acts as a rigid body. Significant motions result from small forces near resonances (i.e., regions of low impedance). The impedance head must also measure motions corresponding to accelerations much less than 1 g (386 in. per/sec^2) in order to measure accurately high impedances at antiresonances in the structure. For this reason, accelerometers are preferred for making impedance measurements at high frequencies, since the outputs from velocity and displacement pickups are quite small for small amplitude motions at frequencies much above 1000 cps.

Another requirement for accurately measuring large impedances is that the motion transducer should not respond to force excitation particularly when the acceleration tends to zero. If false outputs result from the motion transducer due to dynamic stresses applied to the case of the impedance head, the indicated impedance would be less than the actual impedance. The impedance head should be designed so this interaction does not occur.

On the other hand, the interaction of the force transducer responding to applied accelerations normally occurs in an impedance head. This output from the force transducer equals the mass of the end of the impedance head plus any externally attached mass times their acceleration. This characteristic is used to dynamically calibrate the force transducer in the impedance head.

The mass of the impedance head should be small and its stiffness large so that the effect of the impedance head on the response of the structure is not significant. If the head has these characteristics, the measured data on many structures need not be corrected for the head mass and stiffness.

One type of impedance head and an accompanying force generator are shown in Fig. 1. The impedance head is 1 inch high and nearly

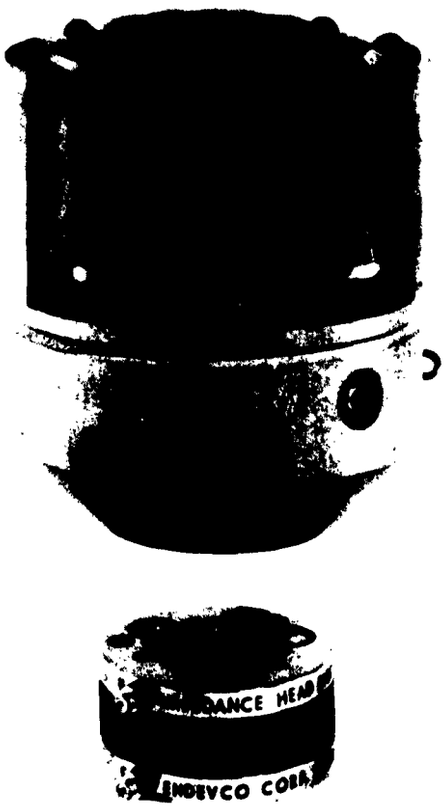

Fig. 1 - Electrodynamic force generator and impedance head used for measuring the impedance of structures

2 inches in diameter. It has three piezoelectric force pickups and three piezoelectric accelerometers built into the head. A bolt is attached to the force generator and passed through the hole in the center of the head to rigidly connect the head and outer casing of the impedance head to a structure. The force generator consists of an electrodynamic vibration exciter with its driving coil rigidly connected to the outer casing. The permanent magnet of the exciter which serves as a reaction mass is flexibly attached to the casing by thin leaf springs. It is rated at 1-pound driving force which is sufficient for testing many structures.

CALIBRATION

Sensitivity

The sensitivities of the force pickup and accelerometer parts of the impedance head were performed on an electrodynamic vibration

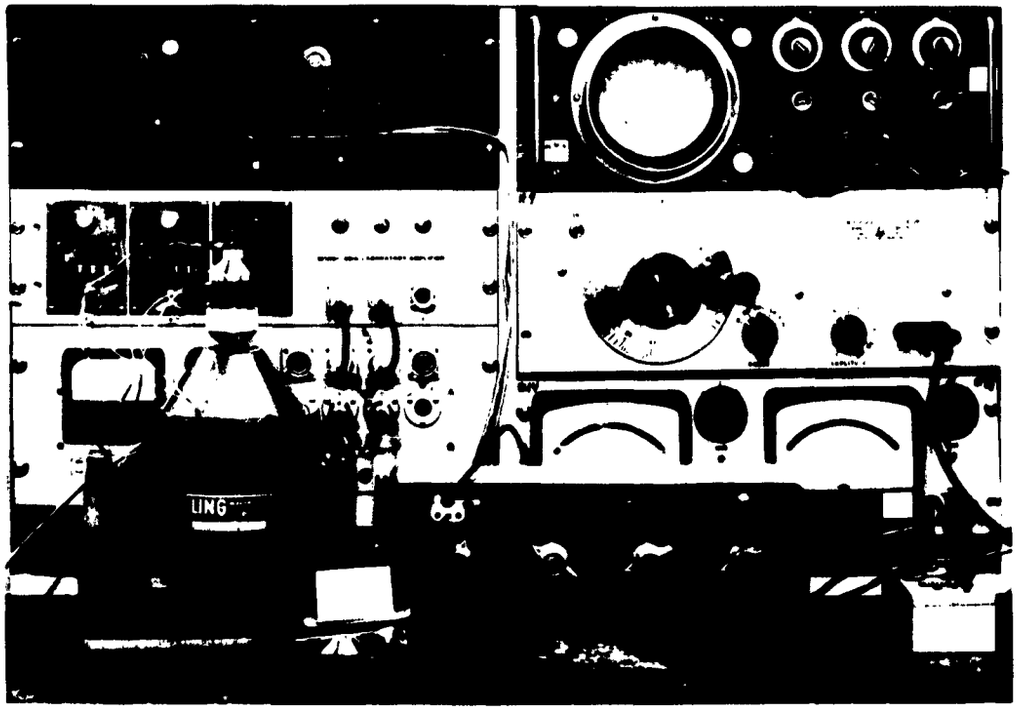

Fig. 2 - Setup used to calibrate the force pickup and accelerometer in the impedance head

exciter using the test setup shown in Fig. 2. The sensitivity of the force pickup was determined by measuring its output with two different weights attached to the impedance head. The ratio of the outputs from the force pickup to standard accelerometer mounted on top of the impedance head was measured. The measurement was repeated with a 2-pound weight inserted between the standard pickup and tapered adapter block on top of the impedance head. The force sensitivity was the change in force pickup output divided by 2 pounds and the applied acceleration. From this force sensitivity determination performed at one frequency, the total weight acting on the force pickup including the effective portion of the mounting bolt through the head and the effective end weight of the head was determined. Knowing the total weight the frequency response was determined by measuring the force pickup to standard accelerometer outputs from 10 cps to 5000 cps without the 2-pound weight attached. This part of the calibration was repeated, measuring the ratio of the output of the accelerometer in the head to the standard accelerometer output, to determine the accelerometer sensitivity over the same frequency range. The 2-pound weight was not used at the higher frequencies in order to avoid relative motion between the standard accelerometer and impedance head. A voltage ratio circuit [11] was used to reduce calibration errors.

The results of the calibration are shown in Fig. 3. The sensitivity of the accelerometer in the impedance head is nearly constant throughout the frequency range, increasing slightly near 5000 cps. Also, the sensitivities of the force pickup are nearly constant in the same frequency range. The sensitivity for use with an aluminum 1/2-inch-diameter bolt is 5.8 mv/lb. The sensitivity is reduced to 5.1 mv/lb when a 1/2-inch-diameter steel bolt is used. This change in sensitivity occurs since a small portion of the total force is applied to the bolt while the rest of the force is applied to the head. Of course, the force sensitivity is the voltage output divided by the total force. The portion of the total force applied to the bolt is the ratio of the bolt stiffness to head stiffness. The impedance head stiffness computed from the modulus of elasticity and geometric dimensions of the various parts is 2.7×10^7 lb/in. Therefore, the change in sensitivity resulting from using different size bolts can be computed. The computed change in sensitivity for the steel and aluminum 1/2-inch-diameter bolts is approximately 12 percent which agrees closely

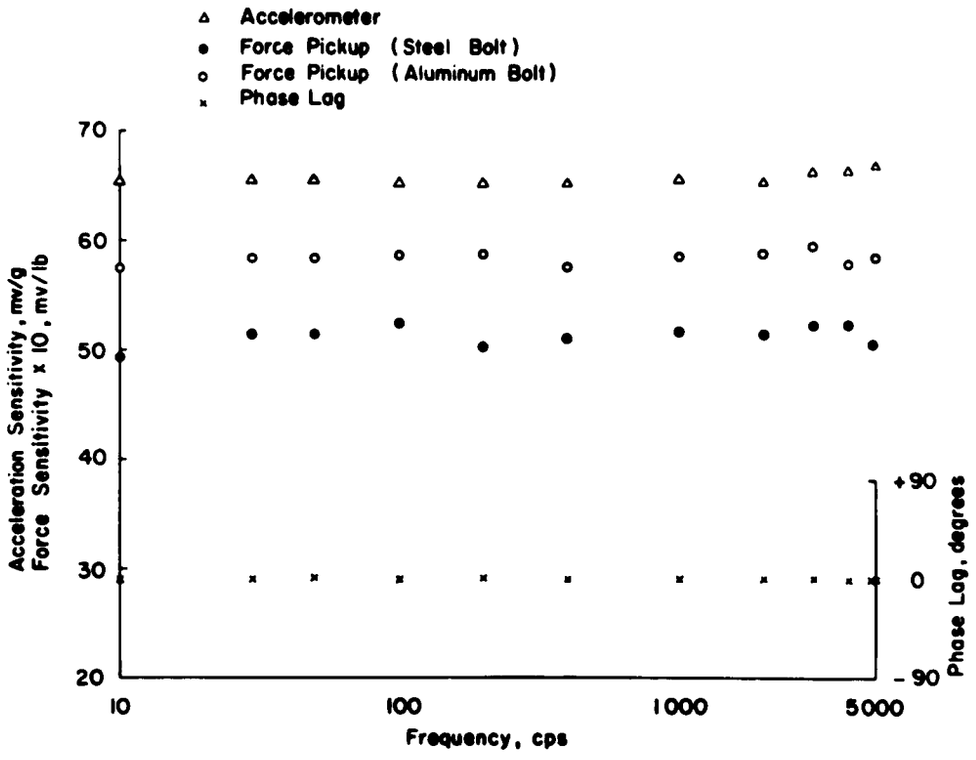

Fig. 3 - Calibration results on an impedance head. The force pickup and accelerometer were calibrated by comparison with a standard accelerometer. The phase-angle measurements were made with a dual-beam oscilloscope.

with the results shown in Fig. 3. When no bolt is used, the increase in sensitivity is 7 percent compared to the value obtained with the aluminum bolt.

The phase angle between the force and acceleration outputs is zero degrees throughout the frequency range. This indicates that the acceleration motion and force applied to a structure are faithfully reproduced in the output signals from the head and no correction to the measured phase angle of the impedance need be made.

The effective end weight of the impedance head was measured by repeating the above described force calibration with several different weights attached. The output from the force pickup corresponding to 1-g acceleration was measured for each weight applied externally to the impedance head. These data were plotted and the points fitted with a least squares line. The results for two impedance heads are shown in Fig. 4. The intercepts of the lines with the abscissa indicates the effective end weight of the impedance head is about 0.3 pound.

Amplitude Linearity.

The amplitude linearities of the impedance head were verified on electrodynamic vibration exciters equipped with resonant beams and on a shock motion calibrator.

Calibrations up to 112 pounds and 100 g were made on vibration exciters. With a small weight on top of the impedance head, sufficiently high accelerations were achieved by mounting it at the center of a free-free beam. In order to achieve sufficiently high forces, it was necessary to mount the head on the end of the beam. A standard accelerometer was mounted on top of the head and the calibration was made using the same method used for the above sensitivity calibrations.

Accelerations up to 502 g were applied on shock motion calibrators similar to that described in Ref. 12. The impedance head and standard accelerometer were attached to an anvil. Two-inch-diameter and 4-inch-diameter hardened steel balls were dropped on the anvil. Rubber paddings were used on the impact

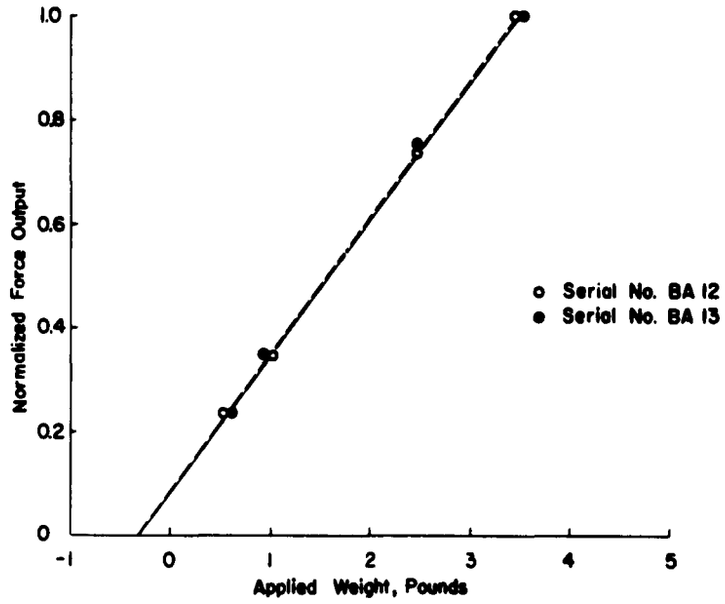

Fig. 4 - Normalized force output measured with different applied weights. The impedance head apparent end weight is indicated by the abscissa intercept (0.3 pound).

surface to obtain the desired accelerations. The amplitude linearity was determined by measuring the ratio of the standard accelerometer to impedance head accelerometer outputs which were photographed on the screen of an oscilloscope. The results are given in Table 1 and Fig. 5. The deviations from amplitude linearity are less than the measurement errors. The Model 2225 standard accelerometer (Fig. 5) was previously calibrated throughout its useful acceleration range by the absolute method described in Ref. [12].

TABLE 1
Amplitude Linearity of Endevco
Impedance Head Model 2110

Force Gage		Accelerometer	
Applied Force (lb)	Deviation (%)	Applied Acceleration (g)	Deviation (%)
0.03	+1.0	0.03	0.0
0.1	+0.5	0.1	0.0
1	0.0	1	0.0
17	-0.5	10	0.0
28	0.0	50	0.0
56	0.0	100	+0.4
70	0.0	95	0.0
84	0.0	192	+0.1
112	+0.5	412	+0.9
		502	0.0

Resonance Frequency

Resonance frequency measurements were also made on the shock machine. Less padding was used on the anvil to reduce the pulse duration in order to produce resonance frequency excitation in the impedance head. The results are shown in Fig. 6. The oscillogram, Fig. 6A, indicates the resonance frequency of the accelerometer part of the impedance head is about 28,000 cps. The theoretical response for an ideal pickup, Eq. 10 in Ref. 13, with a 28,000-cps resonance frequency is in close agreement with the slight rise near 5000 cps noted in the sinusoidal calibration (Fig. 3) of the impedance head. The beating present in Fig. 6A apparently is due to the individual accelerometers in the head having slightly different resonance frequencies. The accelerometer part of the impedance head consists of three individual accelerometers connected in parallel with a single output.

The response was measured also with the force pickup in the impedance head subjected to shock excitation. Measurements were made on two different structures. The first structure consisted of four parts including the impedance head for a total length of about 4 inches. The second structure had five parts for a total length of 7 inches. The corresponding responses from the force pickup indicates a structural resonance of 20,400 cps and 10,300

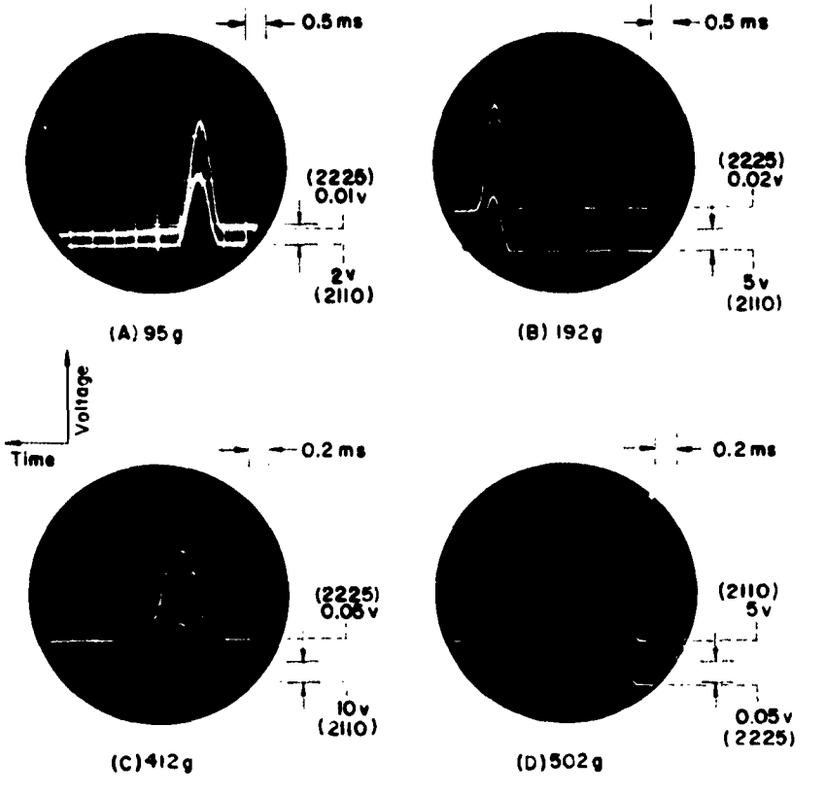

Fig. 5 - Comparison calibrations performed on a shock machine to verify the amplitude linearity of the accelerometer in an impedance head. The standard accelerometer (2225) and impedance head (2110) were mounted on an anvil in a drop-ball shock machine and the ratios of the outputs compared.

cps, Figs. 6B and C, respectively. These frequencies correspond to the resonance frequencies for the above two structures. This indicates that the impedance head is capable of making measurements at very high frequencies. Considering the mass-stiffness characteristics of the impedance head only, computations would indicate its resonance frequencies would occur at frequencies much higher than those present in Figs. 6B and C.

Other Characteristics

In addition to the calibrations just presented, tests were performed to establish the other characteristics of the impedance head.

The force sensitivity of the accelerometer part of the impedance head was determined on a hydraulic testing machine. The applied load was released instantaneously with a quick-acting valve. An oscilloscope was used to measure the output from the accelerometer. No significant output from the accelerometer was measured with an applied load of 5000 pounds which was the capacity of the testing machine. This indicated the response of the accelerometer is of the order of 0.0001 g/lb or less which corresponded to the resolution obtainable with the test equipment. Since this interaction in the impedance head is so small, it is capable of measuring very large impedances accurately.

The other characteristics including transverse sensitivity of the accelerometer, capacitances, internal resistances, and the like, are typical to that of other piezoelectric transducers. Both the force pickup and accelerometer are insulated from the case of the impedance head in order to eliminate electrical noise in auxiliary electronic instruments.

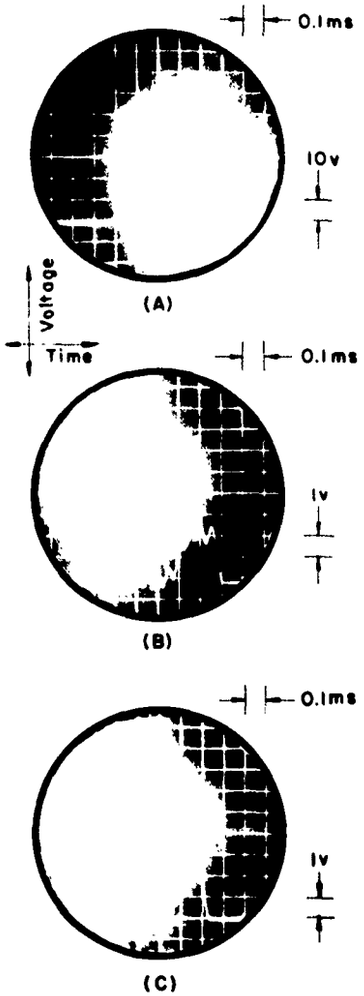

Fig. 6 - Resonance response of an impedance head. (A) Resonance frequency of the accelerometer part of the impedance head is 28,000 cps. (B) and (C) Force response with the impedance head mounted in two structures resonate at 20,400 cps and 10,300 cps, respectively.

IMPEDANCE OF A BEAM

In order to illustrate typical ranges of impedance and frequency, measurements were made on an uniform beam. The test setup is illustrated in Fig. 7. The force generator and impedance head were connected rigidly to a 3/4- by 3- by 36-inch aluminum beam (2024-T4) with a 1/2-inch-diameter steel bolt. The bolt passed through a steel tapered adapter block provided with a 1/2-inch clearance hole. The contact area of the block with the beam is an annulus with an area of 0.23 inch^2. The force and acceleration outputs from the impedance head were connected to a pair of voltage amplifiers and directly to voltmeters and a dual beam oscilloscope. No filtering circuits were used. The power amplifier used with the force generator was operated at sufficiently low levels so no distortion was present, except through very narrow frequency ranges at resonance where the force or acceleration tends to zero. The magnitude of the impedance was computed from the measured voltage outputs times the force pickup and accelerometer sensitivities determined from the above calibrations. No corrections were made to the data for the apparent weight of the impedance head, bolt, or tapered adapter block. The phase angle of the apparent weight was measured directly on a dual-beam oscilloscope and by Lissajous figures.

The results are given in Fig. 8. The experimentally measured resonances and the theoretically computed resonances for the beam are given in Table 2. The cantilever beam resonance at 78 cps was characterized by a single nodal point at the center of the beam and large

TABLE 2
Resonance Frequencies of a Beam
Measured with an Impedance Head

Measured Resonance Frequency (cps)	Theoretical Resonance Frequency (cps)	Normal Mode	
		Number	Type
78	74	1st	Fixed-free
121	117	1st	Free-free
482	460	2nd	Fixed-free
619	631	3rd	Free-free
1340	1289	3rd	Fixed-free
1513	1560	5th	Free-free
2560	2526	4th	Fixed-free
2790	2900	7th	Free-free
4080	4176	5th	Fixed-free
4400	4652	9th	Free-free

displacements at both beam ends. The free-free beam frequencies excited were odd numbered modes characterized by an antinodal point at the center of the beam. It was difficult to excite the even-mode frequencies because of the effect of the bolt and adapter block when the center of the beam tends to form an inflection point. It is interesting to note that an attempt to correct for the apparent mass of the impedance head, bolt, and adapter block would not alter the results at or near the antiresonances

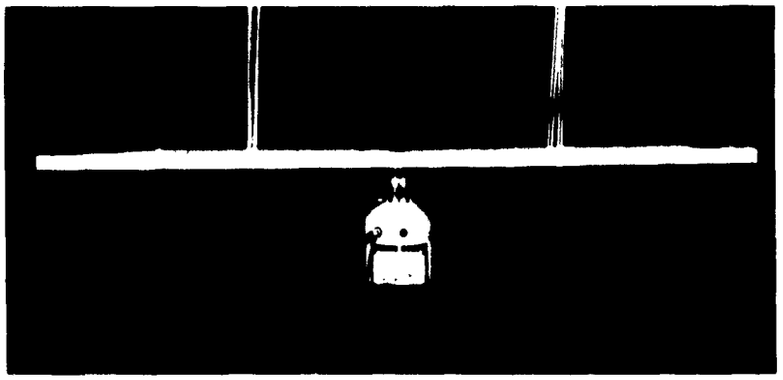

Fig. 7 - Mechanical impedance head and force generator connected to a free-free beam. The beam is suspended from overhead by rubberbands.

(regions of high impedances). Also, an attempt to correct for this apparent mass at resonances (regions of low impedances) would produce only small differences between the measured results and theoretical resonances. In the case of this beam, good results were obtained without correcting for the impedance head and fixture apparent weight.

CONCLUSIONS

Although several different methods have been used to measure mechanical impedance, the direct measurement method with force and motion transducers is becoming attractive. Impedance heads are available for making measurements over wide-frequency and impedance ranges. Accurate impedance measurements are easily made with small heads that are sufficiently stiff. Measurements made on an aluminum beam indicate good accuracy is maintained without correcting for the effective end-mass of the impedance head.

ACKNOWLEDGMENTS

L. C. Ensor and N. Der performed the tests and W. Nazarenko prepared the figures. Their work and the contributions of others are appreciated.

REFERENCES

[1] S. Levy and R. R. Bouche, "Calibration of Vibration Pickups by the Reciprocity Method," Journal of Research, National Bureau of Standards, Vol. 57, No. 4, October, 1956, pp. 227-243.

[2] G. M. Coleman, "Methods for the Measurement of Mechanical Impedance," ASME Colloquium on Mechanical Impedance Methods for Mechanical Vibrations, 1958, pp. 69-75.

[3] R. E. Blake and R. O. Belsheim, "The Significance of Impedance in Shock and Vibration," ibid., pp. 101-107.

[4] V. H. Neubert and W. H. Ezell, "Dynamic Behavior of a Foundation-Like Structure," ibid., pp. 77-86.

[5] D. Muster, "Mechanical Impedance Measurements," ibid., pp. 87-99.

[6] J. E. Ruzicka and R. D. Cavanaugh, "Vibration Isolation of Non-Rigid Bodies," ibid., pp. 109-124.

[7] R. Plunkett, "Experimental Measurement of Mechanical Impedance or Mobility," Journal of Applied Mechanics, Vol. 21, 1954, pp. 250-256.

[8] J. W. Young, Jr. and R. O. Belsheim, "Experimental Measurement of Mechanical Impedance," Naval Research Laboratory Report No. 5458, May 24, 1960, 23 pp.

[9] W. R. Runyan and R. E. Anderson, "Mechanical Impedance Measurements of

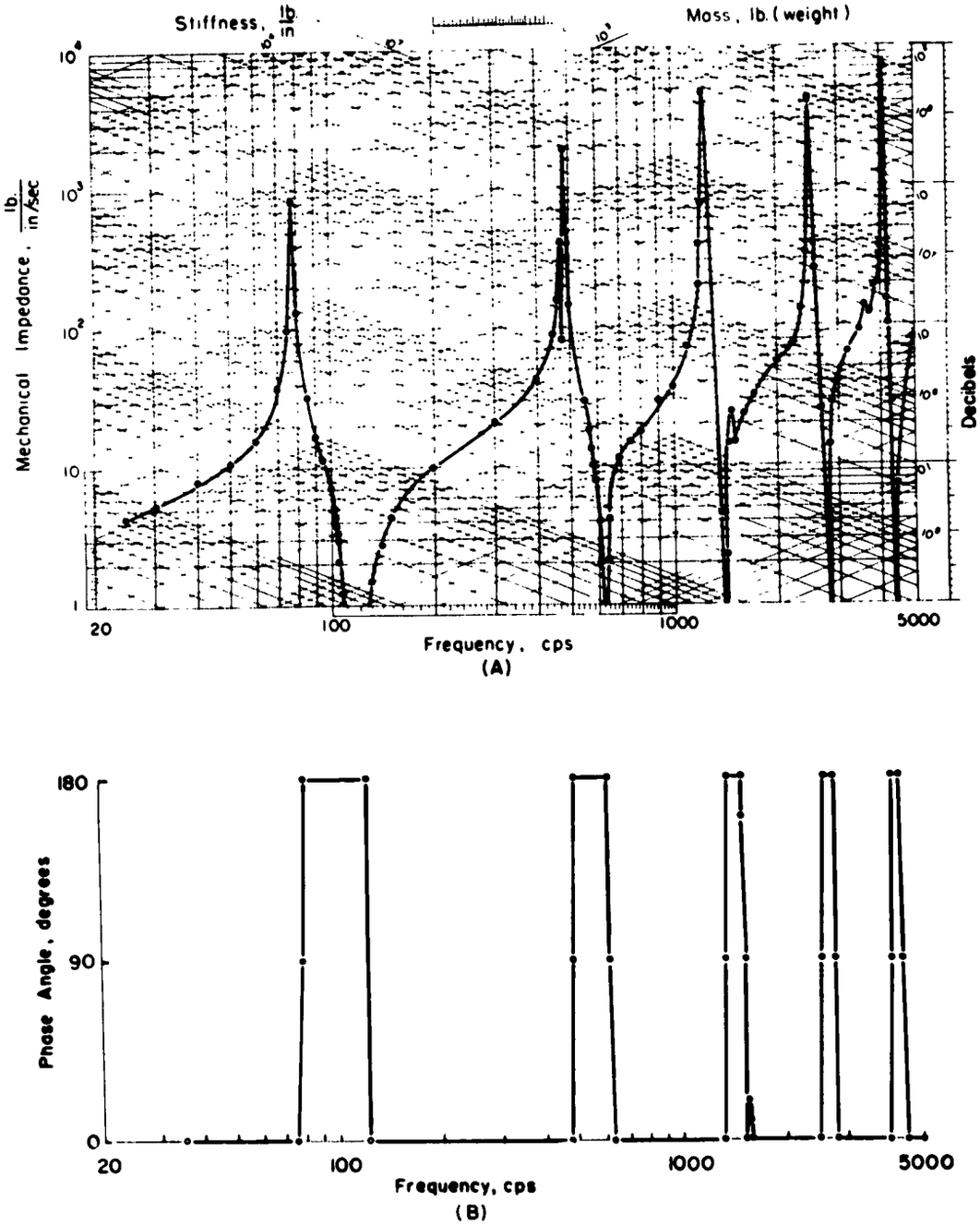

Fig. 8 - Mechanical impedance of an aluminum beam measured with an impedance head: (A) The magnitude of the impedance, apparent weight, or apparent stiffness is indicated by the appropriate scales. (B) This plot is the phase angle of the apparent weight.

Soils," Journal of Acoustical Society of America, Vol. 28, No. 1, January 1956, pp. 73-76.

[10] E. L. R. Corliss and W. Koidan, "Mechanical Impedance of the Forehead and Mastoid," Journal of Acoustical Society of America, Vol. 27, No. 6, November 1955, pp. 1164-1172.

[11] R. R. Bouche, "High Frequency Response and Transient Motion Performance Characteristics of Piezoelectric Accelerometers," Proc. Instrument Society of America (to be published).

[12] R. R. Bouche, "The Absolute Calibration of Pickups on a Drop-Ball Shock Machine of the Ballistic Type," Proc. Institute of Environmental Sciences, 1961, pp. 115-121.

[13] "American Standard Methods for the Calibration of Shock and Vibration Pickups," S2.2-1959, American Standards Association, Inc., 10 East 40th Street, New York 16, New York.

DISCUSSION

Mr. Murfin (Sandia Corp.): In your table of resonances (Table 2), all those with even modes under free-free, as you say, would be difficult to excite since they have an inflection point at the point of support. If those are replaced by the higher modes of fixed-free beams, the agreement between the theoretical frequencies and the measured frequencies is really astonishing. I get the first eight to match almost perfectly and the last two not quite so good.

Mr. Bouche: I see you had the time to do a little bit more work than I did.

Mr. Murfin: It is also interesting that in the fixed-free, there is rigid body motion, hence you would expect to get a high impedance which matches up quite nicely.

Mr. Bouche: I take it then that you have continued the theoretical analysis and computed the resonances for the four that I did not indicate in the paper. Is that correct?

Mr. Murfin: Yes, I have.

NOTE: As a result of Mr. Murfin's comments, additional computations have been made by Mr. Bouche. The results are included in Table 2 and in the text.

Mr. Trummel (Jet Propulsion Laboratory): I wonder if you could comment on the effect of the stiffness of the gage on frequency limitations?

Mr. Bouche: I can comment on it to a certain extent. As I indicated, the stiffness of the total gage is 2.7×10^7 pounds per inch. But, if one considers only the portion of the impedance head between the top of the force transducers and the point where the impedance head is attached to the structure, we have a much higher stiffness because there is only a thin steel plate in this region. Its stiffness is about a factor of 10 greater, about 3×10^8 pounds per inch. Now, from the practical point of view my experimental results on the beam that I measured showed stiffnesses which were quite large. This may demonstrate an approximate figure for the maximum stiffness that could be measured. In that case I obtained readings which were in excess of 10^7 pounds per inch, nearly 10^8 pounds per inch.

Mr. Trummel: Well, in some of our experience in measuring impedance we found that we couldn't quite use that large an area for attachment. In some cases you have to use an adapter which would effectively give you a much less stiff attaching spring constant. You have never talked about the effect of that on how far out in the frequency range you can go. If you use that large an area you stiffen your structure much more than you should.

Mr. Bouche: This would reduce the range, however, I think, in most practical structures that occur in the field, in most cases we don't reach stiffnesses quite this large.

Voice: What are the low-frequency measuring limits of your impedance head? How far is it flat?

Mr. Bouche: I performed by calibrations down to 10 cps, but I expect the impedance head itself will be flat to much lower frequencies, say of the order of 2 cps. The primary limitation here is the electronic equipment that is used with the impedance head. Piezoelectric transducers inherently have a relatively large internal electrical impedance and the impedance is a function of its capacity. So, at very low frequencies, one must use amplifiers or cathode followers that have high impedances. If a high

enough input impedance is maintained in the cathode follower, there is no reason to expect that the transducer will not be flat down to 2 cycles. It is a little bit more difficult to calibrate at 2 cycles than at 10 cycles.

* * *

APPLICATIONS OF IMPEDANCE INFORMATION

Ralph E. Blake
Lockheed Missiles and Space Company
Sunnyvale, California

Only a few applications of impedance information have yet been made to the solution of engineering problems. However, engineering research is being carried on by several groups to develop methods, apparatus, and theorems for application to some important problems in shock and vibration. The greatest current effort is on developing more effective sound and vibration isolation systems. Improvements in methods of making field measurements of dynamic environment and methods of simulation in the testing laboratory are also being studied. Ultimately, any area of shock and vibration work which deals in complicated linear systems should benefit from applications of the techniques and knowledge being developed.

INTRODUCTION

This paper is concerned with practical, engineering application of impedance techniques and theories such as those discussed in the two previous papers. Although applications to engineering problems are just beginning, engineering research is making rapid progress toward further uses, particularly in some rather important areas of shock and vibration. In general, we might hope to apply impedance ideas to any problem in which we know the dynamic-response characteristics of some parts and need to know the response when the parts are joined together. Complexity of the details is not a problem so long as the parts are linear.

The engineers working on structural impedance have had to "write the book" as they went along, developing equipment and techniques before running the experiments that they really wanted. Progress can be expected to become more evident as they build up from these foundations. One of the most important aspects of this progress is the least predictable. As masses of data are gathered and studied and as more cases are worked out theoretically, we can hope that new generalizations, or laws, will be developed. Such general laws of behavior of complex mechanical systems may someday enable us to tackle problems which look too complicated and unwieldy today.

In addition to describing some of the current applications, I will discuss the present work toward future applications. Then I wish to illustrate some generalizations that have begun to show up in the results already reported.

This paper does not pretend to survey all of the activities in the field. First, I am sure that I have not seen all the pertinent reports. But those that I have seen have too much material to permit me in the time allowed to do more than select a few examples. I asked Dr. Belsheim to send me reports from his files to help me brush up on recent work. But I was staggered to get a carton-full; it was a stack, 6 inches high, with a grand total of over 1000 pages. If structural impedance work is still in its infancy, it's a big baby.

THE ISOLATION MOUNTING PROBLEM

Most of the work on structural impedance thus far has been aimed at reducing the machinery noise emitted by a Navy ship or submarine which might be picked up by an enemy hydrophone. The hull and its sound radiation characteristics can be studied only in expensive field tests. Machinery noise generation and transmission can be measured in engineering laboratories. Impedances of machinery and foundations can be measured. Then, the effect of various possible flexible mounts and foundations can be studied theoretically and experimentally. The goal is to find design features and techniques to minimize the transmitted sound. All of these steps are being actively

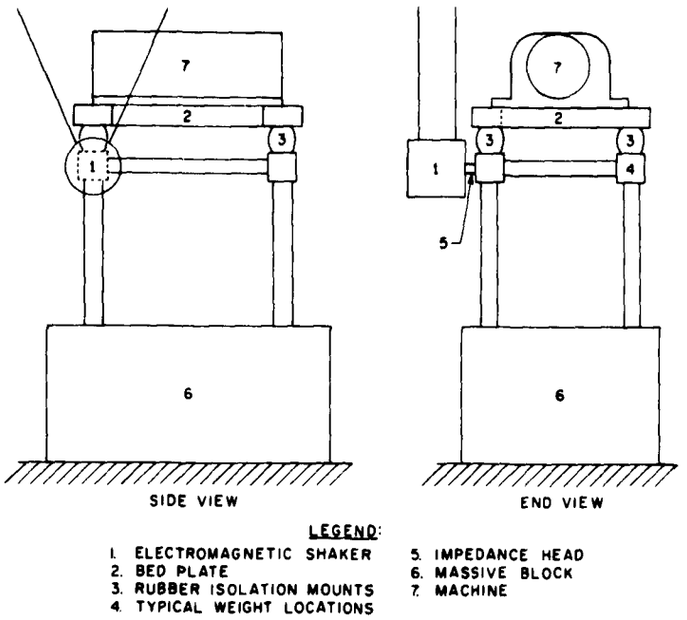

Fig. 1 - Machine-bed plate isolation system foundation

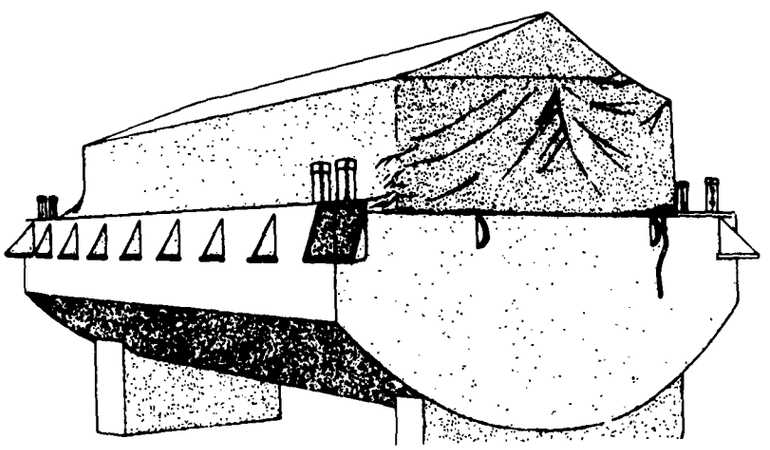

Fig. 2 - Test barge "Dezi-Belle" in air

carried out; the following few examples may indicate the scope and nature of the work.

Figure 1 shows an experimental setup [1] at the Electric Boat Division. Impedance measurements are being made on a special foundation structure while it supports a piece of naval machinery on some rubber mounts. In this test, the foundation is on a massive block.

Figure 2 is a view of a barge [2] at the Electric Boat Company which is structurally very much like a section of submarine hull. By adding foundations inside, the sound transmission path from foundation to hull to water can be studied. Figure 3 shows a point impedance measurement [2] that was made on the foundation in the barge. The complexity of the structure can be inferred from the number of

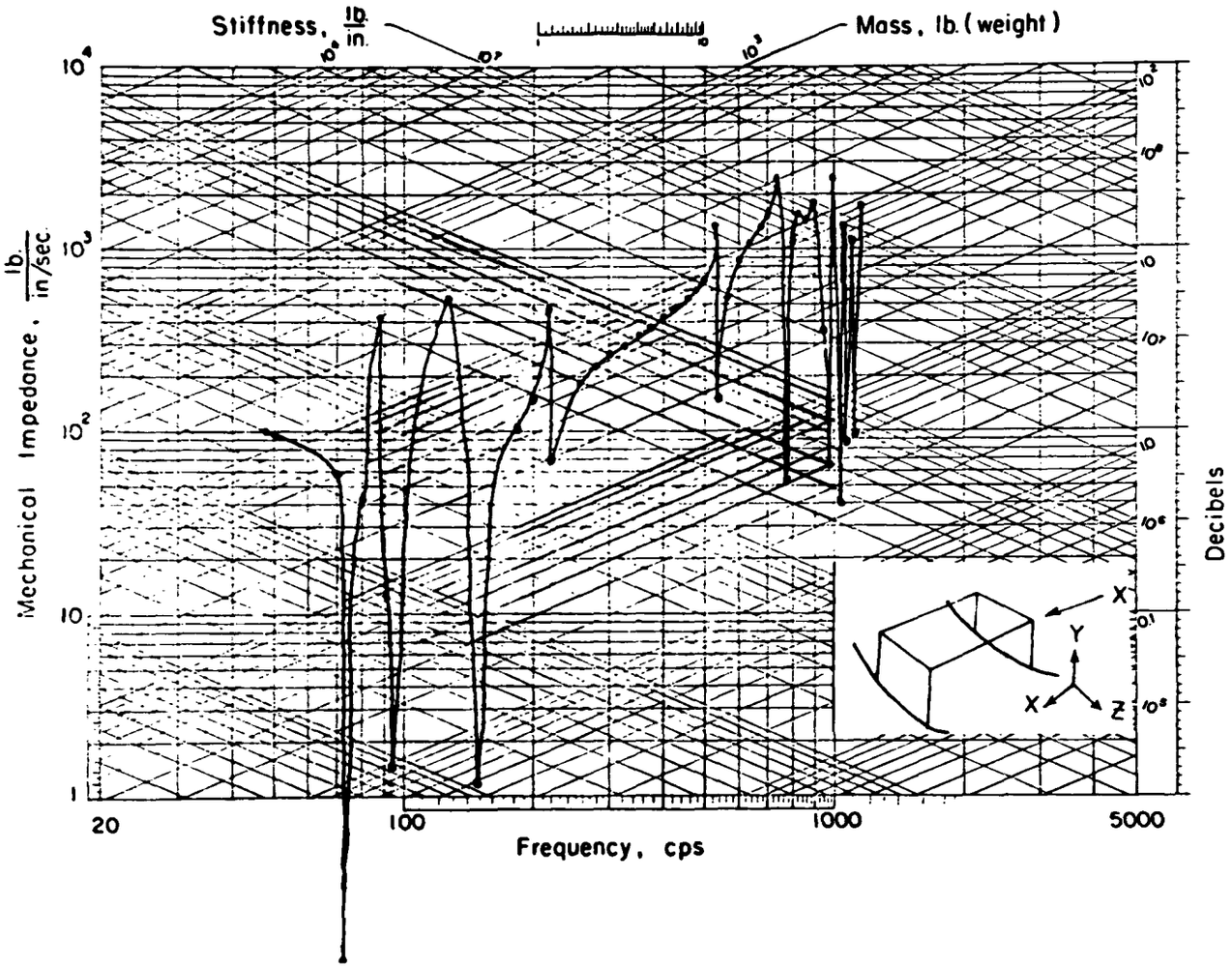

Fig. 3 - Measured point impedance, foundation G in barge in water, X direction

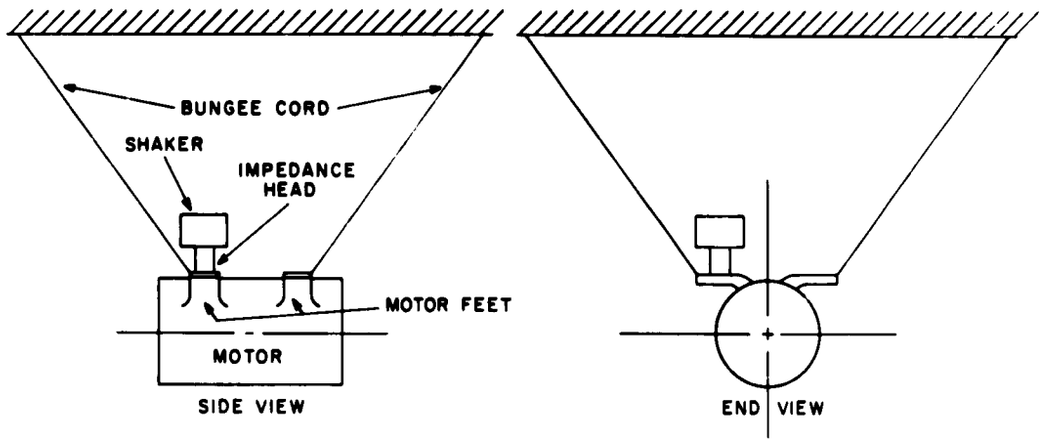

Fig. 4 - Experimental setup for external excitation tests

resonant peaks on the record. I would guess that over a hundred similar impedance measurements have been made.

Figure 4 shows the apparatus used at the Arthur D. Little Company [3] for some impedance measurements on the mounting feet of an electric motor. One of the transfer impedances measured between one foot and another is shown on Fig. 5. Now, the Reciprocity Theorem says that the transfer impedance will be the same if one interchanges the force-input and velocity-output points. But the interchange in this experiment gave the result shown on Fig. 6. Perhaps the unsatisfactory comparison between these curves was due to nonlinearity of the structure. But the experimenter hesitated to state this as a conclusion without more direct evidence. This action is in keeping with the need to proceed cautiously and check everything in this unfamiliar game until we learn to avoid the pitfalls. We expect most structures to be linear but should not assume it for any structure.

Theoretical and laboratory studies of various resilient mounts are being carried on by several investigators [4, 5, 6]. The dynamic modulus and damping of many rubber-like materials have been measured up to several thousand cps. These have then been used in theoretical analyses and digital computer studies to show the transmission with various types of machine and foundation impedances.

So far, the conclusions that have been drawn are concerned with parts of the over-all sound transmission path. For example, it has been reported that wave transmission effects become important in rubber mounts at high frequencies [4], that foundation resonances seriously increase sound radiated into the water [1], and the like. It is hoped that such generalizations will grow in number and scope until engineering design improvements can be made in the hardware. Of course much that is learned will apply to any isolator problem.

SHOCK AND VIBRATION MEASUREMENT AND TESTING

Most of us at this symposium dealt with shock and vibration as an environment which might damage some structure or equipment. We go out in the field and measure acceleration-time histories which we hope are typical. Then we set up laboratory test machines to duplicate the worst features of the field environment. These machines are then used to test the structure. It is usually true that the dynamic system on which the measurement was made is somewhat different from the one on which the equipment will be used. Most often the equipment itself is new and will supplant the one used during the field trial.

Now, Norton's Theorem [7] shows that a change in the equipment impedance will change the input motion, so that our measurement does not tell us what the test machine should do. It is common practice to assume that the measurement is "typical" and that several measurements will somehow envelope the one we need. It is true that a small equipment will not influence the motion of a heavy foundation at low frequencies; but this assumption, in practice, becomes increasingly untenable as frequencies get higher and supporting structures get trimmed to minimum weights. The best defense

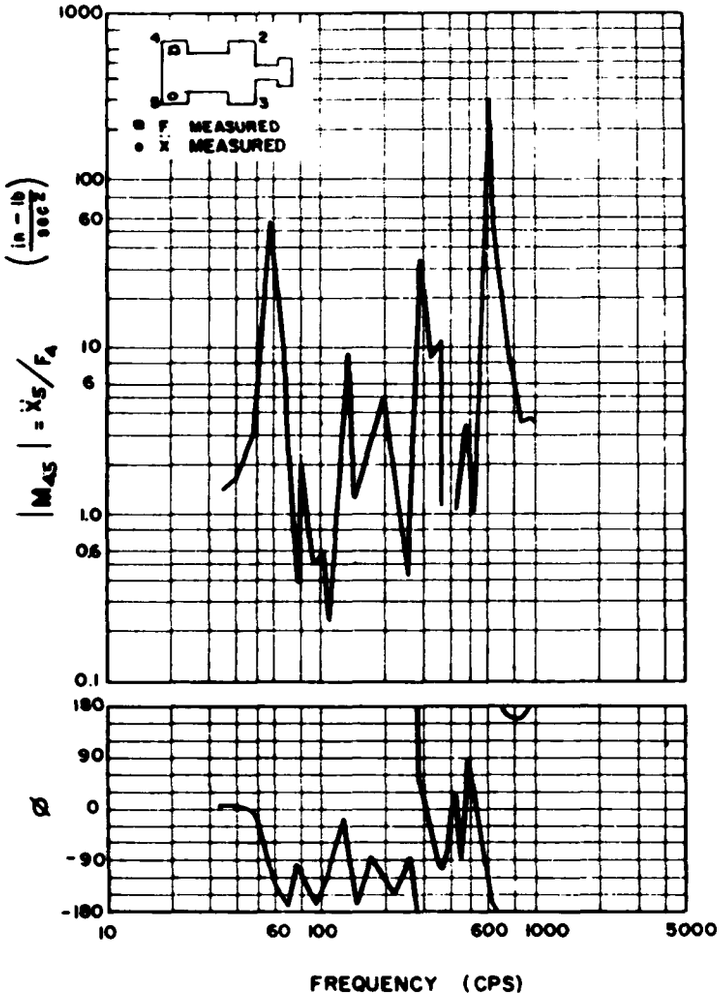

Fig. 5 - Transfer mobility and the phase versus frequency (G. E. 3-hp motor)

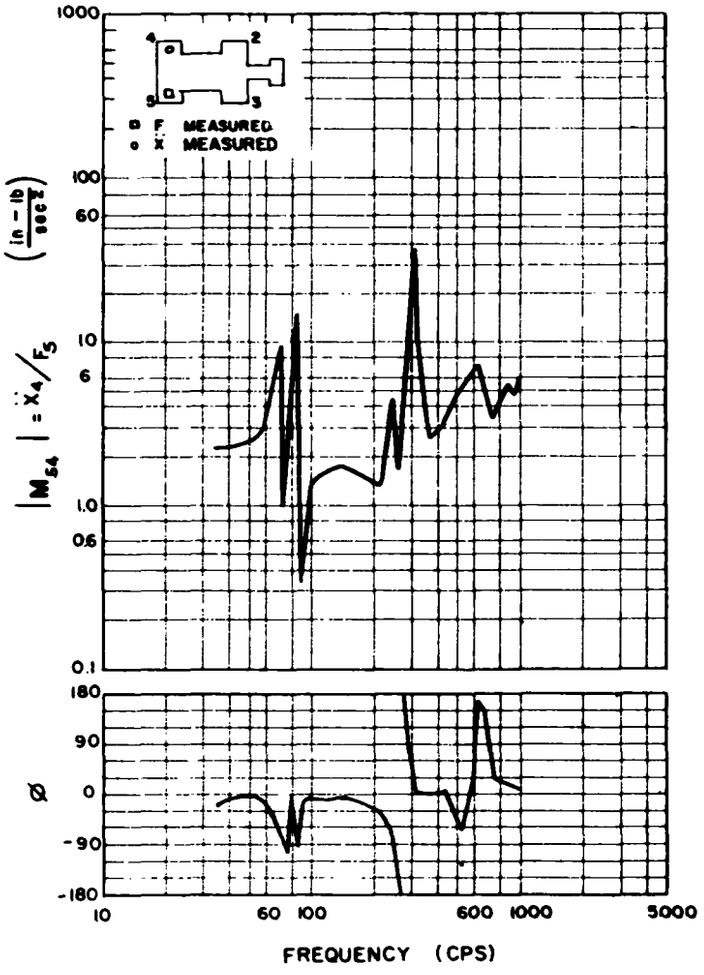

Fig. 6 - Transfer mobility and the phase versus frequency (G. E. induction motor)

of the assumption is that there is no real alternative available, and it has not led to disaster, so far as we know.

Although we may have no alternative today, we can hardly be comfortable with the knowledge that our methods do not have a firm basis. This problem of what we should measure in the field, how we should present data, and what the testing machine should duplicate has interested me for many years.

Our first real evidence that something was wrong came from comparing the actual strength of some heavy naval equipment with that required by an envelope through the peaks of shock spectra measured at the equipment mounting points [8]. Although the equipment easily survived the shock, our calculations called for considerable strengthening. Further study showed that the heavy equipment had produced valleys (or "dips") in the shock spectra at the equipment design frequencies. In this instance we had overestimated the design acceleration by a factor of five. The overdesign is much less for equipment that is lighter relative to its foundation [9, 10].

It would seem that a quantitative expression of what we mean by "lighter relative to its foundation" would require measurements of impedance of equipment and foundation through the frequency range of interest. Testing would be more true-to-life if the output impedance of the test machine duplicated the important characteristics of a foundation [11].

So, our present position is that we can see that what we are doing is inadequate. Theory tells us what to do, but this would not be practical in most cases [7]. What is needed is more experience and data to show us what parts of the theoretically perfect approach can be safely neglected. In short, further research is needed to seek out practical approximations.

AN APPLICATION TO TESTING

Dr. Belsheim and his colleagues at U. S. Naval Research Laboratory (USNRL) have made an interesting application of impedance information to the testing of some rocket payloads [12]. The only measurement of the vibration of the rocket motor to which the satellite was to be attached was made during a static firing. Then the impedance of the motor attachment point was also measured with the setup shown in Fig. 7. This impedance was recorded as an "apparent weight" (force divided by acceleration) as

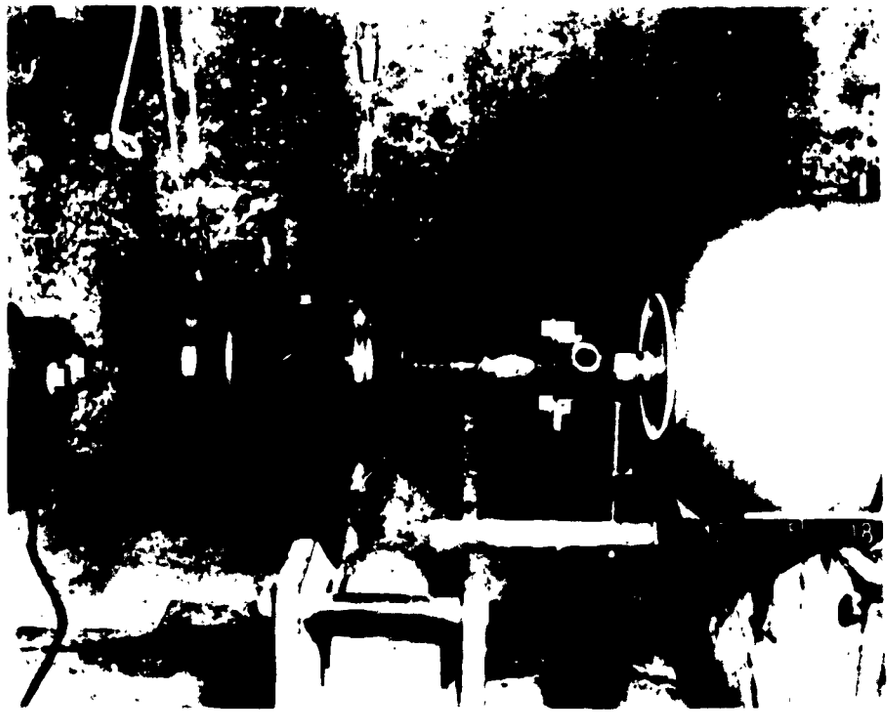

Fig. 7 - Gage location and shaker attachment on X-248 motor

shown in Fig. 8. The apparent weight of the static-firing fixture was measured, as well as that of the payload (Fig. 9). From this group of measurements, it became possible to estimate the input vibration which would have occurred if the payload had been attached in the place of the test stand.

AN APPLICATION TO VIBRATION MEASUREMENT

I have strongly implied that vibration measurements should be combined with a measurement of the impedance, but we are not yet able to make use of these on a routine basis. At Lockheed, we have been using a very simple type of impedance measurement to check on the installation of vibration pickups in the Polaris missile. A simple spring scale is used to apply a known force to the pickup location through a piece of fine music wire, as shown in Fig. 10. Cutting the wire causes a sudden step change in the force. The resulting transient oscillations, such as Fig. 11, are recorded with an oscilloscope and camera.

Suppose a 10-pound step force excited a 10-g oscillation at 1500 cps, as it did in Fig. 11. We conclude that a 1500-cps resonance involves the motion of only a pound or so of structure. Hence a 1500-cps peak in a flight record is due to a "local resonance" and is not representative of the hundreds of pounds of structure that we are interested in. Although the lightweight and high frequency of modern pickups have largely done away with resonance of the pickup or its bracket, resonance of the local structure can produce just as misleading a signal.

With this simple step force system, we have been able to show whether a pickup mounting is stiff enough; we have also been able to edit some high peaks out of our flight vibration spectra. If we had needed it, the transient response could have been analyzed into an impedance curve.

DEVELOPMENT OF GENERALIZATIONS

In this brief and incomplete survey, I have tried to show the scope and promise of work toward application of impedance information. In order to be able to think about such complex structures and intricate impedance data, it is clear that we must discover some simplifying principles. In the reports already published there are many examples of summing up the important trends noted in the data.

In a Westinghouse report [5], we read "The terminating impedance of the heavier structures usually has a resistive component about equal to the reactive at frequencies above about 200 cps."

An Electric Boat Division report says, "Damping and the use of concentrated masses are effective in reducing the transmission efficiency of foundations."

Every report has several conclusions of this general type. It is this sort of boiling down of the data, together with some additional sweeping generalizations, which will enable us to solve problems which seem too complex now.

Although the laws which we hope to find are largely unpredictable, we can search for them by trying to ask the right questions. I will close with a discussion of some studies which we have made at Lockheed to find possibly useful trends.

In the August 1960 session [11] of this symposium, a theoretical study of a very simple three-mass model of a vehicle-equipment system was presented. Results showed how the response of the "equipment" varied with natural frequency, mass, and damping. The behavior of this simple system suggested some interesting effects which should be watched for in real complex systems.

More recently, I have been interested in the implication of Norton's Theorem that a foundation vibration can become much more severe if the equipment impedance is suitably changed. There is a value of equipment impedance which will make the resonant frequency of the total system coincide with any given forcing frequency. Such a resonant condition defines the worst that could happen to an equipment at that frequency. It would be of some interest to see how a vibration measurement which one might obtain in the field compares with this worst possible case.

A computer program which had been used at Lockheed for studying a 50-degree of-freedom representation of a missile was readily adapted to this new investigation. The vibration response at an output point near one end of the missile was calculated for a unit sinusoidal force near the other end. This is the transfer admittance plotted on Fig. 12 for no equipment at the output point. Then, it was assumed that an undamped equipment was fastened to the output point of the missile (which was damped to a Q of 25). The reactive admittance of the equipment was assumed to be equal and opposite

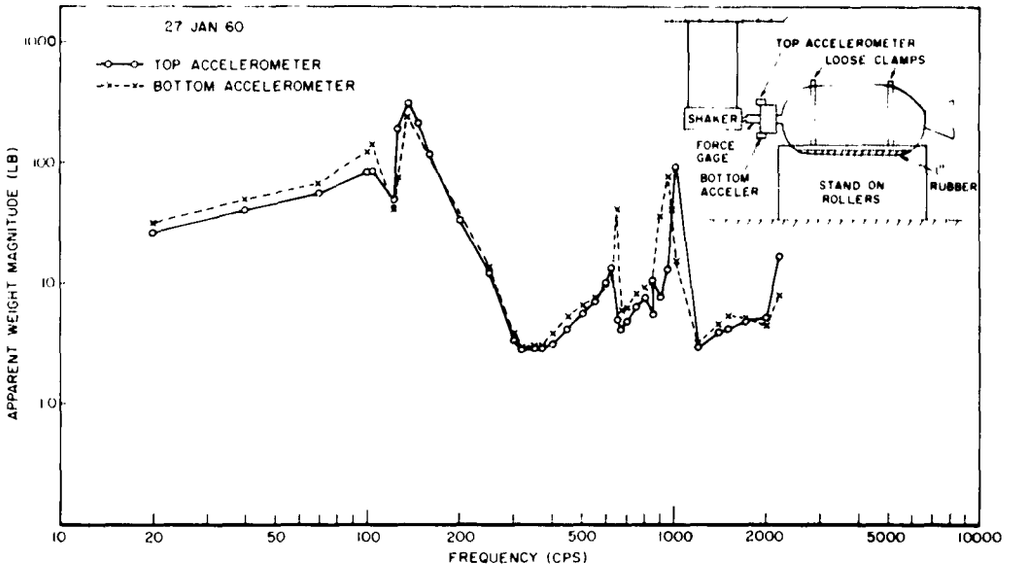

(a) Apparent Weight Magnitude

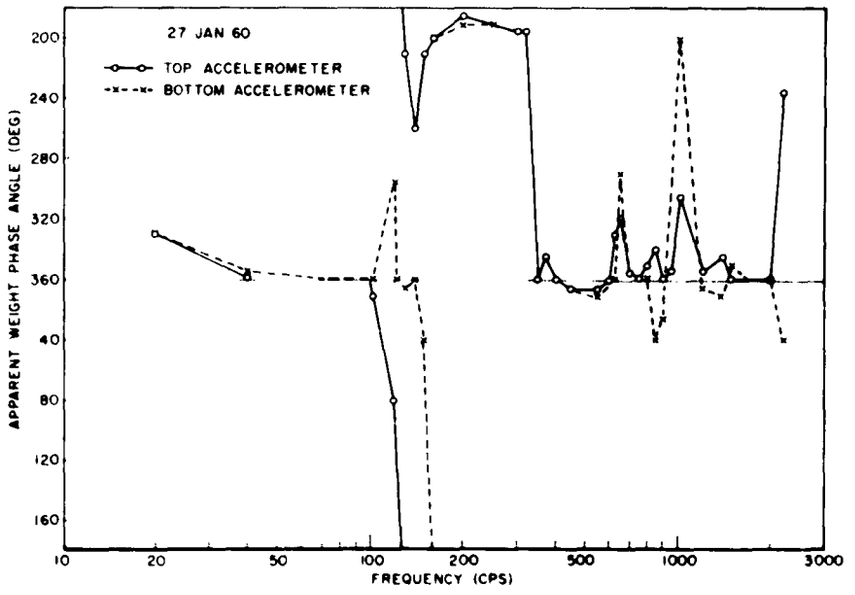

(b) Apparent Weight Phase Angle

Fig. 8 - Apparent weight of burned-out X-248 motor

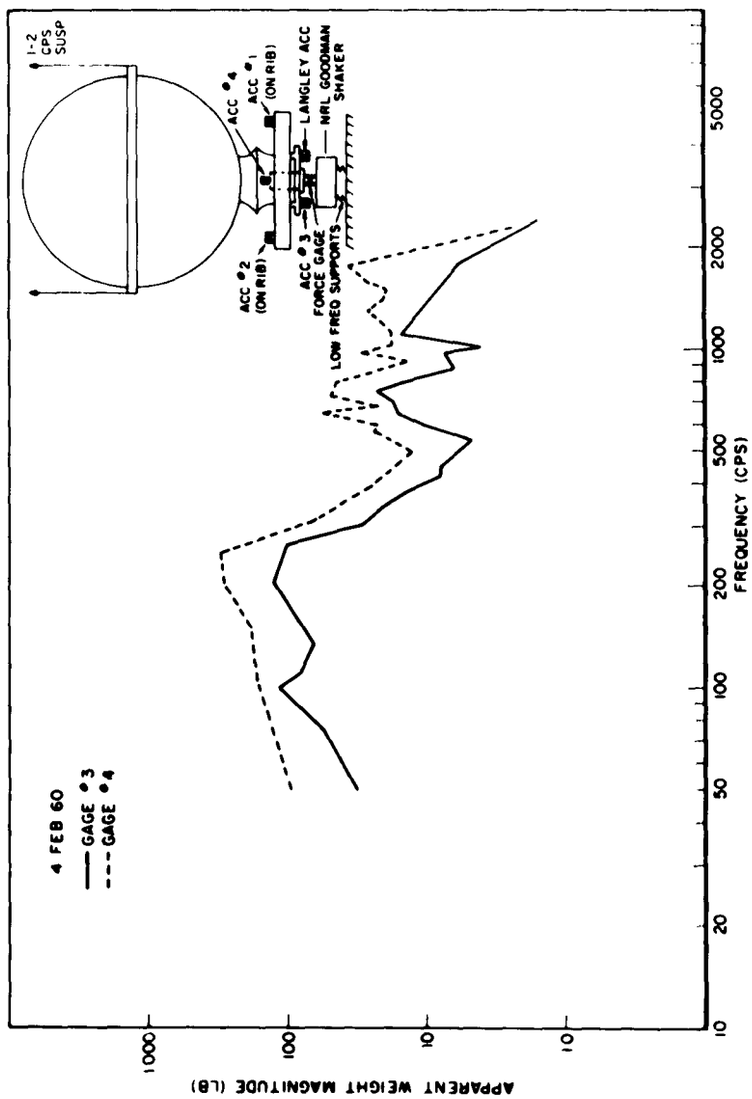

Fig. 9 - Driving-point, apparent-weight magnitude of shotput payload

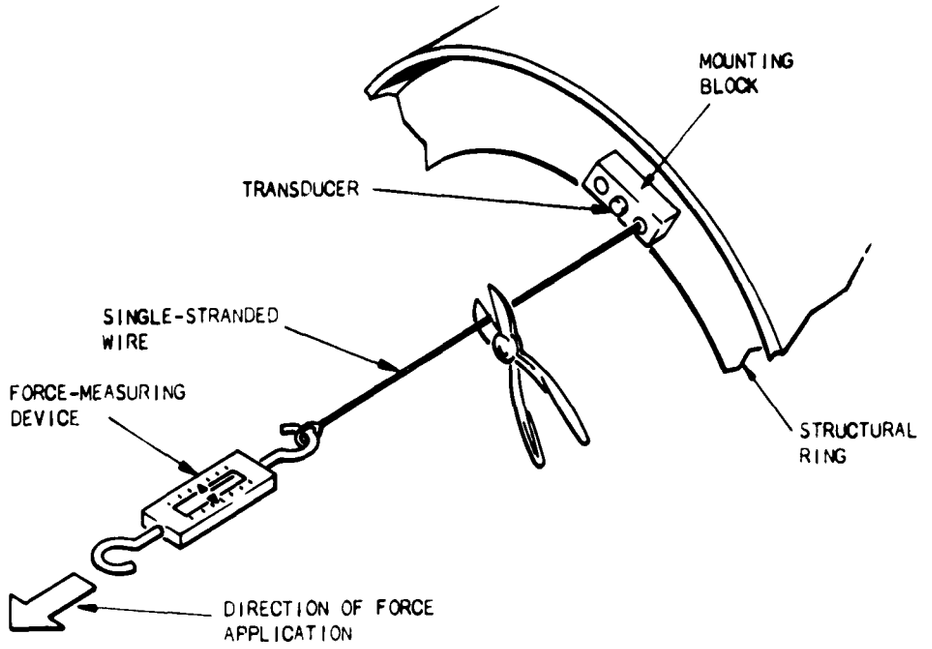

Fig. 10 - Schematic of cut-wire step force application

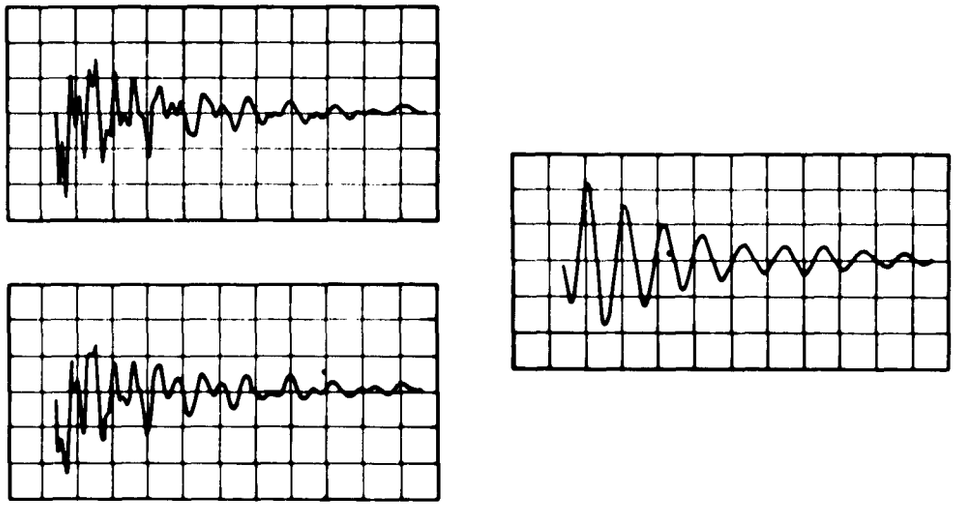

Fig. 11 - Typical transient responses of vibration transducers

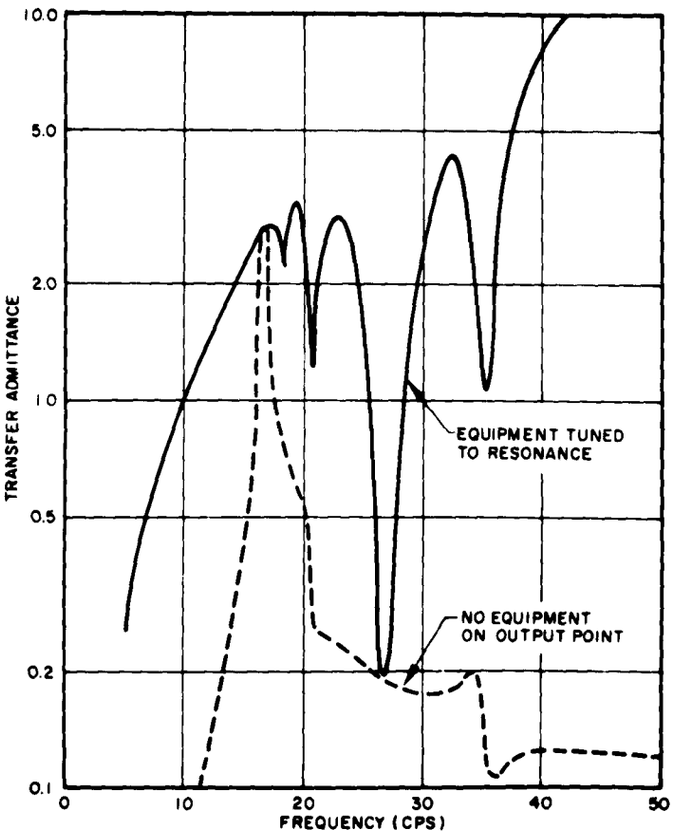

Fig. 12 - Theoretical transfer admittances through a missile structure

to that of the output point of the missile. This produced a resonant response of the system with amplitude limited only by the damping of the missile. The foundation response on Fig. 12 for this case of "Equipment Tuned to Resonance" shows an increase by a factor which often exceeds 10.

The acceleration input to the equipment is only half the story; the force input is also of interest. As a basis for comparison, we first computed the force which would act against an equipment which was an infinite rigid mass. The ratio of this "blocked force" to the input force is shown in Fig. 13. The force for an "Equipment Tuned to Resonance" is also plotted. The latter exceeds the blocked force by the same ratio as that for the admittance curves of Fig. 12. The resonant output force was often many times larger than the input force.

Curves of the type shown on Figs. 12 and 13 could be plotted from any measurement of vibration of a structure, if one also measured the resistive and the total admittances of the pickup location. The curves suggest how unconservative a given measurement could be in the worst circumstances.

This study by itself should not be regarded as conclusive. It was cited as an illustration of the sort of probing and questioning which we should be doing to establish a more reliable basis for shock and vibration practices.

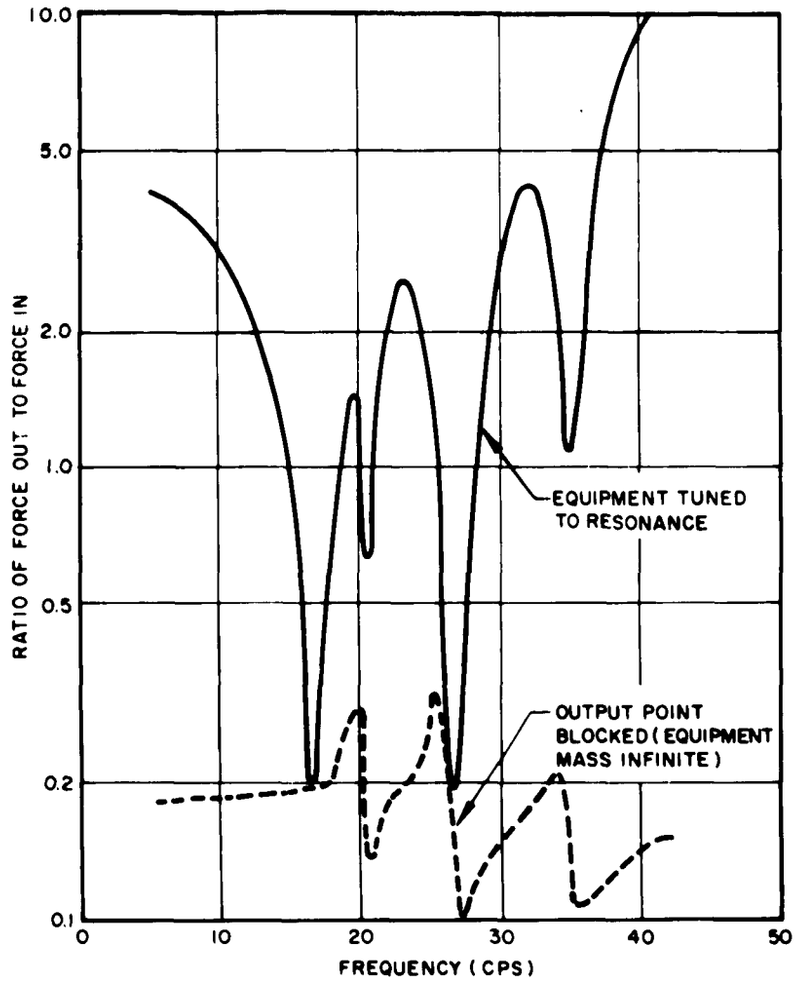

Fig. 13 - Theoretical force transmission through a missile structure

REFERENCES

[1] Electric Boat Division, "Phase IV Dynamic Behavior of a Foundation under Machine Excitation," Report TSD5-064, NOBS66253, April 1959.

[2] Electric Boat Division, "Phase III Dynamic Behavior of Foundations and Hull-Like Structures," Report P58-218, NOBS66253, December 1958.

[3] Arthur D. Little Company, "Experimental Investigation of Internal Mechanical Impedance of Machinery," Report C-60904, NOBS-72335, December 1958.

[4] A. O. Sykes, "Vibration Isolation when Machine and Foundation are Resilient and Wave Effects Occur in the Mounts," David Taylor Model Basin Report 1404, September 1960.

[5] D. V. Wright and A. C. Hagg, "Practical Calculation and Control of Vibration Transmission through Resilient Mounts and Basic Foundation Structures," Westinghouse Research Laboratories Report 405FD 208-R2, December 1, 1959, BuShips Contract NOBS72326.

[6] J. C. Snowdon, "Reduction of the Response to Vibration of Structures Possessing Finite Mechanical Impedance," University of Michigan Willow Run Laboratories, Report 2892-4-T, November 1959.

[7] R. E. Blake and R. O. Belsheim, "The Significance of Impedance in Shock and Vibration," ASME Colloquium on Mechanical Impedance Methods, ASME, 1959.

[8] R. O. Belsheim and R. E. Blake, "Effects of Equipment Dynamic Reaction on Shock Motion of Foundations," U. S. Naval Research Laboratory, Report 5009, October 1957.

[9] G. J. O'Hara, "Shock Spectra and Design Shock Spectra," U. S. Naval Research Laboratory, Report 5386, November 1959.

[10] R. E. Blake and T. Ringstrom, "The Influence of Mass and Damping on the Response of Equipment to Shock and Vibration," Shock Vibration and Associated Environments, Part IV. Office of the Secretary of Defense, August 1960.

[11] R. E. Blake, "The Need to Control the Output Impedance of Shock and Vibration Machines," Shock and Vibration Bulletin No. 23, Office of Secretary of Defense, June 1956, pp. 59-64.

[12] R. O. Belsheim and J. J. Harris, "Apparent Weight Measurements of Rocket Payload and Test Structures," Naval Research Laboratory Report 1099, December 1960.

DISCUSSION

Mr. Gertel (Allied Research): I just want to probe a little bit on the data that you presented on the experiments performed by the Arthur D. Little Company, showing transfer impedances which didn't match going forwards and backwards. Is it possible that if, perhaps, rotational impedance, say torques and rotational accelerations, were measured rather than the forces and translational accelerations, there might have been a better correlation? Was that the problem?

Mr. Blake: It seems possible to me. I haven't worked that out. But it is conceivable that there was some sort of rotational constraint offered by the impedance head, although I am not familiar with the apparatus.

Mr. Gertel: What I was thinking is that the picture showed the item of equipment mounted from bungee cords. Probably the elastic center was fairly central to the equipment, yet the forces were applied on a mounting foot which was eccentric to the elastic center of this bungee system. This suggests that the rotational motions were more strongly involved, or were at any rate present, in addition to the translational observations.

Mr. Blake: I don't think that I can add to your comment. I suspect that the flexible cord didn't play any part at this frequency. Theoretically, this theorem is supposed to be good regardless of whether there is translational motion present.

Mr. Gertel: It was just a thought. Now I had one other experience I wanted to relay about this go slow on impedance. Like Bob Plunkett, I'm in favor of impedance and I'm all for women and motherhood. We recently had a very strange experience. We had some damped elastomer on which we were making some impedance measurements. In plotting the forces and accelerations on impedance paper, we came out with a beautiful spring-like characteristic indicating no damping present whatsoever in this particular elastomer. As an additional check, we ran a conventional transmissibility test, where a mass was mounted on top of this elastomer and the input-output relationships were plotted. The mass involved was about 20 pounds and the frequency was about 60 cycles. We wound up with a transmissibility of 4-1/2, indicating that there was a considerable amount of damping present in this elastomer. The impedance equipment or the impedance-measuring experiment would have led us to believe that there was absolutely no damping in this particular item. It gave us a very weird, strange, misleading kind of result as the additional experiment showed. I just mention that to indicate that there are some subtle things, which I don't understand, which happened in this particular experiment. There are lots of subtle things happening in impedance work which some of us would like to learn more about.

Mr. Nutt (Whitworth Gloster Aircraft Ltd., England): In describing the experiment to determine the transmissibility from one point to another, you remarked that the possible explanation of the discrepancy was nonlinearity in the system and then went on to say that this was unusual. This is not our experience. We find that practically every structure, well in fact, if one wants to be a purist, every structure is nonlinear up to a point, but that most missile structures are nonlinear to a significant degree. Would you agree with this?

Mr. Blake: Yes, I'm afraid so. I'm optimistic about structures being linear but one experience of mine is that perhaps they are not. Our attempts to measure Polaris vibration in flight show a very bad scatter of successive measurements in successive flights for pickups at the same point. One possible explanation is that these missiles, off the same production line, are not in fact dynamically the same. Maybe there are subtle differences in the joints—I wish I knew. But that the missile is not linear is our best contender for an explanation.

Voice: About one year ago, we ran some impedance tests on an old vehicle. We were interested in the apparent mass, and I was really surprised that after we went through the first natural frequency, our apparent mass instead of 190 pounds with the fixture was only about 20 pounds. It really amazed me. The other thing I would like to ask you is if you have say a spent rocket case with some of the viscolastic material in there, would your curves on the impedance plot be shifted to the right or left as you would have in a nonlinear type vibration or would there be no effect at all on this?

Mr. Blake: You are asking the influence of some propellant inside?

Voice: That's right, because you have the viscolastic material acting as a nonlinear-type damping system.

Mr. Blake: I don't think I can answer your question.

Voice: Perhaps Dr. Belsheim may be able to answer that.

Mr. Blake: I believe his test was with a motor empty and full.

Dr. Belsheim: I had one empty and one full and there was quite a difference in the apparent weight looking into the motor in each of these two cases. Considerably more damping showed up apparently in the loaded motor, but this is rather inconclusive and I wouldn't want to say much more.

Mr. Blake: Surely if you were above what I will call the first natural frequency of the propellant, it could go either way.

* * *

APPLICATION OF MECHANICAL ADMITTANCE DATA TO THE SOLUTION OF A PRACTICAL PROBLEM

Roy W. Mustain
Nortronics Division, Northrop Corporation
Hawthorne, California

This paper describes the practical application of mechanical admittance (reciprocal of impedance) data to the numerical solution of a vibration isolation problem. The dynamic solution follows the methodology of the design procedure which was formulated by the SAE G-5 Aerospace Shock and Vibration Committee under the chairmanship of Dr. C. T. Molloy. The solution results in the selection of the most favorable vibration isolator to protect rigid equipment from dynamic excitations of a nonrigid supporting structure. The equipment mass, the fragility of the equipment, the free vibration of the supporting structure, and the mechanical admittance of the supporting structure are processed by techniques given in the G-5 Document, "Design of Vibration Isolation Systems." The solution is presented in steps and produces optima values of stiffness and damping for the selected vibration isolator. An envelope of transmissibility curves for all permitted system designs is established.

INTRODUCTION

The concepts and fundamentals of mechanical impedance which are essential to an understanding of this paper have been discussed and described adequately in the previous presentations of this session. The primary goal of the learned SAE G-5 Aerospace Shock and Vibration Committee has been the preparation of the document, "Design of Vibration Isolation Systems." The intent of this worthwhile G-5 Document is to provide the design engineer with the methodology necessary to select the optimum vibration isolation design through the application of mechanical impedance techniques.

Whereas the formulation of the design procedure and its supporting mathematical equations will be covered in the G-5 Document, the presentation of the procedure proper and the mathematics (especially derivations) will be minimized in this paper. However, formulations and procedural explanations will be given wherever needed for clarity of presentation.

This numerical solution will serve as a guide for engineers desiring to apply the design procedure of the document. This solution presents a practical application which determines whether vibration isolators are necessary to protect delicate airborne equipment. Then, if isolators are required, the solution provides data needed to select a satisfactory isolation system.

THE SAMPLE PROBLEM

A specific source receiver configuration has been selected for treatment in this numerical illustration. This practical application assumes (1) that the supporting structure is a nonrigid mass which is dynamically linear with resonant vibrational characteristics, (2) that the equipment behaves as rigid mass, (3) that the vibration isolators are linear massless spring-dashpot elements, (4) that there is mainly translational vibrations in each of three mutually perpendicular directions, and (5) that the susceptibility to failure of the equipment can be described by either random or sinusoidal fragility curves. The procedure is limited to the selection of center-of-gravity isolation systems [1].

Required Data

The weight of the equipment, the fragility levels of the equipment, the free vibration of the supporting structure, and the mechanical admittance of the supporting structure are required to adequately accomplish the solution of the problem. The weight of the equipment (W) in this example is 100 pounds. The fragility of the equipment $|U_f|$ is given in the accompanying graph (Fig. 1). Levels $|U_f|$ are displayed which can be expected to cause equipment failures. This graph also shows the free vibration of the supporting structure $|U_s|$, i.e., the vibration amplitudes which exist at the support points without the load of the equipment. The mechanical admittance of the supporting structure is given in Fig. 2. The mechanical admittance of the source is the ratio of the complex amplitude of velocity to the complex amplitude of sinusoidal force producing that velocity, both quantities being measured at the structural support of the equipment [2]. The mechanical admittance of the source, Y_s, is equal to $A_s + jB_s$ where A_s and jB_s are the real and imaginary parts of the admittance, respectively. The reciprocal of admittance is the mechanical impedance which is equal to $R_s + jX_s$ where R_s and jX_s are the real and imaginary parts of the mechanical impedance, respectively. At first the G-5 procedure was based on the utilization of mechanical impedance. However, it has been found advantageous to use the mechanical admittance because the isolator-source combination produced a modified source whose admittance is the sum of the admittance of the source and of the isolator [3].

The success of future dynamic progress depends on the utilization of mechanical impedance heads and force generators with improved recording media which provide accurate

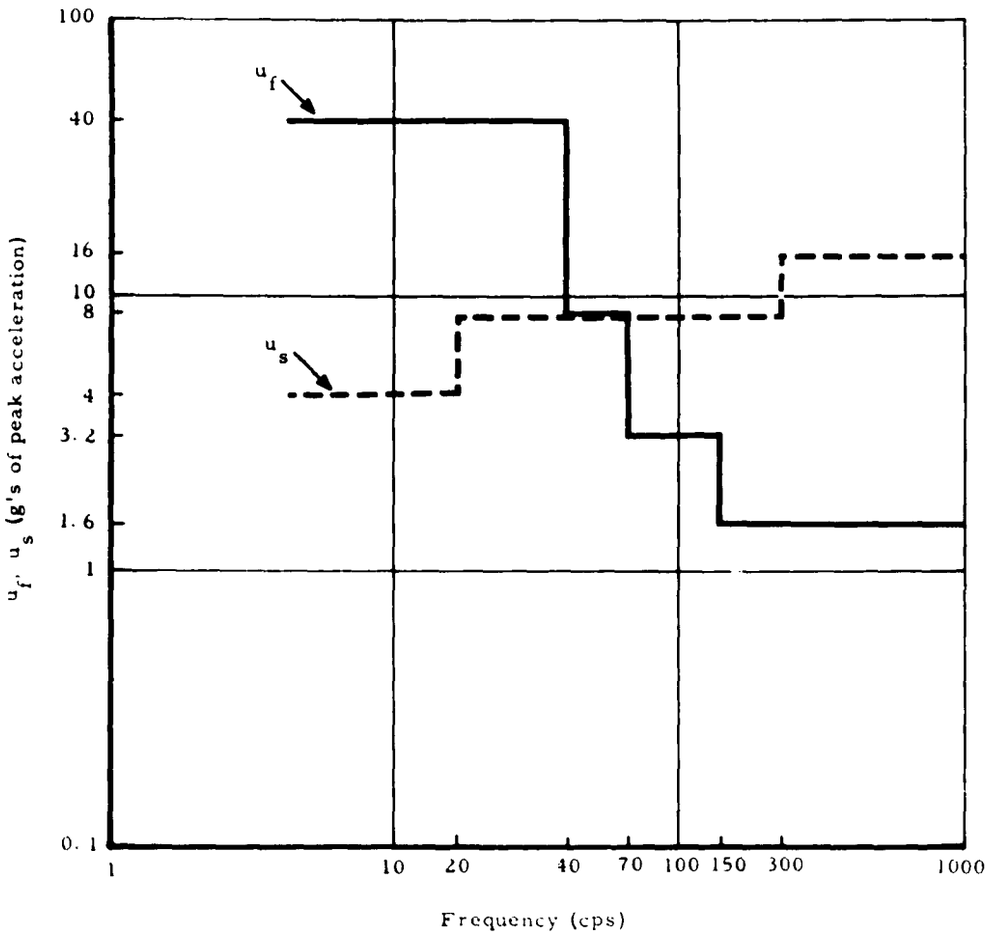

Fig. 1 - Plots of fragility amplitude and free-source amplitude

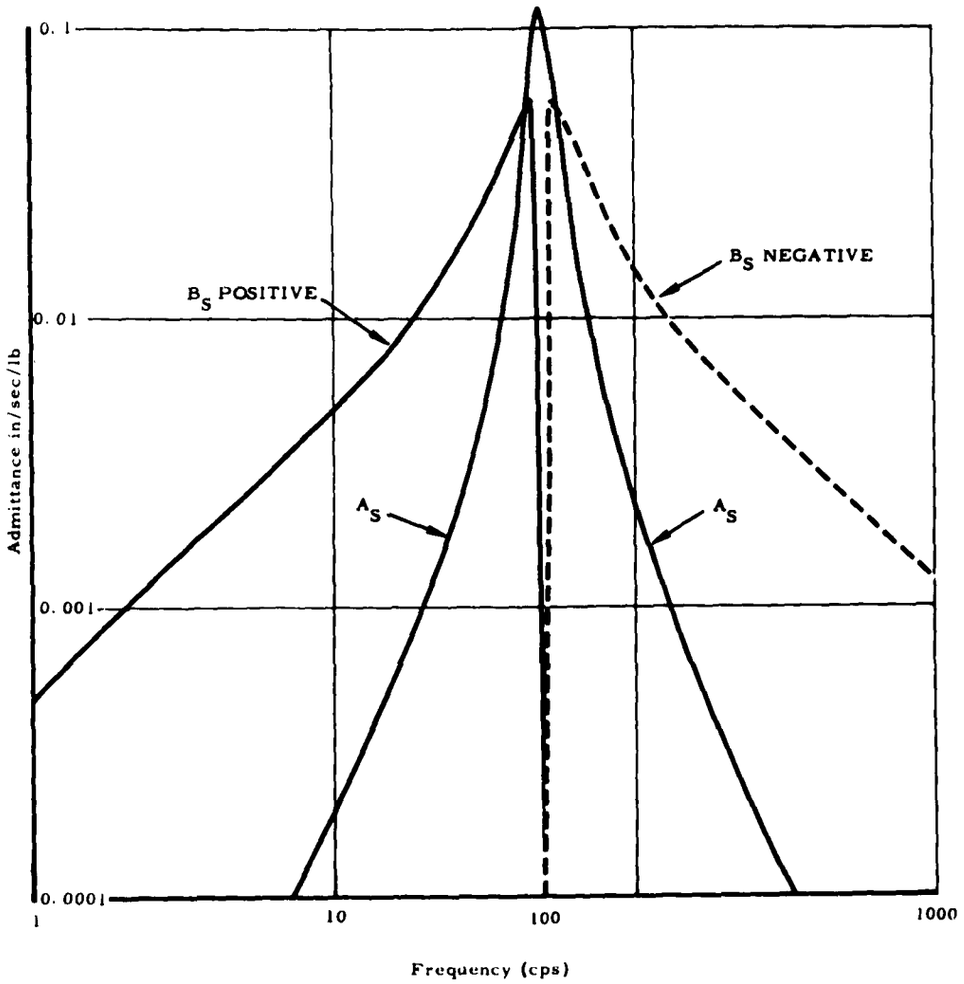

Fig. 2 - Mechanical admittance of supporting structure

measurements of force, motion, and phase relationships. The ideal instrumentation system will supply automatic plots of the real, A_s, and the imaginary, B_s, parts of the admittance as a function of frequency. Presently, no equipment has been devised to automatically plot the data as presented in Fig. 2. However, some systems are being developed that are very close to that stage. One system [4] being developed will automatically record the following data as a function of frequency: (1) the ratio of the acceleration amplitude to the force amplitude, and (2) the phase angle that the acceleration lags the force. The determination of the admittance amplitude, $|Y_s|$, can be accomplished by automatically plotting the ratio of (1) on special charts which show both the admittance amplitude, $|Y_s|$, and the ratio of (1) as a function of frequency. It then becomes a simple calculation to use the admittance amplitude, $|Y_s|$, and the phase angle, θ, to determine the real, A_s, and imaginary, B_s, parts of the admittance [4]:

$$A_s(f) = |Y_s(f)| \sin \theta \qquad (1)$$

$$B_s(f) = |Y_s(f)| \cos \theta \qquad (2)$$

Determination of the Need for Isolation

The first step in the procedure is the calculation and the plotting of the dimensionless admittances $\bar{A}_s$ and $\bar{B}_s$ as a function of frequency. This is accomplished by using the value of W (100 pounds) along with the real (A_s) and an imaginary (iB_s) values of the original

data given in Fig. 2. These data are inserted into the following equation from the procedure to obtain the dimensionless admittance $\bar{A}_s$ and $\bar{B}_s$:

The value of $2\pi/g$ is 1.62×10^{-2}.

$$\bar{A}_s(f) = \frac{2\pi Wf}{g} A_s(f) \quad (3)$$

$$\bar{B}_s(f) = \frac{2\pi Wf}{g} B_s(f) . \quad (4)$$

The values of $\bar{A}_s(f)$ and $\bar{B}_s(f)$ for this problem are shown in the log-log graph of Fig. 3. Distinction between the positive and negative values of $\bar{B}_s$ is made by plotting the positive values as a solid curve and the negative values as a dashed curve. Since $\bar{A}$ is always positive, the $\bar{A}_s$ curve is displayed as a solid line.

The next step in the procedure is the calculation and plotting of the maximum allowable transfer function, H_m. The G-5 procedure determines a criterion of maximum allowable transfer function, H_m, as an upper limit for the vibration of the equipment. This transfer function is given as [2]

$$H_{ms}(f) = \left| \frac{U_f(f)}{U_s(f)} \right| \quad (5)$$

for the sinusoidal case, and is given as

$$H_{mr}(f) = \sqrt{\frac{S(u_f)}{S(u_s)}} \quad (6)$$

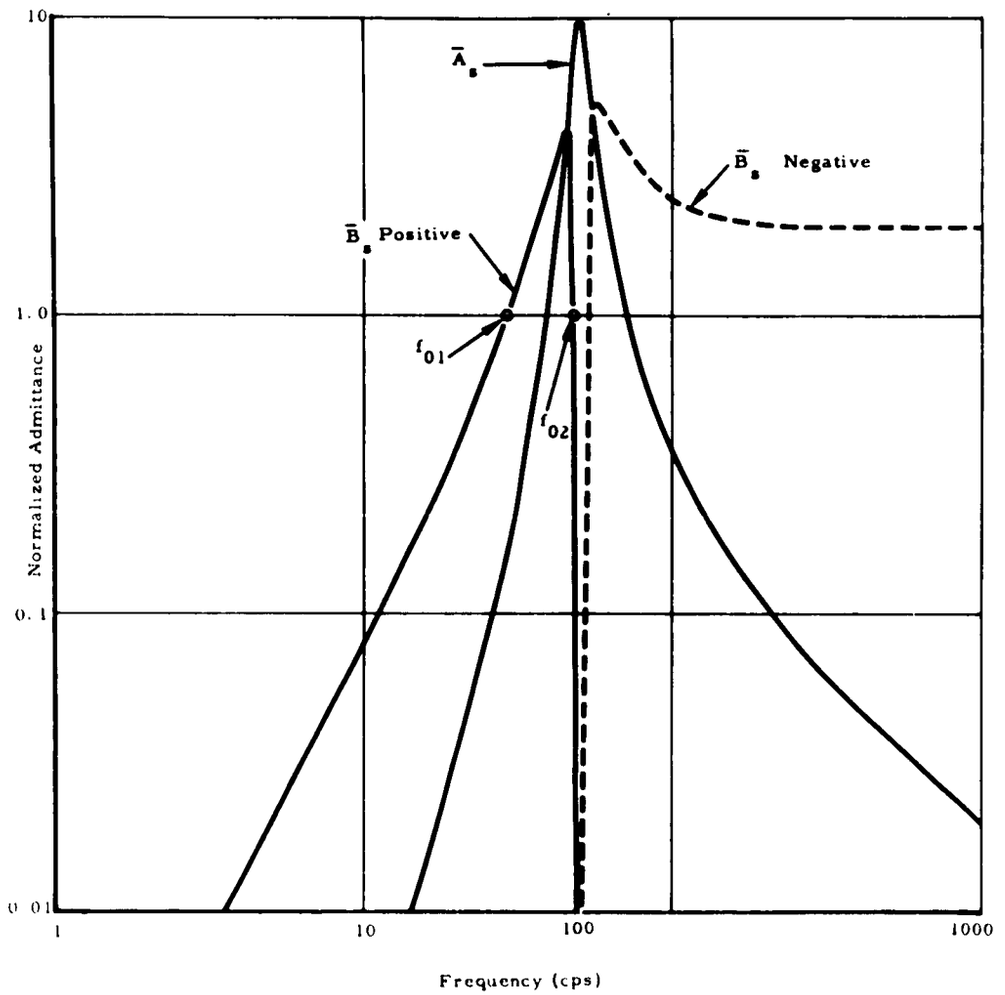

Fig. 3 - Normalized mechanical admittance of supporting structure

for the random case. Where

U_s is the complex amplitude of sinusoidal input displacement expressing the fragility limit of the equipment, inches.

U_f is the complex amplitude of sinusoidal output displacement of the unloaded source vibration, inches.

$S(u_f)$ is the spectral density displacement which the equipment can withstand as a function of frequency, in.^{2}/cps.

$S(u_s)$ is the spectral density displacement of the unloaded source, in.^{2}/cps.

The fragility of the equipment and the free vibration of the source may be expressed also in terms of velocity or acceleration provided that the same units are used consistently in the above equations. The data from Fig. 1 are used to compute H_m for this sample numerical solution. The calculated values of H_m for each frequency are displayed in Fig. 4. Cross-hatching lines have been placed above the H_m curve to show that the curve is an upper limit. The lower frequency limit of H_m is designated f' and the upper frequency limit is designated f". The frequency range f' to f" is the range within which all succeeding transmissibility or transfer function curves are to be plotted. In this problem f' is 5 cps and f" is 1000 cps.

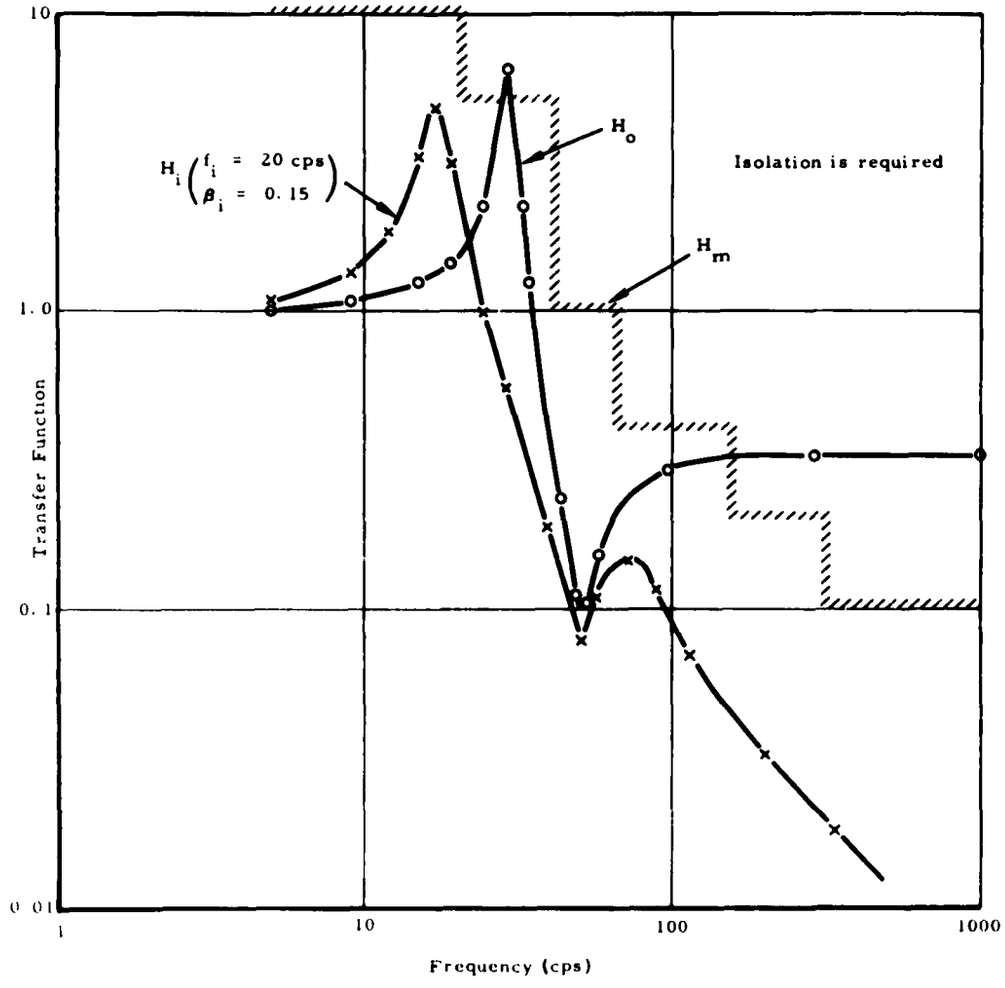

Fig. 4 - Plots of H transfer function

Another transfer function, H_o, is calculated and added to Fig. 4. H_o is defined to be the absolute value of the ratio of the velocity of the load mass to the free velocity of the source when the mass is attached directly to the source:

$$H_o(\omega) = \left| \frac{\dot{U}_o(\omega)}{\dot{U}_s(\omega)} \right| . \quad (7)$$

Since

$$\frac{\dot{U}_o(\omega)}{\dot{U}_s(\omega)} = \frac{1}{1 + i\omega m Y_s(\omega)} , \quad (8)$$

$H_o(\omega)$ can be equated to:

$$\left(\left[1 - m\omega B_s(\omega) \right]^2 + \left[m\omega A_s(\omega) \right]^2 \right)^{-1/2} . \quad (9)$$

Applying the relationships of Eqs. (3) and (4), the transfer function $H_o(\omega)$ becomes [2]:

$$\left(H_o(\omega) = \left[1 - \bar{B}_s(\omega) \right]^2 + \left[\bar{A}_s(\omega) \right]^2 \right)^{-1/2} . \quad (10)$$

The H_o curve is found by using data in Fig. 3 and by filling in Tables 1 and 2. First, the peaks of H_o are determined by inspection of Fig. 3. The peaks and valleys of H_o are located at or near the frequencies where $\bar{B}_s(f)$ equals one. Therefore, these frequencies occur at the intersection of the $\bar{B}_s$ positive curve with the ordinate value of 1.0. The points for this problem are shown in Fig. 3. The lowest frequency intersection (29 cps) is labeled as f_{01} and the next intersection (48 cps) is labeled f_{02}. The other intersections need not be labeled. Since $\bar{A}_s$ is a relatively small value at f_{01}, the f_{01}

TABLE 1
Determination of Frequencies for Transfer Function Calculations

$f' = \underline{5}$ cps $\qquad$ $f'' = \underline{1000}$ cps

	Multiples of Center Column					PEAKS and VALLEYS	Multiples of Center Column				
	0.1	0.3	0.5	0.7	0.9		1.1	1.4	2	6	50
H_o	53	9	15	20	26	$f_{01} = 29$	32	~~41~~			
H_o				34	43	$f_{02} = 48$	53	67	196	288	1000
H_i		5	9	12	15	17	19	24	~~34~~		
H_i, $f_i = 20$ cps			28	39	50	56	62	78	112	336	1000

TABLE 2
Calculation of H_o

① f (cps)	② $\bar{A}_s$	③ $\bar{B}_s$	④ $\lvert 1 - ③ \rvert$	⑤ $④^2$	⑥ $②^2$	⑦ ⑤+⑥	⑧ $1/\sqrt{⑦}$ H_o
5	0	0.0200	0.980	0.960	0	0.960	1.02
9	0	0.066	0.934	0.872	0	0.872	1.07
15	0.0122	0.187	0.813	0.660	0.000	0.660	1.23
19	0.0290	0.315	0.685	0.469	0.001	0.470	1.46
24	0.068	0.560	0.440	0.194	0.005	0.199	2.24
✓ 29	0.155	———	0	0			6.43
32	0.280	1.33	0.33	0.109	0.078	0.187	2.31
34	0.440	1.67	0.67	0.449	0.194	0.643	1.25
43	2.50	3.80	2.80	7.84	6.25	14.09	0.266
✓ 48	9.0	———	0				0.111
53	8.0	-4.7	5.7	32.5	64	96.5	0.102
67	4.4	-3.95	4.95	24.5	19.4	43.9	0.151
196	0.39	-2.4	3.4	11.6	0.15	11.8	0.2911
288	0.068	-2.	3.	9.	0.00	9.00	0.33
1000	0.0200	-2.	3.	9.	0.00	9.00	0.33

intersection represents a peak in the H_o curve and since $\bar{A}_s$ is relatively high at f_{02}, the f_{02} intersection represents a valley [1]. The methodology of the G-5 procedure is followed to determine the minimum number of points necessary to properly define the H_o curve. It is shown in the procedure that the transfer function curve for a single peak or valley is satisfactorily determined by values at frequencies which are the following multiples of the frequency at which the peak or valley occurs: 0.1, 0.3, 0.5, 0.7, 0.9, 1.0, 1.1, 1.4, 2, 6, 50. These multiples have been computed for this sample problem and are listed in Table 1. The values of f_{01} (29 cps) and f_{02} (48 cps) are entered in the center column of Table 1, with the smallest value being listed first. Entries were made to the left of f_{01} and the lowest multiple of 0.1 was deleted and replaced by the value of f' which is to equal to 5 cps. Then entries were made to the right of f_{02} and the highest multiple was deleted and replaced by f''. Since the ratio of f_{01}/f_{02} is less than 0.75, the following procedure [1] was used to fill in the H_o points of Table 1: successive entries were made — 1.1 f_{01} to the right, 0.9 f_{02} to the left, 1.4 f_{01} to the right, 0.7 f_{02} to the left. At this point the frequency multiples crossed and the last entry on the right (41) was deleted.

The frequencies determined in Table 1 for the H_o curve are used in Table 2 to compute Eq. (11) from the procedure:

$$H_o(f) = \left(\left[1 - \bar{B}_s(f)\right]^2 + \left[\bar{A}_s(f)\right]^2\right)^{-1/2}. \quad (11)$$

Table 2 which is taken from the procedure is a convenient form for efficiently computing values of H_o. The frequencies found in Table 1 are entered into column 1 of Table 2 with the lowest frequency at the top of the column. The check marks to the left of column 1 indicate frequencies which represent actual intersections. For these two frequencies (29 and 48 cps) a zero has been entered in column 4 and a horizontal line has been entered in column 3 since it is not needed. Values of $\bar{A}_s$ and $\bar{B}_s$ taken from Fig. 3 are listed in columns 2 and 3, respectively. Negative signs have been included wherever applicable for values of $\bar{B}_s$. Zeroes have been entered for values of $\bar{A}_s$ and $\bar{B}_s$ which are less than 0.01. The computations indicated in columns 4 through 8 are straightforward and yield the H_o curve. The values in column 8 are equal to H_o.

The H_o data for this example are displayed in Fig. 4 for comparison with the H_m curve. The peak of the H_o curve is labeled f_{01} (29 cps) and the valley is labeled f_{02} (48 cps).

Whereas the peak, f_{01}, of the H_o curve exceeds the upper bound of H_m and H_o exceeds H_m above 150 cps, vibration isolation is required and this sample problem is continued to determine a satisfactory isolation system.

Determination of a Minimum Natural Frequency for the Isolation System

The definition of an adequate isolation system requires the determination of a range of acceptable natural frequencies. The lower limit of the frequencies corresponds to a minimum stiffness for the isolators and is a function of (1) the maximum permitted displacement, U_{max}, across the isolators and (2) the available sway space in the particular installation [1]. The maximum permitted displacement, U_{max}, of the equipment relative to its static position, for this problem is given as 1 inch and the largest peak acceleration of the supporting structure, a_{max}, is given as 10 g. This information is used in Eq. (12) to find f_{min} [1]:

$$f_{min} = 3.13\sqrt{\frac{a_{max}}{U_{max}}} = 9.9 \text{ cps}. \quad (12)$$

Determination of the Region of Permissible Damping and Natural Frequency Parameters for the First Peak in the Transfer Function which Considers Isolators and Structural Admittance

An approximation to the transfer function, H_i, of the desirable isolation system is provided by the family of classical transmissibility curves of Fig. 5. Figure 5, in the form of an overlay, is placed on Fig. 4 of this problem to establish approximate damping values for the first peak in the transfer function, H_i, of the equipment-isolator combination. The ordinate of H equal to one for the overlay is juxtapositioned on the H equals one ordinate of Fig. 4. With this juxtaposition maintained, the overlay is moved laterally on Fig. 4. The frequency range above f_{02} is ignored during this overlay estimation. The overlay is adjusted so that f_{n1} equals f_{min}. The largest and smallest values of β in Fig. 5 (in the range from 0.01 to 0.5) for which all of the corresponding curve in Fig. 5 lies below H_m in the frequency range below f_{02} are noted. The extreme values of β at the frequency f_{min} are plotted on Fig. 6. These 0.5 and 0.05 β are indicated as points 1 and 2, respectively.

Additional usage of the overlay is required to further define the approximate region of

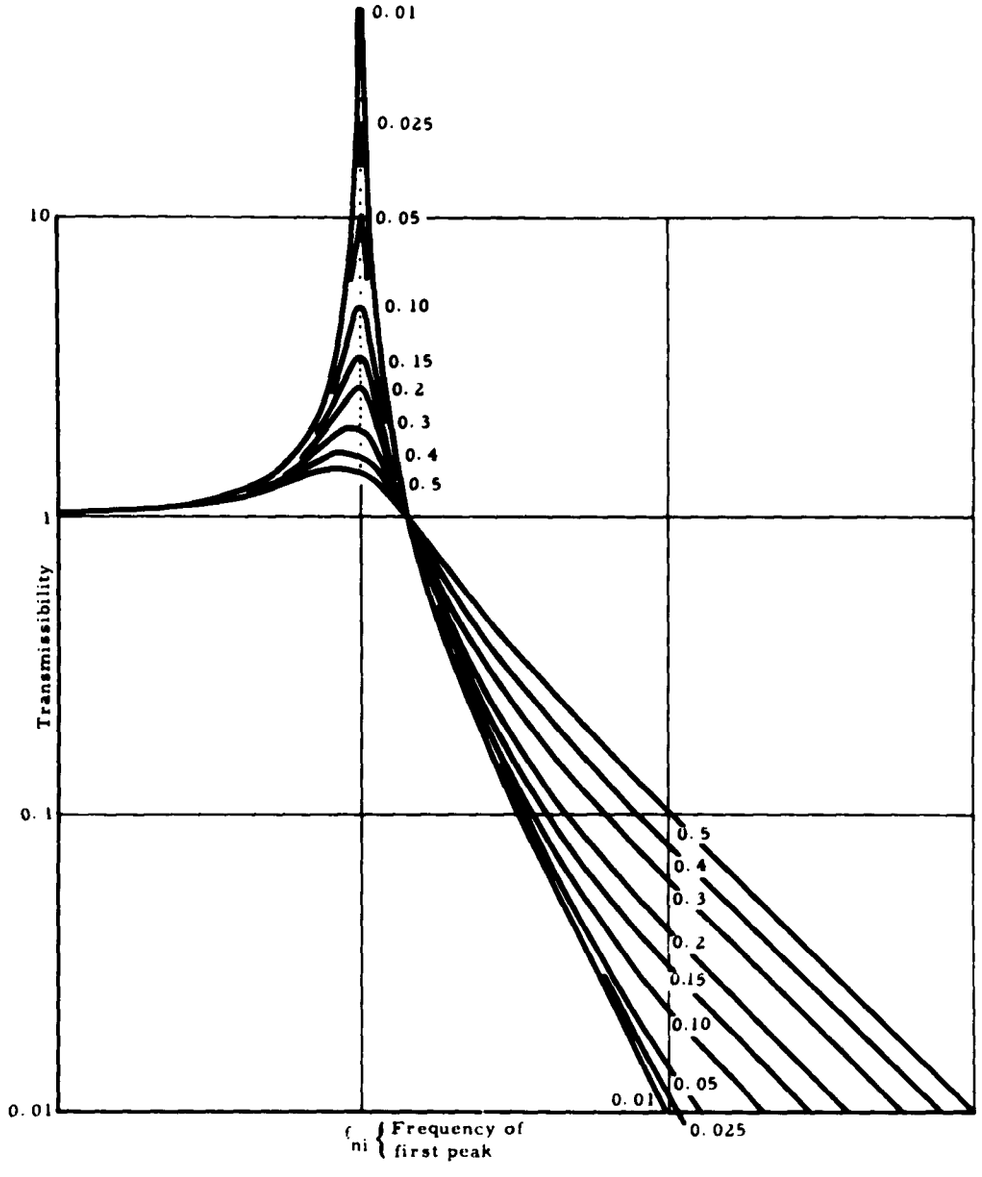

Fig. 5 - Family of curves approximating the transmissibility achieved at low frequencies when isolators are placed between the equipment and the supporting structure

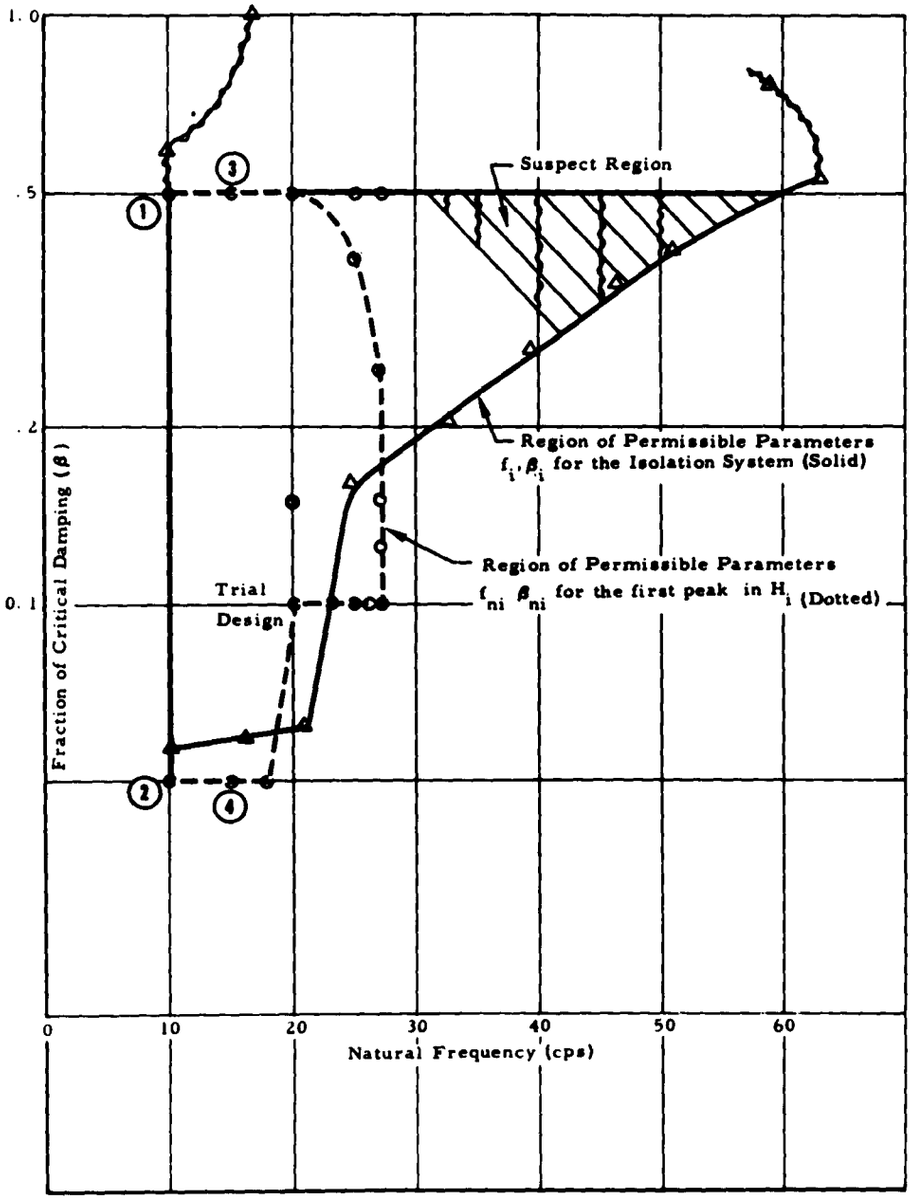

Fig. 6 - Regions of permissible natural frequency and damping parameters

TABLE 3
Limiting Values of β_{n1}

$$\beta_{n1(max)} = 1/2\sqrt{\frac{1}{\bar{B}_s(f_{n1})} - 1}$$

$$D_{n1} \text{ at } \beta_{n1(min)} = \bar{A}_s(f_{n1})$$

① f_{n1} (cps)	② $\bar{B}_s(f_{n1})$	③ 1/2	④ ③ - 1	⑤ $\sqrt{④}/2$ $\beta_{n1(max)}$	⑥ $\bar{A}_s(f_{n1})$	⑦ $\beta_{n1(min)}$
10	0.081	12.4	11.4	1.68	0	<0.01
15	0.185	5.40	4.40	1.05	0.012	<0.01
18	0.277	3.61	2.61	0.81	0.024	0.012
20	0.353	2.74	1.74	0.66	0.035	0.018
25	0.625	1.60	0.60	0.387	0.077	0.040
27	0.799	1.25	0.25	0.250	0.130	0.067

permissible damping for the first peak. Figure 5 is adjusted again so that f_{n1} coincides with a frequency that is 5 cps higher than f_{min} or until a frequency is encountered wherein there is a noticeable change in one of the extreme values of β_{n1}, whichever occurs first. Once more, the largest and smallest values of β are noted and plotted on Fig. 6. These values are shown by points 3 and 4, respectively, on Fig. 6. This process is continued until a frequency is reached wherein no transmissibility curve, for any of the β values, falls below H_m or until $f_{n1} = 0.9\ f_{01}$, whichever occurs first.

Now that extreme values of β for a range of f_{n1} values have been determined and plotted in Fig. 6, the next step is to correct this region by using Table 3 to obtain limiting values of β_{n1}. The β_{n1} values must lie between a maximum value $\beta_{n1(max)}$ and a minimum value $\beta_{n1(min)}$ in order that the damping be obtainable by spring-dashpot isolators. Equations (13), (14), and (15) which are taken from the procedure are used to define the limits for the maximum and minimum damping at each distinct value of f_{n1}. Table 3 provides a convenient and efficient form for computing Eqs. (13) and (14). The maximum limit at each f_{n1} frequency is defined by Eq. (13):

$$\beta_{n1(max)} = \frac{1}{2}\sqrt{\frac{1}{\bar{B}_s(f_{n1})} - 1}\ . \qquad (13)$$

Equation (14) gives the expression for a dimensionless parameter D_{n1} when β_{n1} is at minimum

$$D_{n1} \text{ at } \beta_{n1(min)} = \frac{2\beta_{n1(min)}}{1 + 4\beta^2_{n1(min)}} = \bar{A}_s(f_{n1}). \qquad (14)$$

where

$$D(\beta_i,\ f/f_i) = \frac{2\beta_i (f_i/f)}{(f_i/f)^2 + 4\beta_i^2}\ . \qquad (15)$$

and is displayed graphically in Fig. 7 which is taken from the procedure. Figure 7 presents a family of curves of $D(\beta_i,\ f/f_i)$ versus f/f_i for constant values of β_i. Thus, having established $\bar{A}_s(f_{n1})$ values which are equal to D_{n1} at β_{n1} (min), it is easy to obtain the β_{n1} (min) values graphically from Fig. 7. The values of f_{n1} (10, 15, 18, etc.) for this problem are listed in column 1 of Table 3. Corresponding values of $\bar{B}_s(f_{n1})$ and $\bar{A}_s(f_{n1})$ which are taken from Fig. 3 of this problem are shown in columns 2 and 6, respectively, of Table 3. Using the input data of column 2, the straightforward calculations of columns 3, 4, and 5 are completed to yield $\beta_{n1(max)}$ values which are equal to

$$\frac{1}{2}\sqrt{\frac{1}{\bar{B}_s(f_{n1})} - 1}$$

of Eq. (13).

The input data, $\bar{A}_s(f_{n1})$, of column 6 are equivalent to values of Eq. (14) and are used to enter Fig. 7 to obtain the values of $\beta_{n1(min)}$ in column 7. The $\beta_{n1(min)}$ values of column 7 are obtained from Fig. 7 by using $D = D_{n1} = \bar{A}_s(f_{n1})$ and f/f_i is equal to 1. Therefore, the ordinate of Fig. 7 is entered with the values of $\bar{A}_s(f_{n1})$ from column 6 of Table 3 and the abscissa is entered only at f/f_i equal to 1. The data in columns 5 and 7 are compared with the β_{n1} extremes previously plotted on Fig. 6. The β_{n1} points which are outside of the limits defined by columns 5 and 7 of Table 3 must be

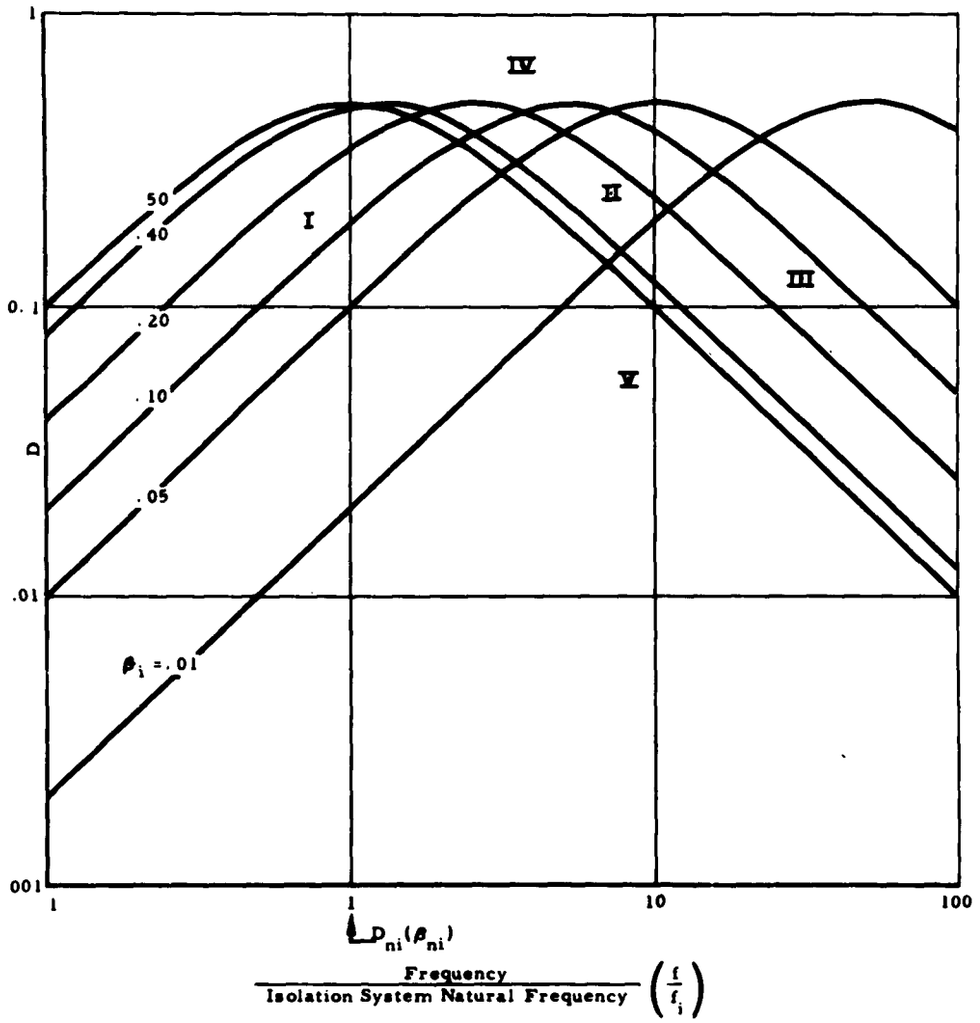

Fig. 7 - Plot of $D(\beta_i, f/f_i)$ versus f/f_i for constant β_i

$$D(\beta_i, f/f_i) = \frac{2\beta_i (f_i/f)}{(f_i/f)^2 + 4\beta_i^2}$$

changed to equal the value at the nearest limit. These changes are shown on Fig. 6 where the original β_{n1} points at 25 and 27 cps have been crossed out and lowered to match the $\beta_{n1\,(max)}$ points of column 5 at 25 and 27 cps. These newer points at 25 and 27 cps are 0.387 and 0.35, respectively.

The points in Fig. 6 which were established in the above steps are connected by dashed lines in Fig. 6. This area is labeled the "Region of Permissible Parameters f_{n1}, β_{n1} for the first peak of H."

Determination of the Region of Permissible Damping (β_i) and Natural Frequency (f_i) Parameters for the Equipment-Isolator System

The isolator/source parameters f_{n1} and β_{n1} for the range of low frequencies from f_{min} to f_{02} were established in the previous section. Now in this section, these same parameters, f_{n1} and β_{n1}, are used to obtain the required isolator parameters f_i and β_i. Data from Section 4 are entered into Table 4 to compute Eqs. (16), (17), (18), and (19) which are also given in the procedure. First, values of f_{n1} and their corresponding values of β_{n1} for this sample exercise are taken from Fig. 6 and entered into columns 1 and 2 of Table 4. Two values of β_{n1} are entered in column 2 for each f_{n1} frequency. For example, Fig. 6 shows β_{n1} equal to 0.5 and 0.05 at 10 cps. This is shown in column 2 of Table 4 wherein a double entry is made for the β_{n1} values at 10 cps. Two asterisks are noted in column 2 to indicate that two values of β_{n1}, 0.387 at 25 cps and 0.25 at 27 cps, were determined in Table 3 as maximum values of β_{n1}. Column 3 of Table 4 displays values of D_{n1} which are taken from Fig. 7 of the procedure. The D_{n1} values are found by entering Fig. 7 with f/f_i equal to 1 and with β_i equal to β_{n1} as listed in column 2 of Table 4. Column 4 contains values of $\bar{A}_s(f_{n1})$ which are taken from Fig. 3 of this problem. The value of $\bar{A}_s$ for 10 cps is less than 0.01 and, in agreement with the procedure, is entered as a zero in column 4. Column 5 is equivalent to column 3 minus column 4 and thus, column 5 satisfies Eq. (16). For column 5 is equal to:

$$\bar{A}_i(f_{n1}) = D_{n1} - \bar{A}_s(f_{n1}). \qquad (16)$$

Column 6 of Table 4 yields $D_{n1}/2\beta_{n1}$ values which are part of Eq. (17):

$$\bar{B}_i(f_{n1}) = \frac{D_{n1}}{2\beta_{n1}} - \bar{B}_s(f_{n1}). \qquad (17)$$

Column 6 values are obtained by dividing column 3 values by twice the β_{n1} values given in column 2. Values of $\bar{B}_s(f_{n1})$ which are taken from Fig. 3 are shown in column 7. Finally, the $\bar{B}_i(f_{n1})$ values for Eq. (17) are established in column 8 by subtracting column 7 values from column 6 values. This subtraction is the same as

$$\frac{D_{n1}}{2\beta_{n1}} - \bar{B}_s(f_{n1}). \qquad (17)$$

At this point in this section, required admittance parameters, $\bar{A}_i$ and $\bar{B}_i$, of the isolators have been found and are listed in columns 5 and 8, respectively. Table 4 calculations will be continued to determine f_i and β_i by completing Eqs. (18) and (19) of the procedure:

$$f_i = \sqrt{\frac{\bar{B}_i(f_{n1})}{\bar{A}_i^2(f_{n1}) + \bar{B}_i^2(f_{n1})}}\, f_{n1} \qquad (18)$$

$$\beta_i = \frac{1}{2}\,\frac{f_i}{f_{n1}}\,\frac{\bar{A}_i(f_{n1})}{\bar{B}_i(f_{n1})}. \qquad (19)$$

The $\bar{A}_i^2(f_{n1})$ and $\bar{B}_i^2(f_{n1})$ values needed under the radical sign of Eq. (18) are computed and listed in columns 9 and 10, respectively. Then these two columns are added and tabulated in column 11. Following this, the $\bar{B}_i$ values of column 8 are divided by the sums of A_i^2 and B_i^2 which are found in column 11. These quotients are placed in column 12 and are equivalent to the quantities under the radical sign. Next, the square roots of these quantities are found and listed in column 13. The values in column 13 are multiplied by f_{n1} values taken from column 1. In turn, these products are listed in column 14 and they represent the values of Eq. (18) which are equal to f_i. The last column, 15, of Table 4 is determined by inserting values from columns 14, 5, 1, and 8 into Eq. (19) as follows:

$$\beta_i = \frac{1}{2}\,\frac{f_i}{f_{n1}}\,\frac{\bar{A}_i(f_{n1})}{\bar{B}_i(f_{n1})}$$

$$= \frac{1 \times (\text{column } 14) \times (\text{column } 5)}{2 \times (\text{column } 1) \times (\text{column } 8)}. \qquad (19)$$

These computations complete Table 4 and establish the required parameters, f_i and β_i, at low frequencies for the isolators. The data from columns 14 and 15 are plotted on Fig. 6 of the problem. The high values of β_i (1.701, 1.25, and ∞) fall outside the limits of the figure and are simply ignored. A horizontal line is drawn at $\beta = 0.5$, since this value represents an upper-boundary limitation to practical

TABLE 4

Boundary Values of f_i, β_i Combinations

① f_{n1} (cps)	② β_{n1}	③ D_{n1}	④ $\bar{A}_s$	⑤ ③-④ $\bar{A}_i$	⑥ ③/2②	⑦ $\bar{B}_s$	⑧ ⑥-⑦ $\bar{B}_i$	⑨$_2$ ⑤	⑩$_2$ ⑧	⑪ ⑨+⑩	⑫ ⑧/⑪	⑬ $\sqrt{⑫}$	⑭ ①·⑬ f_i	⑮ ⑭⑤/2①⑧ β_i
10	0.5	0.500	0	0.500	0.500	0.081	0.419	0.250	0.176	0.426	0.982	0.99	9.9	0.59
	0.05	0.100		0.100	1.00		0.919	0.010	0.845	0.855	1.06	1.03	10.3	0.056
15	0.5	0.500	0.012	0.488	0.500	0.185	0.315	0.239	0.099	0.338	0.993	0.962	14.4	0.743
	0.05	0.100		0.088	1.00		0.815	0.008	0.663	0.671	1.21	1.10	16.5	0.059
18	0.5	0.500	0.024	0.476	0.500	0.277	0.223	0.226	0.050	0.276	0.808	0.903	17.0	1.01
	0.05	0.100		0.076	1.00		0.723	0.006	0.525	0.531	1.36	1.165	21.1	0.062
20	0.5	0.500	0.035	0.465	0.500	0.353	0.147	0.216	0.022	0.238	0.620	0.788	15.8	1.25
	0.10	0.192		0.157	0.960		0.607	0.025	0.368	0.393	1.54	1.24	24.8	0.161
25	0.387*	——	0.077	——	——	0.625	0	——	——	——	——	——	0	∞
	0.10	0.192		0.115	0.960		0.335	0.013	0.112	0.125	2.48	1.575	39.4	0.271
27	0.25*	——	0.110	——	——	0.780	0	——	——	——	——	——	0	∞
	0.10	0.192		0.082	0.960		0.180	0.0007	0.0324	0.033	5.46	2.34	63.0	0.531
† 23	0.10	0.192	0.058	0.134	0.960	0.500	0.460	0.018	0.211	0.229	2.01	1.42	32.6	0.206
† 19	0.07	0.138	0.029	0.109	0.987	0.315	0.672	0.012	0.454	0.466	1.44	1.20	22.8	0.097
† 27	0.125	0.238	0.130	0.108	0.952	0.799	0.153	0.012	0.023	0.035	4.38	2.09	59.0	0.77
	0.15	0.280		0.150	0.933		0.134	0.023	0.018	0.051	2.63	1.62	43.6	0.902
† 26	0.10	0.192	0.090	0.102	0.960	0.700	0.260	0.010	0.068	0.078	3.33	1.78	46.3	0.349
† 26.5	0.10	0.192	0.096	0.096	0.960	730	0.230	0.009	0.053	0.062	3.71	1.925	51.0	0.401

† Additional points needed to define the region of permissible f_i, β_i.

isolation system designs. The area below this practical level is labeled the "Region of Permissible Parameters f_i, β_i for the Isolation System."

Investigation of the Transfer Function, $H_i(f)$, at the Higher Frequencies

Whereas the isolator parameters f_i and β_i found in the above section have ignored frequencies above f_{02}, it becomes necessary to extend this investigation to include the higher frequencies. In this section, the possibility of the isolator transfer function exceeding H_m, the maximum allowable transfer function, will be determined. The area where trouble may be encountered and where this possibility exists is described as the "suspect" region. The transfer function of an isolator system is given in the procedure as:

$$H_i(f) = \left(\left[1 - \bar{B}_s(f) - \bar{B}_i(f)\right]^2 + \left[\bar{A}_s(f) + \bar{A}_i(f)\right]^2\right)^{-1/2} . \qquad (20)$$

An upper bound is established for the isolator transfer function when the term $(1-\bar{B}_s(f) - \bar{B}_i(f))$ is equal to zero. If the term is not zero, either in a positive or negative case, the transfer function is smaller. The upper bound to the isolator transfer function H_i is given by Eq. (21) from the procedure:

$$\bar{H}_i(f) = \frac{1}{\bar{A}_i(f)\ \bar{A}_s(f)} = \frac{1}{\frac{f^2}{f_i^2} D(\beta_i, f/f_i) + \bar{A}_s(f)} . \qquad (21)$$

Table 5 has been set up to facilitate calculations of the quantity $D(\beta_i, f/f_i)$ as defined in Eq. (21):

$$D(\beta_i, f/f_i) = \frac{f_i^2}{f_c^2}\left(\frac{1}{\bar{H}_i(f)} - \bar{A}_s(f)\right) .$$

The determination of $D(\beta_i, f_c/f_i)$ in Table 5 is accomplished at several frequencies to check the isolator system design in the range of interest above f_{02}. Three check frequencies are worthy of investigation in the sample problem. Sudden reductions in H_m occur on Fig. 4 at 65, 150, and 300 cps. These frequencies are entered in column 1 as values of f_c. Corresponding values of H_m for each value of f_c are taken from Fig. 4 also and entered in column 2 of Table 5. Column 3 represents the reciprocals of $H_m(f_c)$ which are listed in column 2. Values of $\bar{A}_s(f_c)$ are taken from Fig. 3 and are tabulated in column 4. The values of column 3 minus column 4 or the values of $1/H_m(f_c) - \bar{A}_s(f_c)$ are obtained and listed in column 5. An examination of Fig. 6 shows that the highest frequency permitted by the solid region is approximately 50 cps. This value of f_i is made the first entry

TABLE 5
Determination of f_i, β_i Combinations for which Satisfactory Transfer Function Valves are Assured at High Frequencies

① f_c	② $H_m(f_c)$	③ 1/②	④ $\bar{A}_s(f_c)$	⑤ ③ - ④	⑥ f_i	⑦ f_c/f_i	⑧ $\frac{2}{⑤/⑦}$	⑨ Region Fig. 7	⑩ Satisfactory β_i
65	0.4	2.5	1.65	0.85	50	1.30	0.503	IV	none
					40	1.62	0.334	I	>0.12
					30	2.16	0.182	I	>0.043
					20	3.25	0.084	I	>0.013
					10	6.5	0.020	V	all
150	0.2	5.0	0.165	4.84	50	3.0	0.538	IV	none
					40	3.75	0.343	II	0.055 to 0.32
					30	5.0	0.194	II	0.02 to 0.5
					20	7.5	0.086	V	all
					35	4.29	0.263	II	0.024 to 0.42
					32.5	4.62	0.226	II	0.027 to 0.47
300	0.1	10.0	0.065	9.94	50	6.0	0.276	II	0.026 to 0.28
					40	7.5	0.187	II	0.013 to 0.34
					30	10.0	0.099	V	all
					35	8.58	0.135	III	<0.43

in column 6 of Table 5. This value (50) is divided into the value of f_c (65) and the result (1.30) is placed in column 7. Column 5 is divided by the square of the value in column 7 and the quotient is listed in column 8. The values in column 8 are equal to $D(\beta_i, f_c/f_i)$.

The first calculation of $D(\beta_i, f_c/f_i)$ is equal to 0.503 for the condition wherein f_c/f_i equals 1.30 and f_i equals 50 cps. Figure 7 has been divided into five regions. For this first case, Fig. 7 is entered at f_c/f_i equal to 1.30 and D equal to 0.503. This falls into the region which is marked as IV in Fig. 7. The value of IV is entered into column 9.

Information in column 10 is found by using the regions of column 9 according to the following scheme [1].

Column 9 Region in Fig. 7	Column 10 Satisfactory
I	> ———
II	——— to ———
III	< ———
IV	none
V	all

A value of β is found on Fig. 7 for each blank in column 10. Two values of β are determined for region II. One value is read from β curves which are traveling upward to the right, positive slope; the other from β curves which are traveling downward to the right, negative slope.

According to the procedure, the region IV provides no satisfactory values of β_i. Whereupon the above steps of Table 5 are repeated using new values of f_i in increments of 10 cps in descending order until the f_c/f_i versus D point lies in region V or until f_i is less than f_{min}. Computations for $D(\beta_i, f_c/f_i)$ down to 10 cps are displayed in Table 5 for this sample solution. The data in columns 6 and 10 of Table 5 are used to correct the solid region in Fig. 6 which is suspect at high frequencies. The suspect region is indicated by the slashed lines in the high-frequency area of Fig. 6.

Choice of a Trial Isolator Design

The next logical step in the procedure is to select a resilient element having frequency and damping parameters within the range of the acceptable values of Fig. 6. A trial design is selected within the region of permissible parameters (1) that avoids the suspect region, (2) that allows a variation in natural frequency of at least ±10 percent, (3) that permits a variation of ±20 percent in fraction of critical damping, and (4) that is feasible by the current state of the art in the production of vibration isolators. The nominal value of the trial design is shown in Fig. 6. On the basis of the selection rules, the selected isolators have a natural frequency of 20 ± 2 cps and a fraction of critical damping of 0.15 ± 0.03. It is necessary to check this trial design to see that the isolator transfer function does not exceed H_m, the maximum allowable transfer function. For this reason, the isolator transfer function, H_i, is calculated in the next section.

Calculation of H_i the Transfer Function Achieved with the Isolator System Design

The check of the trial design is accomplished by (1) finding the peaks and valleys of H_i, (2) determining the frequencies at which to calculate H_i, (3) calculating the values of the normalized isolator admittance at the frequencies found in (2) and adding these to the values of normalized structural admittance, (4) using these data to calculate H_i, and (5) plotting H_i on the same graph as H_m (Fig. 4) for comparison.

The isolator transfer function, H_i, was previously defined by Eq. (20) from the procedure. The data from Fig. 1 are used in Tables 1, 6, and 7 of the procedure to obtain the isolator transfer function curve for this numerical solution. The peaks and valleys of this curve are determined by using the overlay of Fig. 8 on the data of Fig. 3. Figure 8 provides a curve of the dimensionless admittance of a spring-mass combination with a natural frequency f_i. The frequencies at or near the peaks and valleys of H_i are found at the intersections of the spring part of the admittance of the isolator-equipment combination with the imaginary part of the structural admittance. The overlay of Fig. 8 is placed on Fig. 3 of this problem with the unity ordinates coinciding and the f_i value of Fig. 8 placed at the numerical value of f_i (20 cps) on Fig. 3. Then, the intersections of the overlay curve with the $\bar{B}_s$ curve are noted. Intersections occur near 17 and 56 cps. These values are entered into Table 1 in the column labeled peaks and valleys. The lowest frequency intersection, 17 cps, indicates the presence of a peak and the 56 cps represents a valley.

The G-5 procedure is followed to determine the minimum number of points necessary to properly define the H_i curve. It is shown that the transfer function curve for a single peak or valley is satisfactorily determined by

TABLE 6
Calculation of the Sum of the Normalized
Structural and Isolator Admittances

① f (cps)	② f/f_i	③ D (Fig. C)	④ 2 ②·③ / $\bar{A}_i$	⑤ ②③/2 β_i $\bar{B}_i$	⑥ $\bar{A}_s$	⑦ $\bar{B}_s$	⑧ ④+⑥ $\bar{A}_s + \bar{A}_i$	⑨ ⑤+⑦ $\bar{B}_s + \bar{B}_i$
5	0.250	0.074	0.005	0.060	0	0.020	0.005	0.080
9	0.450	0.132	0.027	0.198	0	0.066	0.027	0.264
12	0.600	0.175	0.063	0.351	0	0.118	0.063	0.469
15	0.750	0.218	0.123	0.544	0.012	0.187	0.135	0.731
17	0.850	0.242	0.175	0.687	0.019	0.243	0.194	0.930
19	0.950	0.268	0.241	0.848	0.029	0.315	0.270	1.163
24	1.20	0.320	0.460	1.28	0.068	0.560	0.528	1.84
28	1.40	0.358	0.701	1.67	1.28	0.87	0.829	2.54
39	1.95	0.435	1.655	2.83	1.10	2.65	2.76	5.48
50	2.50	0.480	3.00	4.00	9.7	0	12.7	4.00
56	2.80	0.490	3.97	4.57	5.2	-4.95	9.17	-0.38
62	3.10	0.500	4.80	5.18	2.2	-4.55	7.0	0.63
78	3.90	0.490	7.45	6.38	0.69	-3.00	8.14	3.38
112	5.60	0.430	13.5	8.02	0.28	-2.22	13.8	5.80
336	16.8	0.192	54.2	10.75	0.058	-2.0	54.3	8.75
1000	50.0	0.066	165	11.0	0.02	-2.0	165	9.0
60	3.00	0.370	3.33	3.70	2.90	-4.8	6.23	-1.1
200	10.0	0.300	30.0	10.0	0.107	-2.0	30.1	8.0

TABLE 7
Calculation of H_i

① f (cps)	② $\bar{A}_s + \bar{A}_i$	③ $\bar{B}_s + \bar{B}_i$	④ $\lvert 1 - ③ \rvert$	⑤ $④^2$	⑥ $②^2$	⑦ ⑤+⑥	⑧ $1/\sqrt{⑦}$ H_i
5	0.005	0.080	0.920	0.845	0.000	0.845	1.09
9	0.027	0.264	0.736	0.540	0.001	0.541	1.36
12	0.063	0.469	0.531	0.282	0.004	0.286	1.85
15	0.135	0.731	0.269	0.072	0.018	0.090	3.33
17	0.194	0.930	0.070	0.005	0.038	0.043	4.83
19	0.270	1.163	0.163	0.027	0.072	0.099	3.18
24	0.528	1.84	0.84	0.707	0.278	0.985	1.01
28	0.829	2.54	1.54	2.37	0.665	3.04	0.573
39	2.76	5.46	4.46	19.9	7.63	27.5	0.190
50	12.7	4.00	3.00	9.0	161	170	0.077
56	9.17	-0.38	1.38	1.90	84.0	85.9	0.108
62	7.0	6.3	0.37	0.137	49.0	49.1	0.143
78	8.14	3.38	2.38	5.65	66.5	72.2	0.118
112	13.8	5.80	4.80	23.0	190	213	0.069
336	54.3	8.75	7.75	60.0	2960	3020	0.018
1000	165	9.0	8.0	64.0	27,300	27,360	0.006
60	6.23	-1.1	2.1	4.41	38.9	43.3	0.152
200	30.1	8.0	7.0	49.0	903	952	0.032

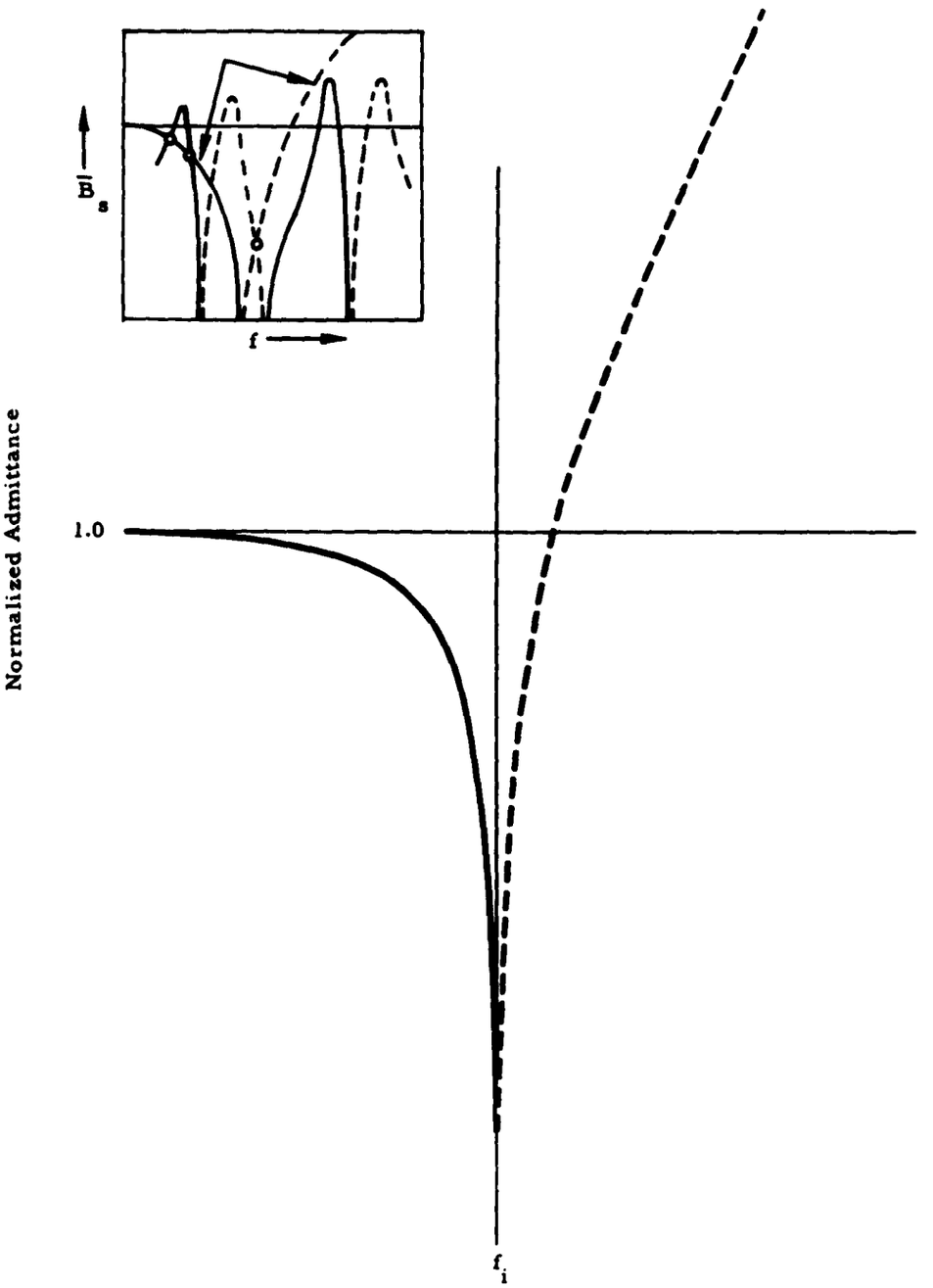

Fig. 8 - Plot of the normalized admittance of springmass combination with natural frequency f_i

values at frequencies which are the following multiples of the frequency at which the peak or valley occurs: 0.1, 0.3, 0.5, 0.7, 0.9, 1.0, 1.1, 1.4, 2, 6, 50. These multiples for H_i of the trial design are listed in Table 1. The values of 17 cps and 56 cps are entered in the center column of Table 1, with the smallest value being listed first. Entries were made to the left of 17 cps until f' was reached. Then entries were made to the right of 56 cps and the highest multiple was deleted and replaced by f''. Since the ratio of 17/56 is less than 0.75, the following procedure was used to fill in the H_i points of Table 1: successive entries were made — 1.1 x 17 to the right, 0.9 x 56 to the left, 1.4 x 17 to the right, 0.7 x 56 to the left, 2 x 17 to the right, 0.5 x 56 to the left. At this point the frequency multiples crossed and the last entry on the right (34) was deleted.

The frequencies determined in Table 1 for the H_i curve are used in Tables 6 and 7 to compute Eq. (20):

$$H_i(f) = \left(\left[1 - \bar{B}_s(f) - \bar{B}_i(f)\right]^2 + \left[\bar{A}_s(f) + \bar{A}_i(f)\right]^2\right)^{-1/2} \qquad (20)$$

Table 6 provides a convenient form for efficiently computing the sum of the normalized structural and isolator admittances. The frequencies for H_i found in Table 1 are entered into column 1 of Table 6 with the lowest frequency at the top of the column. Using 20 cps for f_i, the values of f/f_i are computed and listed in column 2. The $D(\beta_i, f/f_i)$ values of column 3 are obtained by entering Fig. 7 with the f/f_i values of column 2 and with β_i equal to 0.15. The $D(\beta_i, f/f_i)$ values are read from the ordinate of Fig. 7. The values of $D\, f^2/f_i^2$ which are equal to $\bar{A}_i(f)$ are computed by multiplying the square of column 2 values by the corresponding column 3 values. These $\bar{A}_i(f)$ values are listed in column 4 of Table 6. Next, the values of $\bar{B}_i(f)$ which are equal to $fD(\beta_i, f/f_i)/2\beta_i f_i$ are computed by dividing the product of columns 2 and 3 by $2\beta_i$. The values of $\bar{B}_i(f)$ are tabulated in column 5. Values of $\bar{A}_s$ and $\bar{B}_s$ are taken from Fig. 3 and are entered in columns 6 and 7, respectively. Note that the $\bar{B}_s$ values from 56 to 1000 cps are negative. Column 8 of Table 6 is the sum of the real parts of the normalized structural and isolator admittances. Thus, the values in column 8 are obtained by adding the $\bar{A}_i$ values in column 4 to the $\bar{A}_s$ values in column 6. Similarly, column 9 contains the sum of the imaginary parts of the normalized structural and isolator admittances. The values in column 9 are determined by adding the $\bar{B}_i$ values in column 5 to the $\bar{B}_s$ values of column 7.

Now the admittance data complied in Table 6 are used in Table 7 to establish values of $H_i(f)$. The frequencies used in Table 6 are entered into column 1 of Table 7. The admittance values of $(\bar{A}_s + \bar{A}_i)$ and $(\bar{B}_s + \bar{B}_i)$ are taken from Table 6 and are entered into columns 2 and 3, respectively, of Table 7. The absolute values of $|1 - (\bar{B}_s + \bar{B}_i)|$ for this sample exercise are computed and tabulated in column 4 of Table 7. In turn, the square of these values is calculated and listed in column 5. Column 6 contains the square of the values which are listed in column 2 of this table. Thus the values in column 6 are equivalent to the square of the real part of the normalized structural and isolator admittances, $\bar{A}_s + \bar{A}_i$. Values from column 5 are added to values from column 6 and entered in column 7. These sums are equal to that part of Eq. (20) which lies within the outer brackets. Finally, the reciprocals of the square roots of the values in column 7 are computed and are entered in column 8. This completes Table 7 for the values in column 8 are equal to H_i, the isolator transfer function. The data from column 8 of Table 7 are plotted on Fig. 4. Since these data, H_i, are less than the maximum allowable transfer function, H_m, at all frequencies, it is evident that the trial design ($\beta_i = 0.15$ and $f_i = 20$ cps) provides adequate protection to the equipment.

Statement of the Isolation System Design Requirements

It was concluded in the previous section that since H_i does not exceed H_m at any frequency, the equipment is satisfactorily isolated by the trial design selection. Although it appears that the solution has been completed, it is considered worthwhile to continue this study to further define the isolation system and to establish an envelope of permissible transmissibility curves for the isolator-equipment combination.

An envelope of transmissibility curves is determined for all the permitted isolation system designs of Fig. 6. This envelope is established by considering designs on the periphery of the accepted design region (solid line) of Fig. 6. The overlay of Fig. 5, which contains the family of classical transmissibility curves is used to find the transmissibility for each isolation system design of β_i and f_i. Corresponding values of β_i and f_i are taken from the acceptable design region of Fig. 6. Then

transmissibility curves for these β_i, f_i points are obtained from Fig. 5. These curves are traced from Fig. 5 onto a three decade log-log graph. The frequency f_i is indicated on the abscissa and the transmissibility values are plotted on the ordinate. The envelope of transmissibility curves for the permitted isolation system design applicable to this example is shown in Fig. 9.

The selected isolators have a natural frequency of 20 ± 2 cps and a fraction of critical damping of 0.15 ± 0.03. These two ranges are expanded slightly by an examination of Fig. 6. Using the same nominal values, slightly greater ranges of natural frequency, f_i, and damping, β_i, are chosen from the permissible range in Fig. 6. A range of 20 ± 3 cps is selected for the natural frequency and a range of 0.15 ± 0.035 is selected for the damping.

Equation (22) provides an alternate method of stating the isolator specifications [1]:

$$k_i = \frac{4\pi^2 W}{g} f_i^2$$
$$c_i + \frac{4\pi W \beta_i}{g} f_i \qquad (22)$$

The values of the dynamic stiffness, k_i, and the coefficient of viscous damping, c_i, in Eq. (22) are divided by n, the number of isolators, to obtain individual isolator requirements. Four isolators are required for this numerical example. Individually, the isolators have a nominal

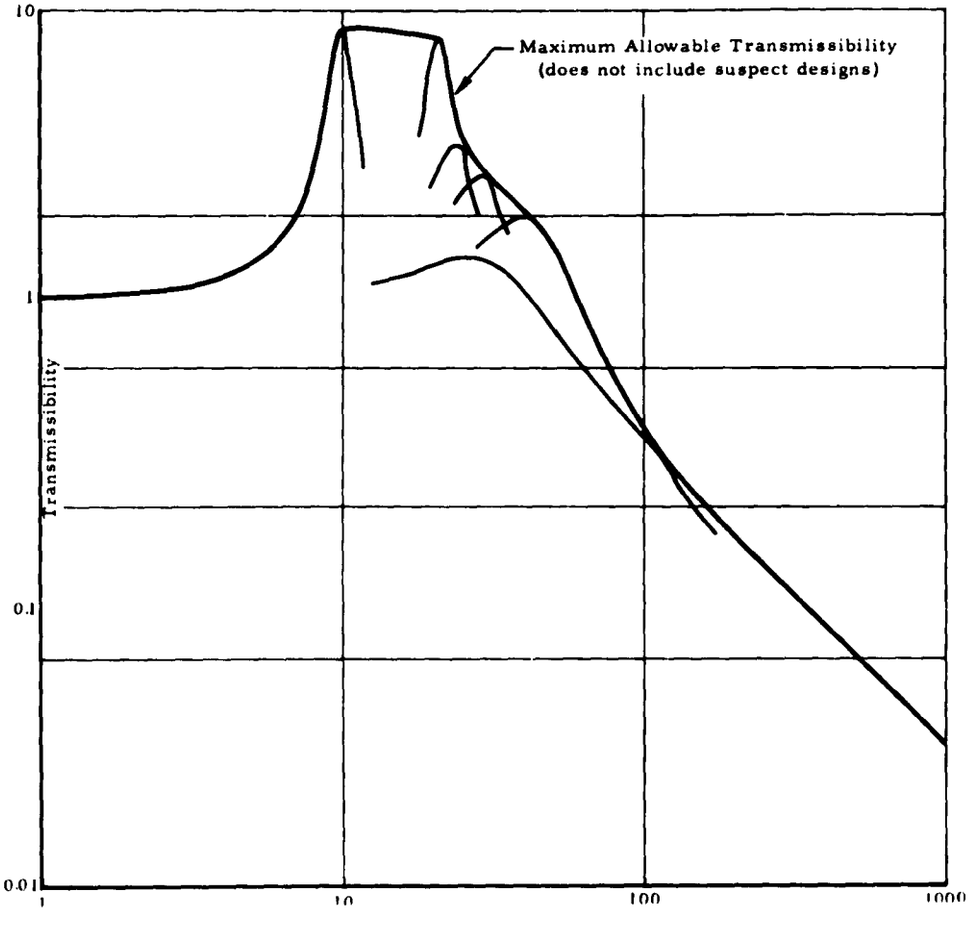

Fig. 9 - Envelope of maximum allowable transmissibilities

dynamic stiffness of 1023 lb/in. for the nominal frequency of 20 cps. Similarly, the dynamic stiffness values for the limiting frequencies of 17 and 23 cps are found to be 739 and 1352 lb/in., respectively. Thus the range of stiffness for the individual isolators runs from 739 to 1352 lb/in. with a nominal value of 1023 lb/in. at the nominal frequency of 20 cps. The values of the coefficient of viscous damping for the individual isolators are computed for (1) the nominal β_i and f_i values, (2) the highest β_i and f_i values, and (3) the lowest β_i and f_i values. For the nominal case (β_i = 0.15; f_i = 20 cps), the individual coefficient of viscous damping is 2.44 lb/in./sec. Likewise, the highest case (β_i = 0.185; f_i = 23 cps) and the lowest case (β_i = 0.115; f_i = 17 cps) values are 3.46 and 1.59 lb/in./sec, respectively. Obviously, this results in a range for the coefficient of viscous damping from 1.59 to 3.46 lb/in./sec with a nominal value of 2.44 lb/in./sec at the nominal β_i and f_i values.

Rotational Frequencies

A satisfactory isolator design has been established in the previous sections and the isolator characteristics have been stated in terms of (1) the natural frequency and the fraction of critical damping, (2) a permissible transmissibility envelope, and (3) the stiffness and the equivalent viscous damping coefficient of the isolation system. Since the procedure is applicable to all directions individually, only calculations for one of the XYZ axes are given in this presentation. This sample problem has encompassed the isolation of equipment which is essentially symmetrical about a centrally located c.g. This sample problem is solved with the selection of four isolators which are mounted symmetrically about the center-of-gravity of the isolated equipment.

This solution has been accomplished while assuming that only translational motion exists in each of the three principal axes. However, this exclusive translational condition seldom occurs in actual practice. It is indeed a rare design which results in translational modes occurring independently without rotational modes. Nevertheless, this numerical solution has been based on the selection of the most favorable design which presents negligible coupling and rocking vibrations. Still, realizing that some small amount of rotational motion may be induced in the equipment, it is considered desirable and appropriate to determine the rotational natural frequencies of the selected isolation system.

The sample problem is extended to investigate rocking frequencies by basing calculations on zero source mechanical admittance [1] and by assuming rigid coupling between supports. The rotational natural frequencies for this example are determined by using the following equation from the procedure:

$$f_{n\alpha} = \frac{1}{\rho_x}\sqrt{f_{ny}^2 a_z^2 + f_{nz}^2 a_y^2}$$

$$f_{n\beta} = \frac{1}{\rho_y}\sqrt{f_{nx}^2 a_z^2 + f_{nz}^2 a_x^2} \qquad (23)$$

$$f_{n\gamma} = \frac{1}{\rho_z}\sqrt{f_{nx}^2 a_y^2 + f_{ny}^2 a_x^2}\,.$$

Where f_{nx}, f_{ny}, and f_{nz} are the translational natural frequencies in the x, y, and z directions, respectively, ρ_x, ρ_y, and ρ_z are the radii of gyration of the equipment about the x, y, and z axes, respectively; and a_x, a_y, and a_z are distances from the c.g. of the equipment to the elastic centers of the individual isolators in the x, y, and z directions, respectively [1].

To determine the three rotational natural frequencies for this problem, the following required data are given:

f_{nx} = 20 cps, f_{ny} = 20 cps, and f_{nz} = 20 cps.
a_x = 12 inches, a_y = 12 inches, a_z = 0.

Equipment dimensions,

20 x 20 x 20 inches.

Then

$$\rho_x = \rho_y = \rho_z = \sqrt{\frac{20^2 + 20^2}{12}} = 8.16 \text{ inches}$$

$$f_{n\alpha} = f_{n\beta} = \frac{\sqrt{20^2 \times 12^2}}{8.16} = 29.41 \text{ cps}$$

$$f_{n\gamma} = \frac{\sqrt{20^2 \times 12^2 \times 20^2 \times 12^2}}{8.16} = 41.59 \text{ cps.}$$

A last final criterion from the procedure is applied to these rotational natural frequencies. These rotational frequencies are considered harmful if they fall within 0.56 to 1.5 of any critical frequency. An examination of Fig. 4 shows the H_i curve to have a salient peak at 17 cps which tends to approach the H_m curve. Then, the critical range for the rocking frequencies runs from 0.56 x 17 to 1.5 x 17 cps or from 9.5 cps to 25.5 cps. Since the rotational natural frequencies found above are outside of this range, the isolators appear to be located in

transmissibility curves for these β_i, f_i points are obtained from Fig. 5. These curves are traced from Fig. 5 onto a three decade log-log graph. The frequency f_i is indicated on the abscissa and the transmissibility values are plotted on the ordinate. The envelope of transmissibility curves for the permitted isolation system design applicable to this example is shown in Fig. 9.

The selected isolators have a natural frequency of 20 ± 2 cps and a fraction of critical damping of 0.15 ± 0.03. These two ranges are expanded slightly by an examination of Fig. 6. Using the same nominal values, slightly greater ranges of natural frequency, f_i, and damping, β_i, are chosen from the permissible range in Fig. 6. A range of 20 ± 3 cps is selected for the natural frequency and a range of 0.15 ± 0.035 is selected for the damping.

Equation (22) provides an alternate method of stating the isolator specifications [1]:

$$k_i = \frac{4\pi^2 W}{g} f_i^2$$
$$c_i + \frac{4\pi W \beta_i}{g} f_i \qquad (22)$$

The values of the dynamic stiffness, k_i, and the coefficient of viscous damping, c_i, in Eq. (22) are divided by n, the number of isolators, to obtain individual isolator requirements. Four isolators are required for this numerical example. Individually, the isolators have a nominal

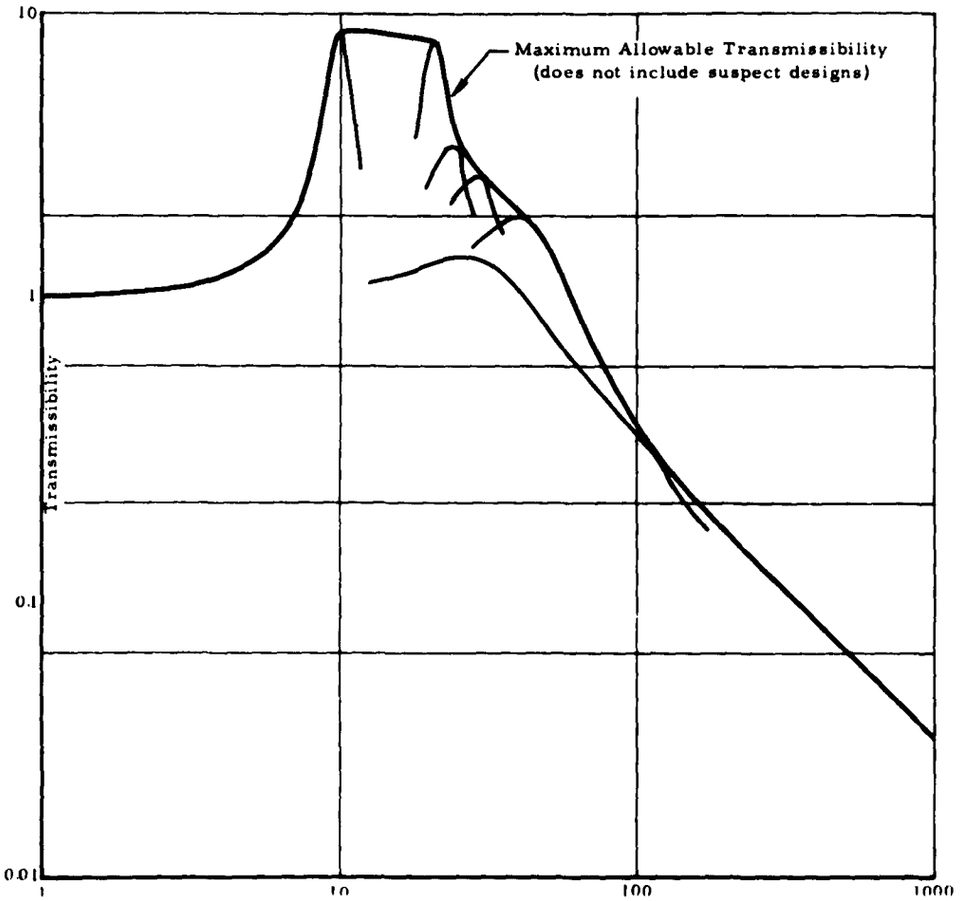

Fig. 9 - Envelope of maximum allowable transmissibilities

a position that will create negligible equipment response to the rocking motions. This completes the numerical solution of the isolation design which is adequate to protect the airborne equipment.

CONCLUSION

Mechanical impedance and admittance data are applicable to many dynamic problems in various fields of mechanical engineering. However, this paper has been confined to the specific utilization of admittance concepts in the reduction of vibration transmission from sources (the supporting structure) to receivers (the equipment). In this regard, this paper has attempted to lead the design engineer through most of the details of a sample vibration isolation problem which was solved by the procedure prepared by the SAE G-5 Committee On Aerospace Shock and Vibration. It is felt that the G-5 procedure is a worthwhile contribution which will be invaluable to the engineer faced with the problem of designing a suitable isolation system to protect delicate airborne equipment. Obviously, this paper has presented an excess of working details on the various steps of the procedure. This intentional overabundance of particulars is merited since experience with the G-5 procedure has shown that the average engineer encounters difficulties when he first attempts to apply the procedure. The philosophy has been followed that too much information is better than insufficient information. As this paper is being prepared (18 July 1961), the G-5 procedure is undergoing revisions which are not reported in this paper. But the essential portions of the procedure have been included in this paper.

It is predicted that mechanical admittance measurements will become commonplace and that the application of mechanical admittance concepts will prevail within the next decade. Future dynamic progress will depend on the development of mechanical admittance measuring systems, the measurement of mechanical admittance on more Aerospace programs, and the application of these data to optimize structural and equipment designs.

ACKNOWLEDGMENT

The author wishes to express his appreciation to the members of the SAE G-5 Committee whose activities form the basis for the major portion of this paper. The inspirational leadership of Dr. C. T. Molloy is gratefully acknowledged. Also, the writer is greatly indebted to Dr. S. Rubin who is responsible for the derivation of the procedure and who supplied most of the mathematics and the sample problem used in this report.

NOMENCLATURE

- A = Real part of mechanical admittance, in./sec/lb
- $\bar{A}$ = Real part of normalized mechanical admittance (Eq. (3)), dimensionless
- B = Imaginary part of mechanical admittance, in./sec/lb
- $\bar{B}$ = Imaginary part of normalized mechanical admittance (Eq. (4)), dimensionless
- D = Function defined by Eq. (15), dimensionless
- H = Transfer function defined by Eqs. (5) and (6), dimensionless
- R = Real part of mechanical impedance, lb/in./sec
- S = Spectral density amplitude of random motion
- U = Complex amplitude of sinusoidal motion
- $V = \dot{U}$ = velocity, in./sec
- W = Weight of equipment = mg, pounds
- X = Imaginary part of mechanical impedance, lb/in./sec
- Y = Complex mechanical admittance, in./sec/lb
- Z = Complex mechanical impedance, lb/in./sec
- a = Peak acceleration, g
- c = Coefficient of viscous damping, lb/in./sec
- f = Frequency = $\omega/2\pi$, cps
- g = Acceleration of gravity, 386 in./sec^2
- $i = j = \sqrt{-1}$
- k = Stiffness of linear spring, lb/in.

m = Mass of equipment = W/g, lb/in./sec^2

u = Displacement, inch

β = Fraction of critical damping, dimensionless

ω = Frequency = $2\pi f$, rad/sec

SUBSCRIPTS

o - Subscript zero indicates that equipment is attached to source without isolators

o_1, o_2 - Used with f to indicate frequencies at which first peak o_1, and first valley o_2 occur on the H_o curve

f - Indicates fragility amplitude

i - Indicates that quantities refer to isolators

m - Used with H to denote maximum allowable transfer function

s - Indicates quantities of source structure.

REFERENCES

[1] SAE G-5 Committee on Aerospace Shock and Vibration, "Design of Vibration Isolation Systems."

[2] Dr. Sheldon Rubin, "Theoretical Background of Procedure," Appendix 3.2 of Ref. 1.

[3] Dr. Sheldon Rubin, "Design Procedure for Vibration Isolation on Non-Rigid Supporting Structures," SAE National Aeronautic Meeting, The Ambassador Hotel, Los Angeles, California, October 5-9, 1959.

[4] H. Himelblau and F. Schloss, "Measurement of Mechanical Admittance," Appendix 3.7 of Ref. 1.

DISCUSSION

Mr. Stern (General Electric): The isolators that you are referring to, are you going to design and make these, or do you plan on buying commercial isolators?

Mr. Mustain: This of course was a sample problem. However, we have ordered from one of the vendors, under a little pressure, an isolator unit 0.18 damping and something higher than 20 cycles per second.

Mr. Stern: Generally you have to use isolators that are commercially available, and the response curves are usually given in the catalog literature of the vendors. This really brings up one of the objections I have to this. Look at the isolators that are used, let's say if you were to go to a conventional spring, just using a spring you won't get any damping. If you use a mesh-type isolator to get damping usually you are worried about icing of the isolator during the humidity test, so you won't isolate that way. The regular rubber isolators get hard as a rock at say -65 degrees. So – for practically all military work you end up with a silicon rubber isolator of some sort, and the spring constants are far from linear. If anything they are pretty close to a tangent function or a hyperbolic sine function. So, how would you actually apply this technique you've evolved to an isolator that you are going to buy from a catalog when you know right away the characteristics are far from those for which you've set up in this plan?

Mr. Mustain: Well I don't think you can buy it off the shelf. You will have to make a special specification, and this is the second procedure that is worked out in this G-5 Document: How to specify a vibration isolator.

Mr. Stern: After all when we finally arrived at the silicon rubber isolator, it does work fairly well compared to what was available before. What I am wondering is do you really think people are going to pay the money and take the time to design isolators when we have some that work fairly well now?

Mr. Mustain: Well, as I said, we're forcing the manufacturer to give us 0.18 damping and it was like pulling teeth but we got it from him.

Mr. Stern: There is a report by Mindlin, I'm pretty sure you are familiar with it, in which he has handled these nonlinear cases quite well. I mean, he has shown how it is quite easy to handle them, and what I wondered was why you haven't made any attempt to handle these cases in this report. Because these are the isolators people use.

Mr. Mustain: Well, we are working on the problem. Procedures have been written by Harry Klein of Ramo-Wooldridge that will cover the specifications to vibration manufacturers and we are considering all these points. It will probably be a more complex specification than any that has ever been prepared in the past.

* * *

STRUCTURAL RESPONSE TO DYNAMIC LOAD*

R. M. Mains
General Engineering Laboratory
General Electric Company
Schenectady, New York

This paper represents an attempt to generalize the problem of calculating responses to random vibration and shock into a set of simple principles, which are sufficient to produce numerical solutions to practical problems. Within the limitations of superposition and linearity, there are no restrictions on the recipes given so that the methods are general. The use of a digital computer with narrow frequency or time intervals leads to solutions as precise as desired, yet the numerical summations can be done by slide rule or hand computer and still give acceptable results. The related subjects of load definition and damage evaluation are discussed so that the prediction of structural response is placed in a proper frame of reference.

LIST OF SYMBOLS

$f(t)$ = a time function

e = base of natural logarithms

t = time

ω = frequency

$i = \sqrt{-1}$

$F(i\omega)$ = the complex Fourier integral transform of $f(t)$

F_{RE} = the real part of $F(i\omega)$

F_{IM} = the imaginary part of $F(i\omega)$

M = mass matrix

C = damping matrix

K = stiffness matrix

X = motion vector

$\dot{X}$, $\ddot{X}$ = time derivatives of X

p = operator, d/dt

$Z(p) = Mp^2 + Cp + K$

$X(t)$ = time function of X

$\chi(i\omega)$ = the Fourier integral transform of $X(t)$

$Y(i\omega)$ = the complex frequency response function

a = the real (or even, or cosine) part of the response vector

b = the imaginary (or odd, or sine) part of the response vector

f_1 = the real (or even, or cosine) part of $f(t)$

f_2 = the imaginary (or odd, or sine) part of $f(t)$

Y_{RE} = the real part of $Y(i\omega)$

Y_{IM} = the imaginary part of $Y(i\omega)$

$g(i\omega)$ = complex spectral density in units^2/cycle

n = number of expected cycles at a given stress level

*This paper was not presented at the Symposium.

N = number of cycles to failure at a given stress level

THE PROBLEM OF DYNAMIC DESIGN

The problem of dynamic design is to produce a piece of equipment, one of a kind or in quantity, which performs a desired set of functions with a given reliability and within cost, size, weight, and other limitations. Once the functional requirements have been established and the economic factors have received due consideration, the problem breaks down into three essential steps: (1) definition of the loads, (2) prediction of the responses of the equipment to these loads, and (3) the evaluation of the resulting performance. In the general sense, loads are any factors which by their action lead to malfunction or damage of the equipment, while responses are the consequences of these loads. The concern of this discussion is with a particular variety of loads and responses: those associated with forces or motions imposed as loads upon a mechanical structure. Such specific loads are usually either static, oscillatory, or transient (or combinations thereof) and are referred to as steady load, vibration, and shock, respectively. For any problem involving the production and use of several pieces of the same equipment over an extended period of time, the loads will usually vary with time, with the particular piece of equipment, and with the individual condition of use. Consequently, the loads tend to be random in character and to have some range within which they are restricted so that they are best described in terms of probabilities and statistics.

The response of a linear structure to a random load is also random, but of a modified character [1]. The way in which the response differs in character of randomness from the load depends upon the structure itself and is predictable for linear structures. This is covered in some detail below.

The development of malfunction or failure under load is usually subject to statistical variation, even for steady loads. As a result, the evaluation of performance under load to determine a reliability (or its inverse, probability of malfunction) becomes a problem of comparing probable malfunction data to produce a reliability estimate. This amounts to predicting the in-service mortality tables in advance of actual service.

HOW LOADS ARE DEFINED

Since we are concerned with force or motion loads on a mechanical structure, the amplitude variation of the load with time or with frequency must be described in order to define the load. Figure 1 shows a number of variations of load, together with the names by which they are usually called. The usual processes for determining load variations are:

(1) By direct measurement in service of a prototype or model.

(2) By deduction from in-service measurement of similar equipment.

(3) By study of the probable environments, deduction of their effect upon the equipment, and translation of this information into loads.

The process of evolution of loads information is usually in reverse order to that given above because the prototype is never available at the beginning of a design. Because equipment reliability is a function of the entire life of each individual in the whole population, it is desirable to describe each kind of load in terms of:

(4) Root-mean-square amplitude.

(5) Distribution of amplitudes (histogram).

(6) Time duration or total design life.

(7) Variations in (4) and (5) with time or at different stages of design life.

For all loads except static loads, the frequency spectrum, $F(i\omega)$, of the loads is needed rather than the time function, $f(t)$, even though load measurements are usually made as time functions. To change from the time function to the frequency spectrum, the mathematical process used is the determination of the Fourier transform (or the infinite series of Fourier component coefficients). This is done by [2]

$$F(i\omega) = \int_{-\infty}^{\infty} f(t)\, e^{-i\omega t}\, dt . \qquad (1)$$

Since for practical problems, $f(t)$ is rarely a convenient analytic function, numerical integration can be performed by substituting

$$e^{-i\omega t} = \cos \omega t - i \sin \omega t , \qquad (2)$$

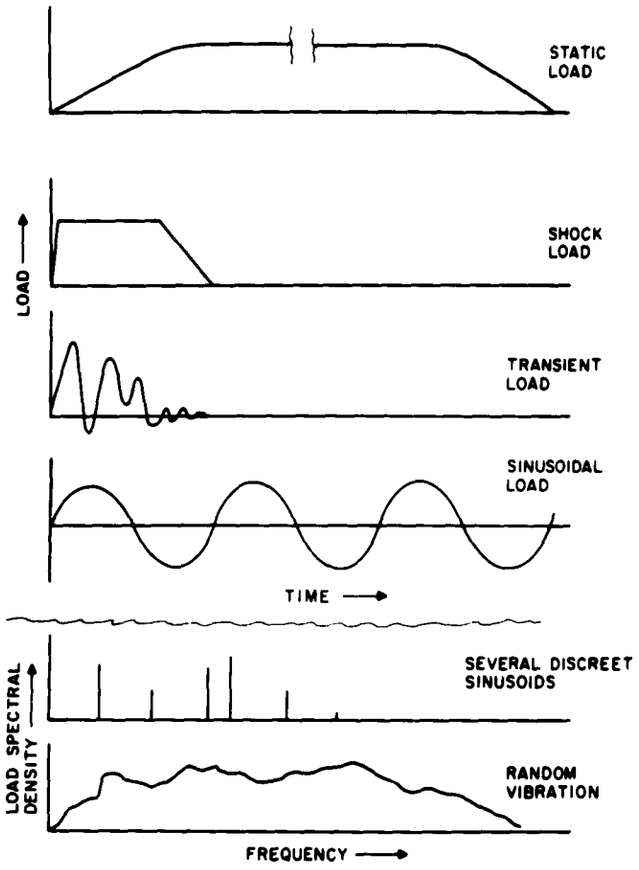

Fig. 1 - Different kinds of load-time functions

whence

$$F_{RE} = \sum_t f(t) \cos \omega t \, \Delta t \qquad (3)$$

$$F_{IM} = \sum_t f(t) \, (- \sin \omega t) \, \Delta t \, . \qquad (4)$$

The same result can be obtained by passing the electrical signal representing $f(t)$ through a series of electrical filters, whose characteristics are known, and deducing from the filter output the values of $F(i\omega)$. The information on phase is usually lost in the filtering process, so that the resulting spectrum, $F(i\omega)$, is useful for calculating responses to random oscillation, but not to transients.

It sometimes happens that the histogram of item (5) will show a regular distribution, such as Gaussian or Rayleigh, and the variations of item (7) will not occur. In such a case the function $f(t)$ may be what is called a "stationary time function" and much of the existing mathematics of statistics can be applied [3]. In other cases, the "stationary time function" requirements may be fulfilled for short intervals in the design life, or may be assumed to be fulfilled so that advantage can be taken of available statistical theory. This is primarily helpful in finding representative functions and testing for correlations and fit of data.

To summarize the problem of definition of loads, consider Fig. 2. We start with the measured time function of the load, $f(t)$, filter it or transform it to get the frequency function of the load $F(i\omega)$. The frequency functions are studied statistically and the results weighted by judgment to account for the degree of uncertainty, the severity of effect of malfunction, and the like. The result is a set of design values of load, statistically described, the general character of which falls in one or more of the categories of Fig. 1.

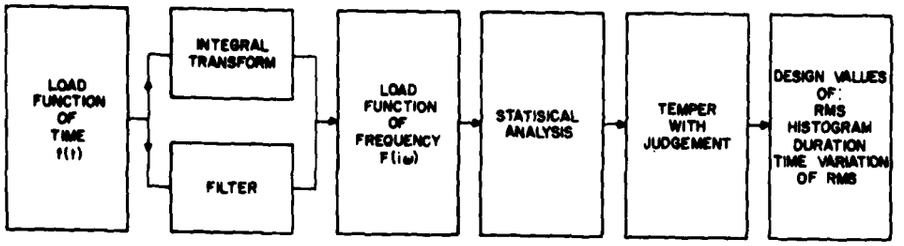

Fig. 2 - Flow chart for load definition

HOW RESPONSES ARE PREDICTED

First, consider the equations of motion of a linear system with lumped parameters,

$$M\ddot{X} + C\dot{X} + KX = f(t) , \qquad (5)$$

in which

M = mass matrix

C = damping matrix

K = stiffness matrix

X = motion vector

$\dot{X}$ and $\ddot{X}$ = time derivatives of X

$f(t)$ = time function of load, a vector.

Now let

$$\frac{d}{dt} = p, \qquad (6)$$

and let

$$Z(p) = Mp^2 + Cp + K ; \qquad (7)$$

then, (5) becomes

$$Z(p)\, X(t) = f(t) , \qquad (8)$$

in which $X(t)$ is used for X simply to emphasize that it is a time function. By Fourier's theorem and Eq. (1) [2]

$$f(t) = \frac{1}{2\pi} \int_{-\infty}^{\infty} F(i\omega)\, e^{i\omega t}\, d\omega . \qquad (9)$$

Define a displacement vector function of frequency, $\chi(i\omega)$ such that

$$X(t) = \frac{1}{2\pi} \int_{-\infty}^{\infty} \chi(i\omega)\, e^{i\omega t}\, d\omega . \qquad (10)$$

Substitute Eqs. (9) and (10) into (8) and get

$$\frac{Z(p)}{2\pi} \int_{-\infty}^{\infty} \chi(i\omega)\, e^{i\omega t}\, d\omega = \frac{1}{2\pi} \int_{-\infty}^{\infty} F(i\omega)\, e^{i\omega t} d\omega . \qquad (11)$$

Carry $Z(p)$ inside the integral and get

$$\frac{1}{2\pi} \int_{-\infty}^{\infty} Z(i\omega)\, e^{i\omega t}\, \chi(i\omega)\, d\omega$$

$$= \frac{1}{2\pi} \int_{-\infty}^{\infty} F(i\omega)\, e^{i\omega t}\, d\omega . \qquad (12)$$

Equation (12) then reduces to

$$Z(i\omega)\, \chi(i\omega) = F(i\omega) . \qquad (13)$$

Premultiply by

$$Z^{-1}(i\omega)$$

and define

$$Y(i\omega) = Z^{-1}(i\omega) , \qquad (14)$$

whence

$$\chi(i\omega) = Y(i\omega)\, F(i\omega) . \qquad (15)$$

In Eq. (15), $Y(i\omega)$ is the calculated or measured mobility matrix. $F(i\omega)$ is obtained by transform from Eq. (1); then $\chi(i\omega)$ can be calculated. Equation (10) then serves to transform $\chi(i\omega)$ into $X(t)$, if the time function is needed.

In the application of these equations to practical problems, two separate cases occur:

(a) Preliminary design, for which calculated or estimated values are put in Eq. (15) and carried through to a solution.

(b) Final design, or design refinement, for which measured data can go into Eq. (15).

At intermediate stages between (a) and (b), the input for Eq. (15) may be partly calculated and partly measured.

For the numerical calculation of $Y(i\omega)$, it is convenient to consider Eq. (5) and let

$$X = a \cos \omega t + b \sin \omega t$$
$$f(t) = f_1 (\cos \omega t) + f_2 (\sin \omega t) . \tag{16}$$

When these substitutions are made in Eq. (5), two equations result, and the order of the matrix solution is doubled,

$$-\omega^2 Ma + \omega Cb + Ka = f_1$$
$$-\omega^2 Mb - \omega Ca + Kb = f_2 ,$$

which can be written as

$$\begin{vmatrix} -\omega^2 M + K & +\omega c \\ -\omega c & -\omega^2 M + K \end{vmatrix} \begin{vmatrix} a \\ b \end{vmatrix} = \begin{vmatrix} f_1 \\ f_2 \end{vmatrix} . \tag{17}$$

Equation (17) now permits the computation of the vector

$$\begin{vmatrix} a \\ b \end{vmatrix}$$

for any desired set of values of ω, with the force vector

$$\begin{vmatrix} f_1 \\ f_2 \end{vmatrix}$$

taken such that all the f_2's are zero, and each f_1 is successively unity while the other f_1's are zero. The resulting a's give the real, or in-phase, components of $Y(i\omega)$, and the b's give the imaginary, or out-of-phase, components of $Y(i\omega)$. For example,

$$\begin{vmatrix} -\omega^2 M + K & +\omega c \\ -\omega c & -\omega^2 M + K \end{vmatrix} \begin{vmatrix} a_1 \\ a_2 \\ a_3 \\ \cdot \\ \cdot \\ \cdot \\ a_n \\ b_1 \\ b_2 \\ \cdot \\ \cdot \\ \cdot \\ b_n \end{vmatrix} = \begin{vmatrix} 1 \\ 0 \\ 0 \\ \cdot \\ \cdot \\ \cdot \\ \cdot \\ \cdot \\ \cdot \\ \cdot \\ \cdot \\ \cdot \\ 0 \end{vmatrix} \tag{18}$$

gives the first row and column of

$$Y_{RE} = \begin{vmatrix} a_1 & a_2 & a_3 \cdots a_n \\ a_2 \\ a_3 \\ \cdot \\ \cdot \\ \cdot \\ a_n \end{vmatrix} \tag{19}$$

and

$$Y_{IM} = \begin{vmatrix} b_1 & b_2 & b_3 \cdots b_n \\ b_2 \\ b_3 \\ \cdot \\ \cdot \\ \cdot \\ b_n \end{vmatrix} . \tag{20}$$

Similarly, with the jth row of the f vector of Eq. (18) taken as unity, the jth row and column of Eqs. (19) and (20) result. Even for as few as 3 degrees of freedom, the bookkeeping involved in these computations is staggering, so that machine computation is advisable. The programming for the machine, however, is relatively simple, since only a simultaneous equation routine and bookkeeping are involved.

To complete the set of relations for numerical computation, recall that

$$e^{i\omega t} = \cos \omega t + i \sin \omega t \tag{21}$$

and apply this to Eq. (10) to get

$$X(t) = \frac{1}{2\pi} \sum_{\omega} \left[X_{RE} \cos \omega t - X_{IM} \sin \omega t \right] \Delta\omega$$
$$+ \frac{i}{2\pi} \sum_{\omega} \left[X_{RE} \sin \omega t + X_{IM} \cos \omega t \right] \Delta\omega . \tag{22}$$

The foregoing discussion is particularly interesting because it leads to the conclusion that any driving function which can be expressed as a function of frequency, Eqs. (3) and (4), together with the system mobility, Eqs. (19) and (20), can be put into Eq. (15) to give the response of the system as a function of frequency. If the response is desired as a function of time, then Eq. (22) provides the means for doing this also. Of course, the units in the various terms of the equations must be compatible, and the conditions of linearity and superposability must apply. When the driving functions are statistically described, then the various equations apply to the

mean-square or root-mean-square values, and Eq. (15) is squared to accommodate this. For example,

$$\left[\bar{X}(i\omega)\right]^2 = \left[Y(i\omega)\right]^2 \times G(i\omega) , \qquad (15a)$$

in which

$\left[\bar{X}(i\omega)\right]^2$ = mean square response density, $(\text{units})^2/\text{cycle}$,

$\left[Y(i\omega)\right]^2$ = square of $|Y(i\omega)|$, in units suitable to change G into x,

$G(i\omega)$ = spectral density in $(\text{units})^2/\text{cycle}$,

and the difference between Eqs. (15a) and (15) is essentially only that between the customary description of a continuous random spectral density as mean-square units/cycle, and a discrete spectrum as just units.

The foregoing is summarized in a group of charts for ready reference, Figs. 3, 4, and 5. Figure 3 summarizes and illustrates the principles involved. Figure 4 shows some time-function → frequency-function transforms for some common driving functions. Figure 5 illustrates what can be done to solve specific problems numerically. These three charts provide the essential recipes for solving numerically any problem to which the limitations of linearity and superposability apply. For a few (2 or 3) degrees of freedom, it is feasible to do the work by hand computation, even though the bookkeeping involved is tedious. The programming for machine computation is simple, since only a few standard subroutines and bookkeeping instructions are needed. The result is a powerful tool which handles all structural dynamics problems, regardless of the particular name given to the driving function, with one response equation serving all cases, Eq. (15).

HOW PROBABLE DAMAGE IS EVALUATED

This part of the process is appreciably less determinant than the definition of loads and the prediction of responses to loads. Investigations on damage accumulation are continuing, and Refs. 3 and 4 contain bibliographies on the subject. Pages 365, 366, and 389 in Ref. 1 give numerical examples of damage accumulation calculations, so such calculations will not be repeated here.

The principles involved in damage evaluation are relatively simple and straightfoward, but their application requires careful bookkeeping. First, one must have a damage factor, such as stress, defined statistically so that a histogram can be drawn to relate stress amplitude to the number of occurrences. Then one must have data-relating stress amplitude to the number of cycles required to produce failure (or malfunction). Finally, one must either have data or make some assumption about how the damage accumulates from each stress cycle until failure occurs.

For example, with a statistically defined set of loads, the methods discussed above can be used to predict responses and generate a histogram of the expected stress amplitudes. Next, S-N data for the material can either be found in the literature or generated by test. It is then common to assume a damage accumulation rule such as the linear one [5], which states that a proportion of total damage accrues at each stress level, σ_i, which is the ratio of the number of expected cycles at that stress level, n, to the number of cycles required to produce failure at that stress level in the virgin material, N. Tests to date show that when these portions of total damage add to something between 0.3 and 3.0, failure occurs. In symbols,

$$\sum_i \frac{n_i}{N_i} = 0.3 \text{ to } 3.0. \qquad (23)$$

This is not a very satisfactory situation for stress damage, and we know more about stress damage accumulation than any other damage producing factor. Much more work needs to be done in this area.

THE EFFECT OF DAMPING ON RANDOM VIBRATION AND SHOCK

First, consider the two cases of a constant spectral density random vibration, and an impulse shock, for both of which the frequency function of load is a straight, horizontal line as in Fig. 4. The response of a structure to these loads is then governed by the appropriate frequency response function, as in Fig. 3. The effect of damping on the response can then be studied by considering how the frequency response function is affected by damping. It is clear that a decrease in any part of the frequency response function decreases the response, and a decrease in area under the frequency-response-function curve correspondingly decreases the response.

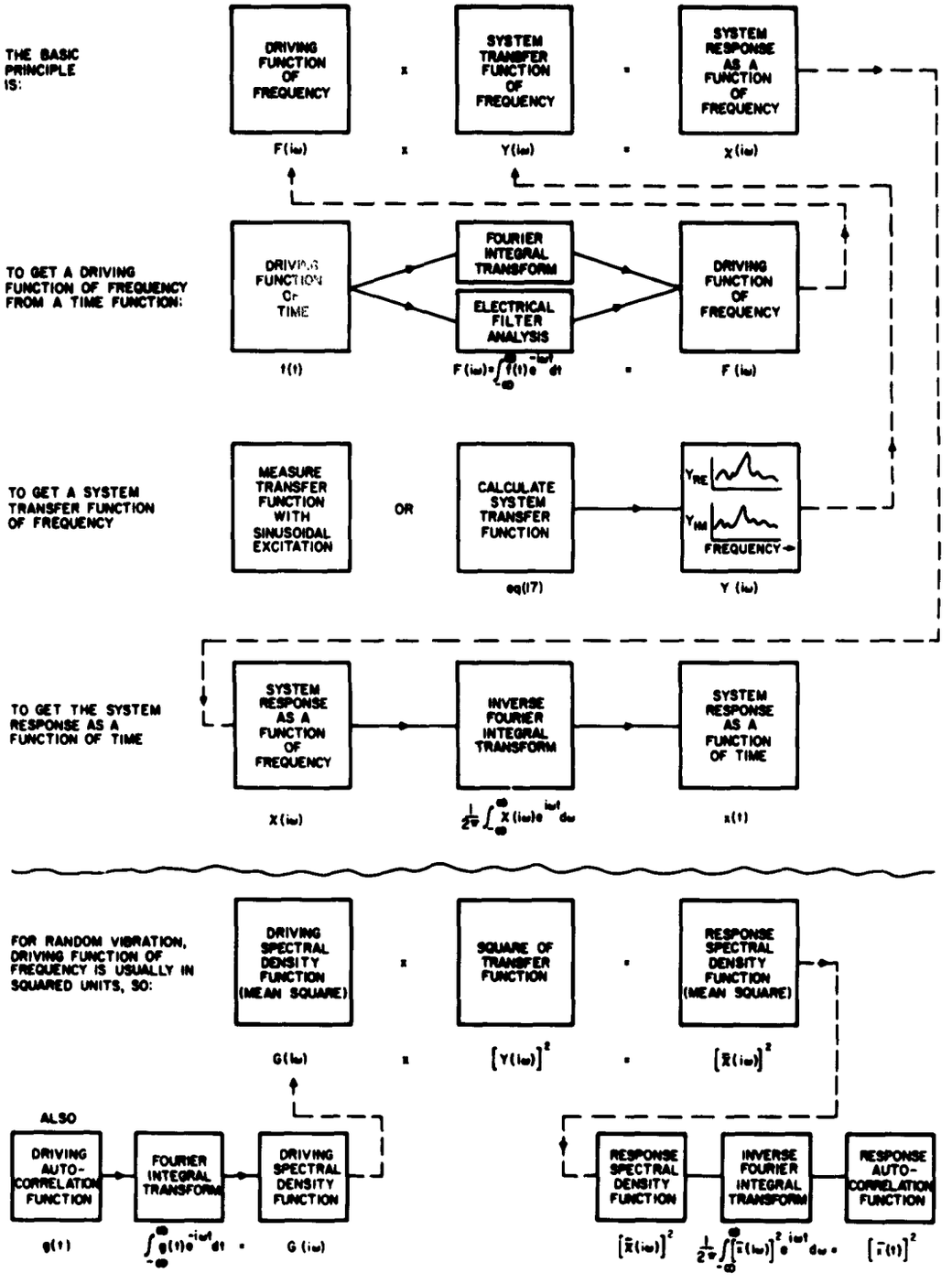

Fig. 3 - Summary of principles for response calculation

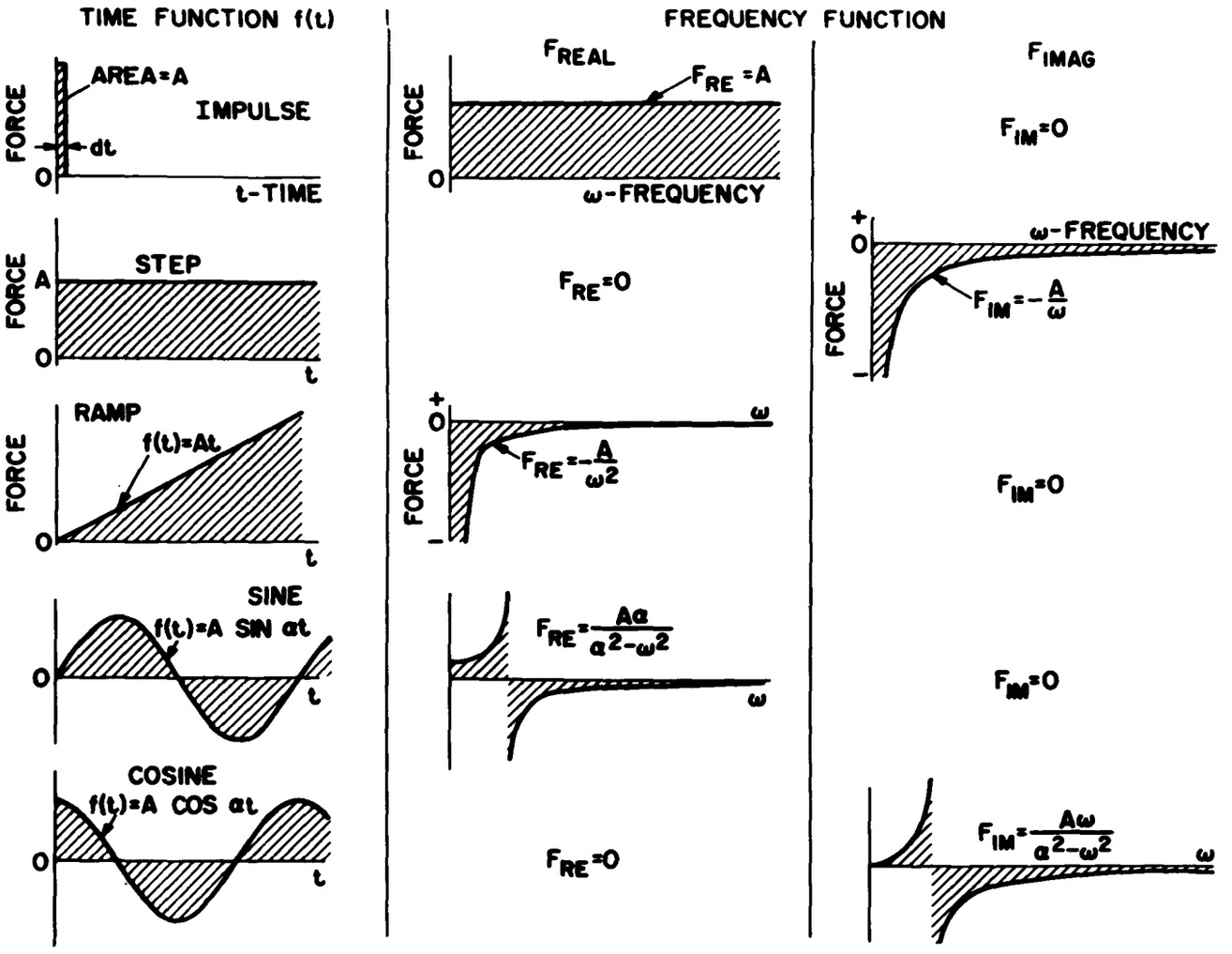

Fig. 4(a) - Sample time-function to frequency-function transforms

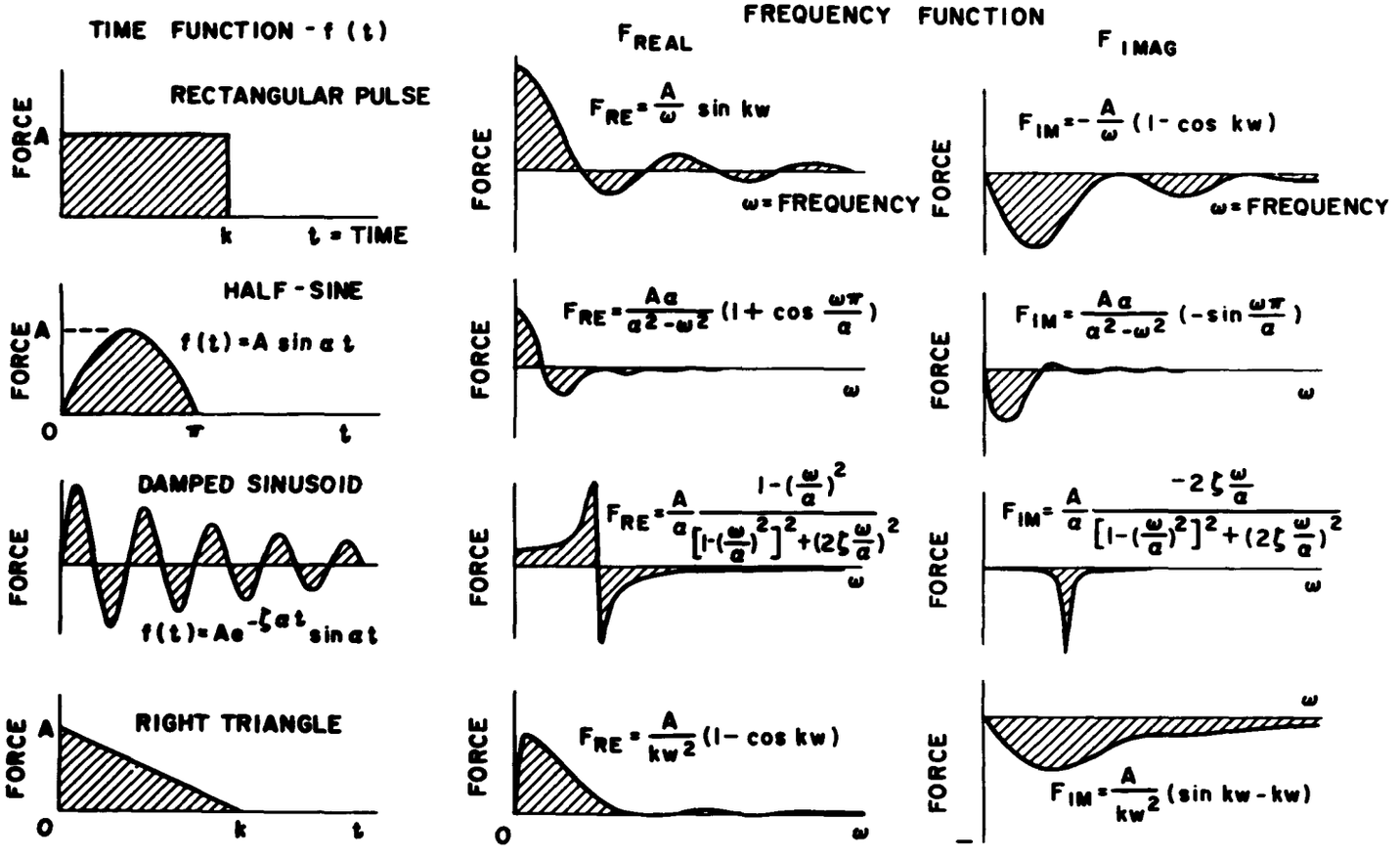

Fig. 4(b) - Sample time-function to frequency-function transforms

FOR SPECIFIC PROBLEMS - (UNITS OF FUNCTIONS MUST BE COMPATIBLE)

EQ (15) CAN BE SOLVED FREQUENCY-BY-FREQUENCY TO GET $X(i\omega)$

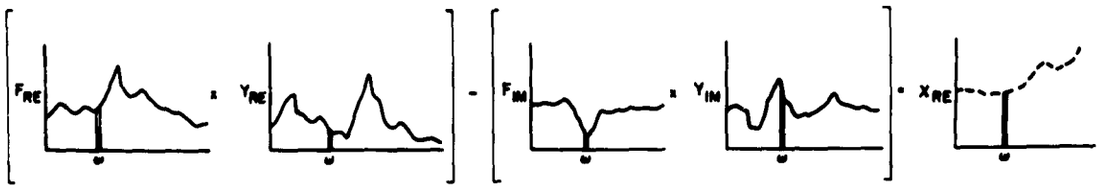

AND SIMILARLY FOR $F_{IM} = Y_{RE} + F_{RE} = Y_{IM} = X_{IM}$

EQ (1), THE DIRECT FOURIER INTEGRAL TRANSFORM CAN BE SOLVED NUMERICALLY BY

$$F_{RE}(i\omega) = \sum_{1} f(t) \cos \omega t \, \Delta t, \quad F_{IM}(i\omega) = \sum_{1} f(t)(-\sin \omega t)\Delta t$$

FOR EACH SPECIFIC FREQUENCY.

EQ. (10), THE INVERSE FOURIER INTEGRAL TRANSFORM CAN BE SOLVED NUMERICALLY BY

$$x(t) = \frac{1}{2\pi} \sum_{\omega} \left[X_{RE} \cos \omega t - X_{IM} \sin \omega t \right] \Delta\omega +$$

$$\frac{1}{2\pi} \sum_{\omega} \left[X_{RE} \sin \omega t + X_{IM} \cos \omega t \right] \Delta\omega$$

FOR EACH SPECIFIC TIME

FOR RANDOM DRIVING FUNCTIONS EXPRESSED AS A MEAN SQUARE SPECTRAL DENSITY, $G(i\omega)$, USE $\left[Y(i\omega)\right]^2 = Y^2_{RE} + Y^2_{IM}$ AND MULTIPLY FREQUENCY-BY-FREQUENCY TO GET THE MEAN SQUARE RESPONSE SPECTRAL DENSITY, $\left[\overline{X}(i\omega)\right]^2$:

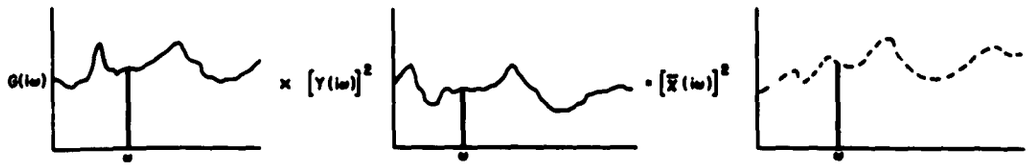

Fig. 5 - Summary for numerical calculation of response

In terms of the frequency-by-frequency multiplication of load function by frequency response function to get the response function (Fig. 5), the response is reduced by:

1. A general decrease in load function level.

2. A general decrease in frequency-response-function magnitudes.

3. A shift of location of load or frequency-response-function peaks so that peaks in one curve do not coincide with peaks in the other curve.

Now a general increase of damping can accomplish item 2, so that a general decrease of response is obtained. Discrete increases of damping can reduce the response in particular frequency ranges by reducing particular peaks of the transfer function. Shifting the location of peaks in the frequency response function is best done by changes in stiffnesses or mass loadings.

Consequently, the effect of damping on response to random vibration and shock is to determine the height of peaks in the frequency response function and its general level. In general, an increase of damping reduces response and a decrease of damping increases response, though there may well be specific cases for which this generalization does not apply. Reference 1, Chapter 5, summarizes

the state of formal knowledge concerning structural damping.

For any specific problem, the effect of experimental changes in damping on a model or prototype transfer function can be measured, and the analytical effects of changes in damping can be determined from Eq. (17). The qualitative effects are as just stated.

SUMMARY

One might well ask what all of the foregoing means in terms of the state of the art in random vibration and shock. What has been discussed here, together with the references in the bibliography, leads us to state that:

1. We can with certainty:

a. Measure loads and describe them statistically.

b. Measure (on prototypes or models) the appropriate transfer functions.

c. Measure (or predict) the probable responses to the loads in terms of known damage producing factors.

2. We can, but with uncertainty:

a. Estimate loads and devise statistical descriptions of them when measurements are not feasible.

b. Devise mathematical models to calculate transfer functions that are needed.

c. Hypothesize damage criteria and apply them to the measured or calculated responses.

d. Judge the validity of the process and data we have used, and form an opinion of the resulting probability of damage.

3. We need more information on:

a. Damage criteria and damage accumulation.

b. The validity of various procedures for devising mathematical models to represent physical problems.

c. Other damage processes than stress fatigue, which <u>may</u> be susceptible to similar treatment.

APPENDIX

Worked Examples

Two examples have been worked, one to show the mathematics, and one to show a numerical calculation.

EXAMPLE 1

Consider the single-degree-of-freedom system shown in Fig. A-1. The equation of motion is:

$$m\ddot{x} + c\dot{x} + kx = c\dot{x}_o + kx_o. \qquad \text{(A-1)}$$

Let

$$\left.\begin{aligned} x &= a\cos\omega t + b\sin\omega t \\ x_o &= A\cos\omega t + B\sin\omega t \end{aligned}\right\}. \qquad \text{(A-2)}$$

Substitute (A-2) in (A-1), and get

$$(-\omega^2 ma + ka + \omega cb)\cos\omega t + (-\omega^2 mb + kb - \omega ca)\sin\omega t =$$
$$+ (\omega cB + kA)\cos\omega t + (-\omega cA + kB)\sin\omega t. \qquad \text{(A-3)}$$

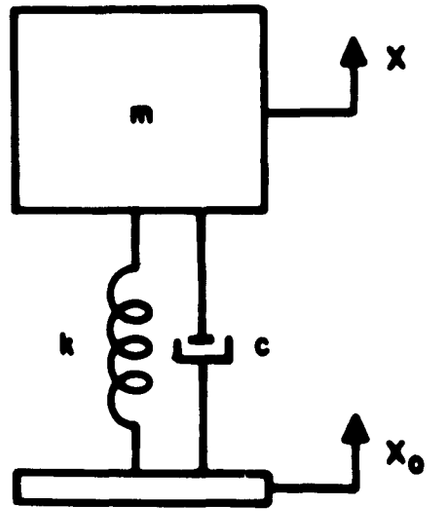

Fig. A-1 - Single-degree-of-freedom system

(A-3) can be written:

$$\begin{vmatrix} -\omega^2 m + k & +\omega c \\ -\omega c & -\omega^2 m + k \end{vmatrix} \begin{vmatrix} a \\ b \end{vmatrix} = \begin{vmatrix} \omega c B + kA \\ -\omega c A + kB \end{vmatrix}, \quad \text{(A-4)}$$

whence

$$a = \frac{(-\omega^2 m + k)k + (\omega c)^2}{(-\omega^2 m + k)^2 + (\omega c)^2} A + \frac{(-\omega^2 m + k)\omega c - \omega c k}{(-\omega^2 m + k)^2 + (\omega c)^2} B, \quad \text{(A-5)}$$

$$b = \frac{(-\omega^2 m + k)(-\omega c) + \omega c k}{(-\omega^2 m + k)^2 + (\omega c)^2} A + \frac{(-\omega^2 m + k)k + (\omega c)^2}{(-\omega^2 m + k)^2 + (\omega c)^2} B. \quad \text{(A-6)}$$

An examination of Eqs. (A-5) and (A-6) shows that the direct frequency response function is

$$Y_D = \frac{(-\omega^2 m + k)k + (\omega c)^2}{(-\omega^2 m + k)^2 + (\omega c)^2}, \quad \text{(A-7)}$$

and the cross-frequency response function is

$$Y_C = \frac{(-\omega^2 m + k)\omega c - \omega c k}{(-\omega^2 m + k)^2 + (\omega c)^2}. \quad \text{(A-8)}$$

If we had made the substitution

$$x = a e^{i\omega t}, \qquad x_o = A e^{i\omega t}$$

at Eq. (A-2), the same frequency response functions would result, except that Y_C would be imaginary. In fact,

$$Y_{RE} = Y_D \quad \text{and} \quad Y_{IM} = Y_C. \quad \text{(A-9)}$$

Now with

$$F(i\omega) = \int_{-\infty}^{\infty} f(t) e^{-i\omega t} dt, \quad \text{(A-10)}$$

we get

$$\left.\begin{aligned} F_{RE} &= \int_{-\infty}^{\infty} f(t) \cos \omega t \, dt \\ F_{IM} &= \int_{-\infty}^{\infty} f(t)(-\sin \omega t) \, dt \end{aligned}\right\}, \quad \text{(A-11)}$$

whence

$$\left.\begin{aligned} x_{RE} &= F_{RE} Y_{RE} - F_{IM} Y_{IM} \\ x_{IM} &= F_{RE} Y_{IM} + F_{IM} Y_{RE} \end{aligned}\right\}, \quad \text{(A-12)}$$

and

$$X(t) = \frac{1}{2\pi} \int_{-\infty}^{\infty} (x_{RE} \cos \omega t - x_{IM} \sin \omega t) \, d\omega + \frac{i}{2\pi} \int_{-\infty}^{\infty} (x_{RE} \sin \omega t + x_{IM} \cos \omega t) d\omega. \quad \text{(A-13)}$$

If we note that F_{RE} is an even function while F_{IM} is odd, that Y_{RE} is even while Y_{IM} is odd, it follows that x_{RE} is even and x_{IM} is odd. As a consequence, the imaginary part of (A-13) vanishes and we have

$$X(t) = \frac{1}{\pi} \int_0^{\infty} \left[(F_{RE} Y_{RE} - F_{IM} Y_{IM}) \cos \omega t + (F_{RE} Y_{IM} + F_{IM} Y_{RE}) \sin \omega t \right] d\omega \quad \text{(A-14)}$$

which is the general equation for the time function of response of a system to any excitation which has a proper Fourier integral transform.

EXAMPLE 2

Consider the four-degree-of-freedom system shown in Fig. A-2. We are concerned with the stretch of the spring, k_{23}, which connects masses 2 and 3, under a step shock input and under a random vibration. The shock load is a 100 in./sec velocity step applied to the foundation, and the random vibration is described in Figs. A-3 and A-4.

The structure is characterized by the mass matrix,

$$M = \begin{vmatrix} 7.13 & 0 & 0 & 0 \\ 0 & 4.38 & 0 & 0 \\ 0 & 0 & 1.13 & 0 \\ 0 & 0 & 0 & 1.89 \end{vmatrix}, \quad \text{(A-15)}$$

the stiffness matrix

$$K = \begin{vmatrix} +40.0 & +6.62 & -2.85 & +5.54 \\ +6.62 & +7.59 & -0.445 & +1.107 \\ -2.85 & -0.445 & +1.057 & -0.395 \\ +5.54 & +1.107 & -0.395 & +9.00 \end{vmatrix} \times 10^5, \quad \text{(A-16)}$$

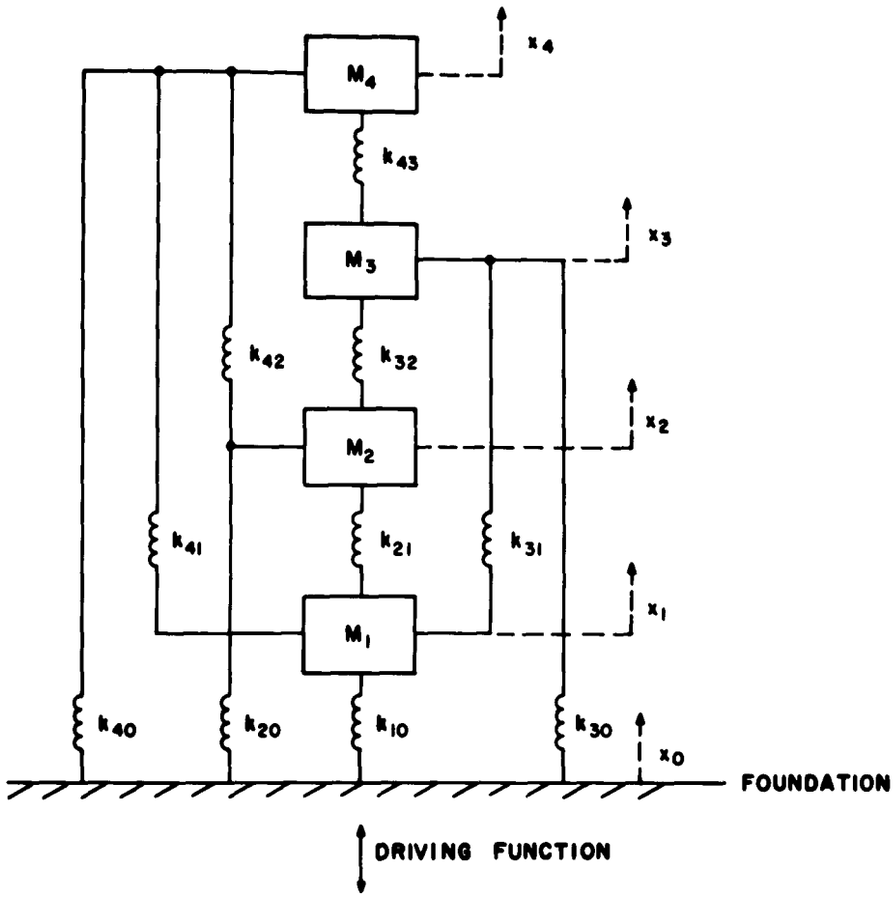

NOTES: EACH SPRING IS PARALLELED BY A VISCOUS DAMPER
MOTIONS ARE CONSTRAINED TO X – DIRECTION ONLY

Fig. A-2 - Four-degree-of-freedom system

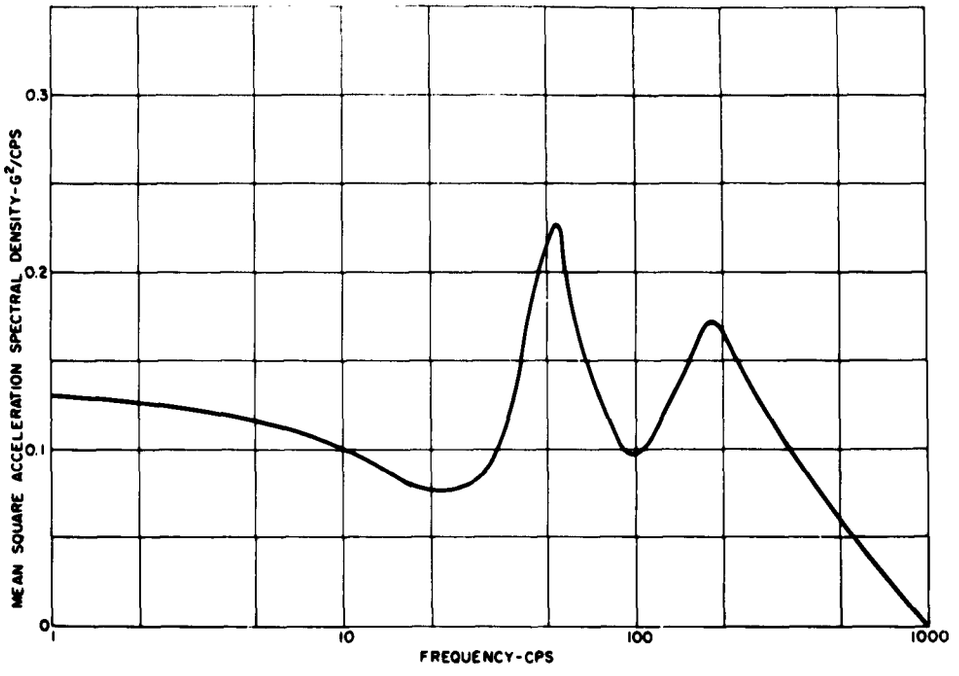

Fig. A-3 - Random vibration spectral density

and the damping matrix

$$C = \begin{vmatrix} +267 & +78 & -50 & +64 \\ +78 & +90 & -12 & +16.6 \\ -50 & -12 & +17.5 & -9.2 \\ +64 & +16.6 & -9.2 & +65.4 \end{vmatrix} . \quad \text{(A-17)}$$

The equations of motion are then

$$M\ddot{x} + C\dot{x} + Kx = f(t) , \quad \text{(A-18)}$$

and we substitute

$$x = a \cos \omega t + b \sin \omega t \quad \text{(A-19)}$$

to get

$$\begin{vmatrix} -\omega^2 M + K & +\omega C \\ -\omega C & -\omega^2 M + K \end{vmatrix} \begin{vmatrix} a \\ b \end{vmatrix} = \begin{vmatrix} f_1 \\ f_2 \end{vmatrix} . \quad \text{(A-20)}$$

Now to get the solution for driving from the foundation, the elements of the f_1 vector must be the sums of the rows of the K matrix and the f_2 vector the sums of the rows of the C matrix times $(-\omega)$:

$$\left.\begin{aligned} f_1 &= \begin{vmatrix} +49.31 \\ +14.872 \\ -2.633 \\ +15.252 \end{vmatrix} \times 10^5 \\ \text{and} \qquad & \\ f_2 &= \begin{vmatrix} +359 \\ +172.6 \\ -53.7 \\ +136.8 \end{vmatrix} (-\omega). \end{aligned}\right\} \quad \text{(A-21)}$$

This produces unit response at zero frequency. Equation (A-21) is put into (A-20), and the equations are solved simultaneously for the a (real) and b (imaginary) vectors for a range of values of ω. The results are shown in Table 1 and Fig. A-5.

To compute the random vibration response frequency spectrum, we use

$$d(i\omega) \times \left[Y(i\omega)\right]^2 = \left[\bar{X}(i\omega)\right]^2 , \quad \text{(A-22)}$$

which is shown in Table 2 and Fig. A-6. Since the principal response is in the frequency

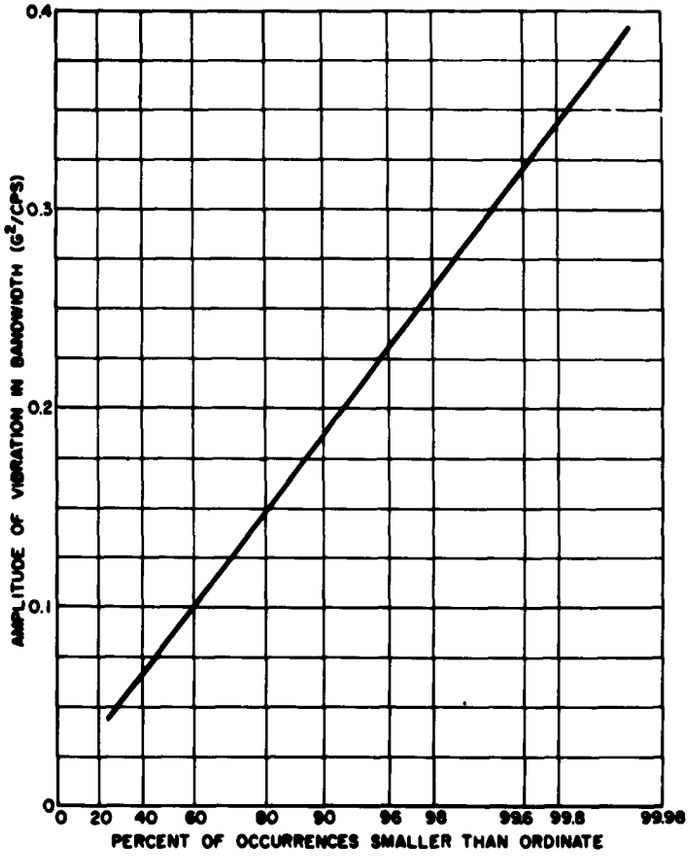

Fig. A-4 - Random vibration probability plot

TABLE A-1
Frequency Response Functions
(Sketch in spring k_{23} per unit foundation motion)

Freq. (cps)	Y_{RE}	Y_{IM}	$[Y(i\omega)]^2$	Freq. (cps)	Y_{RE}	Y_{IM}	$[Y(i\omega)]^2$
0	0	0	0	97.1	+1.999	- 2.150	8.619
$1/2\pi$	$- 1.43 \times 10^{-5}$	$+ 1.326 \times 10^{-9}$	2×10^{-10}	100	+0.911	- 0.6955	1.314
10	- 0.06001	$+ 3.783 \times 10^{-4}$	0.00360	110	+2.124	- 0.2039	4.553
20	- 0.3008	$+ 5.093 \times 10^{-3}$	0.09048	120	+3.512	- 0.6815	12.80
30	- 1.1105	+ 0.04930	1.236	130	+6.302	- 4.924	63.96
40	- 8.298	+ 2.100	73.27	134.8	+1.489	-10.804	118.9
42.9	+ 0.9642	+40.09	1608.1	140	-4.405	- 5.831	53.4
45	+14.246	+ 4.955	227.5	150	-2.860	- 1.494	10.41
50	+ 6.587	+ 0.4930	43.63				
55	+ 6.504	- 0.4172	42.48	180			7.69
59.7	+ 3.206	-13.22	185.0	250			5.00
65	- 0.440	- 0.5472	0.4930	400			2.05
75	+ 1.119	- 0.00580	1.252	700			0.58
85	+ 1.612	+ 0.01065	2.599	1000			0
95	+ 2.753	- 0.7177	8.094				

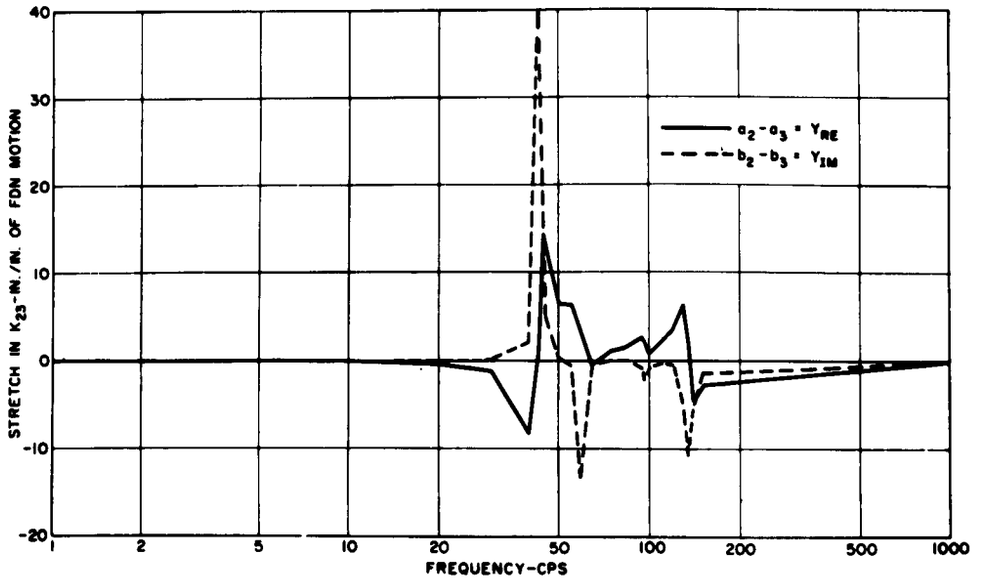

Fig. A-5 - Frequency response function

TABLE A-2

Random Vibration Response

Freq. (cps)	$g(i\omega)$ g^2/cps	$d(i\omega)$ in.^{2}/cps x 10^{-6}	$Y(i\omega)^2$	$\bar{X}(i\omega)^2$ in.^{2}/cps x 10^{-6}	Δf (cps)	$\bar{X}(i\omega)\Delta f$ in.^{2} x 10^{-6}	rms in. x 10^{-3}
0	0.010	0	0	0	0.785	0	0
$1/2\pi$	0.013	0.800	2×10^{-10}	0	5	0	0
10	0.100	0.960	0.00360	3	9.22	28	5.3
20	0.076	45.7	0.09048	4	10	40	6.3
30	0.088	10.4	1.236	13	10	130	11.4
40	0.142	5.32	73.27	389	6.45	2510	50.1
42.9	0.170	4.80	1608.1	7720	2.50	19300	139.
45	0.187	4.38	227.5	998	3.55	3540	59.5
50	0.214	3.29	43.63	144	5	720	26.6
55	0.227	2.37	42.48	101	4.85	490	22.1
59.7	0.188	1.41	185.0	261	5	1305	36.1
65	0.163	0.875	0.4930	0	7.65	3	1.7
75	0.132	0.400	1.252	1	10	10	3.1
85	0.108	0.200	2.599	1	10	10	3.1
95	0.098	0.116	8.094	1	6.05	6	2.5
97.1	0.097	0.105	8.619	1	2.50	3	1.7
100	0.097	0.093	1.314	0	6.45	1	1.0
110	0.102	0.067	4.553	0	10	3	1.7
120	0.112	0.052	12.80	1	10	10	3.1
130	0.124	0.041	63.96	3	7.40	22	4.7
134.8	0.130	0.038	118.9	4	5	20	4.5
140	0.136	0.034	53.4	2	7.60	15	3.9
150	0.145	0.028	10.41	0	20	6	2.4
180	0.172	0.016	7.69	0	50	6	2.4
250	0.135	0.0033	5.00	0	110	2	1.4
400	0.083	0.0003	2.05	0	225	0	0
700	0.030	--	0.58	0	300	0	0
1000	0	--	0	0	150	0	0
						Σ 28180	Σ 168.0

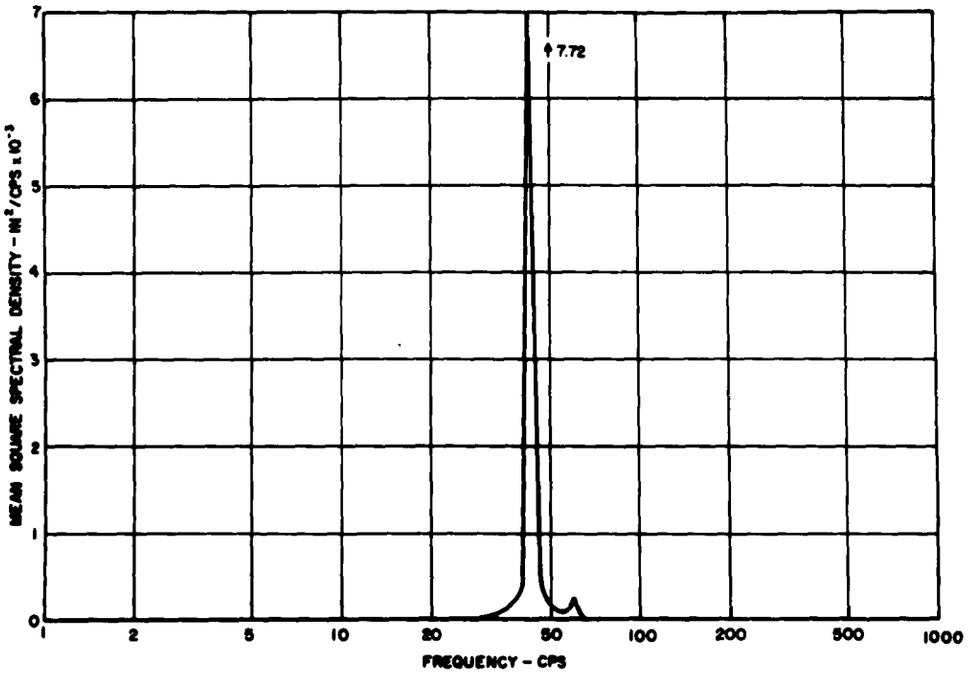

Fig. A-6 - Random vibration response

range around 42.9 cps, a fatigue damage evaluation could be done by assuming that the sum of the responses (0.0281 in.^{2} mean-square response, 0.168 in root-mean-square response) would be predominantly 42.9 cps. The damage evaluation would then follow the process of Ref. 1, p. 389.

To compute the step velocity shock response, we first transform a unit step velocity into F_{RE} and F_{IM}; thus

$$F(i\omega) = \int_{-\infty}^{\infty} 1(t)\, e^{-i\omega t}\, dt\,, \qquad \text{(A-23)}$$

whence

$$\left.\begin{aligned} F_{RE} &= 0 \\ F_{IM} &= -\frac{1}{\omega} \end{aligned}\right\}. \qquad \text{(A-24)}$$

We then get

$$\left.\begin{aligned} X_{RE} &= -F_{IM} Y_{IM} \\ X_{IM} &= F_{IM} Y_{RE} \end{aligned}\right\}, \qquad \text{(A-25)}$$

as in Table 3, and then perform the inverse transform to get $x(t)$,

$$x(t) = \frac{1}{\pi} \sum_{\omega=0}^{\infty} \left[-F_{IM} Y_{IM} \cos \omega t + F_{IM} Y_{RE} \sin \omega t \right] \Delta\omega\,. \qquad \text{(A-26)}$$

The resulting time function, shown in Fig. A-7, can be used in a fatigue-damage evaluation again as before.

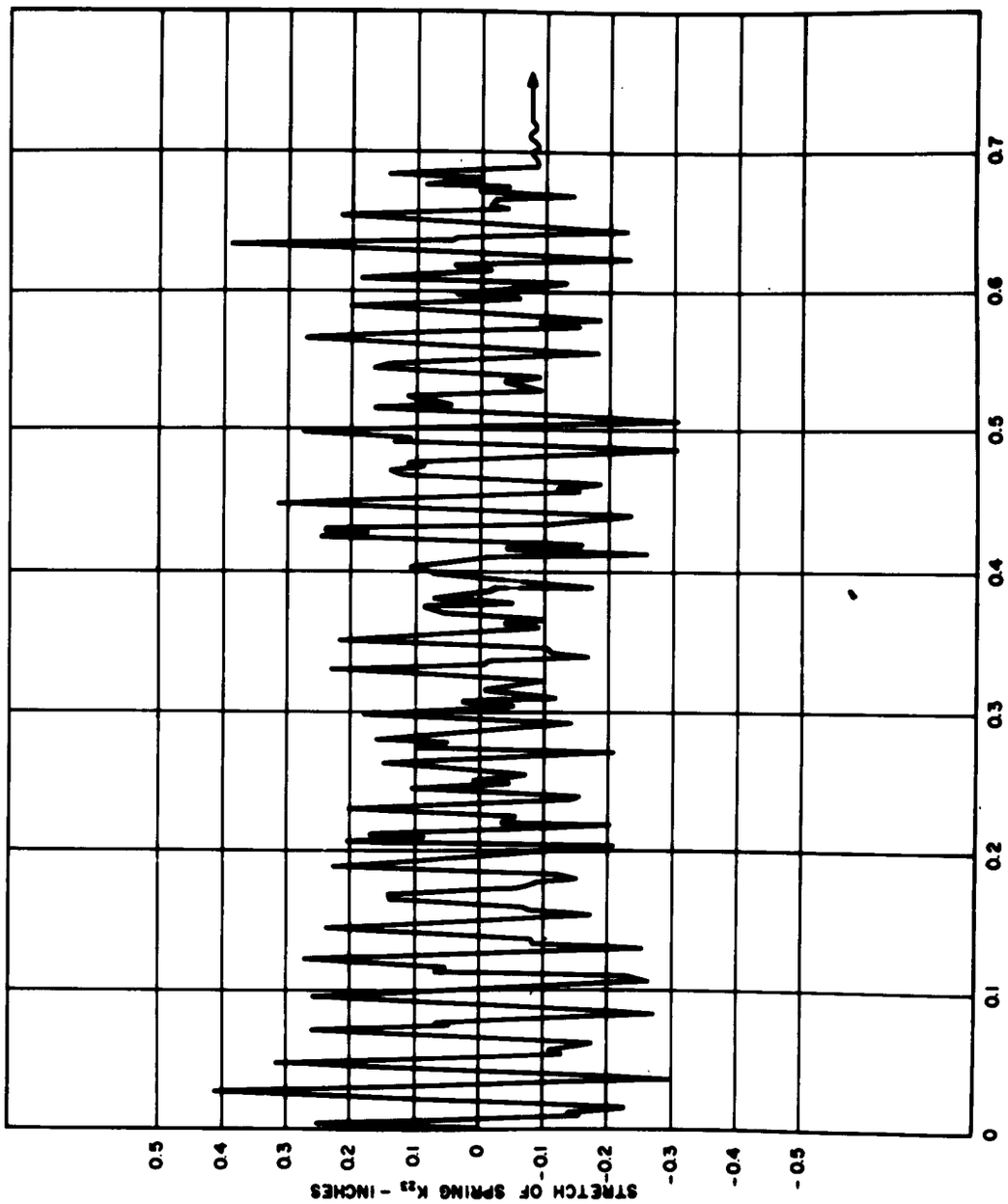

Fig. A-7 - Step shock response

TABLE A-3
Step Shock Response

Freq. (cps)	F_{IM}	Y_{RE}	Y_{IM}	X_{RE}	X_{IM}
0	$-\infty$	0	0	0	0
$1/2\pi$	-1	-1.43×10^{-5}	$+1.33 \times 10^{-9}$	$+1.33 \times 10^{-9}$	$+1.43 \times 10^{-5}$
10	-0.01592	- 0.06001	$+3.783 \times 10^{-4}$	$+6.03 \times 10^{-6}$	$+0.955 \times 10^{-3}$
20	-0.00795	- 0.3008	$+5.093 \times 10^{-3}$	$+4.70 \times 10^{-5}$	$+2.39 \times 10^{-3}$
30	-0.00531	- 1.1105	+ 0.0493	$+2.62 \times 10^{-4}$	$+5.90 \times 10^{-3}$
40	-0.00398	- 8.298	+ 2.100	+0.00837	+0.0330
42.9	-0.00371	+ 0.9642	+40.09	+0.1486	-0.00358
45	-0.00354	+14.246	+ 4.955	+0.1757	-0.0504
50	-0.00318	+ 6.587	+ 0.4930	+0.00157	-0.0209
55	-0.00289	+ 6.504	- 0.4172	-0.00121	-0.0188
59.7	-0.00267	+ 3.206	-13.22	-0.0353	-0.00856
65	-0.00245	- 0.440	- 0.5472	-0.00134	+0.001078
75	-0.00213	+ 1.119	- 0.0058	-1.24×10^{-5}	-0.002385
85	-0.00187	+ 1.612	+ 0.01065	$+1.99 \times 10^{-5}$	-0.003015
95	-0.00168	+ 2.753	+ 0.7177	-1.205×10^{-3}	-0.00463
97.1	-0.00164	+ 1.999	+ 2.150	-3.53×10^{-3}	-0.00398
100	-0.00159	+ 0.911	+ 0.6955	-1.11×10^{-3}	-0.001448
110	-0.00145	+ 2.124	- 0.2039	-2.96×10^{-4}	-0.003224
120	-0.00133	+ 3.512	- 0.6815	-0.907×10^{-3}	-0.00467
130	-0.00122	+ 6.302	- 4.924	-6.00×10^{-3}	-0.00769
134.8	-0.00118	+ 1.489	-10.80	-1.275×10^{-2}	-0.001756
140	-0.00114	- 4.405	- 5.831	-6.65×10^{-3}	+0.00502
150	-0.00106	- 2.860	- 1.494	-1.58×10^{-3}	+0.00303
180	-0.00089	- 2.50	- 1.20	-1.07×10^{-3}	+0.002225
250	-0.00064	- 2.00	- 1.00	-0.64×10^{-3}	+0.00128
400	-0.00040	- 1.30	- 0.60	-0.24×10^{-3}	+0.00052
700	-0.00023	- 0.40	- 0.30	-0.69×10^{-4}	$+0.92 \times 10^{-4}$
1000	-0.00016	0	0	0	0

REFERENCES

[1] Random Vibration, edited by S. H. Crandall, Wiley and Sons.

[2] Mathematical Methods in Engineering, Karman and Biot, McGraw-Hill.

[3] R. M. Mains, "A Generalization of Cumulative Damage," ASME Jour. of Basic Eng., v. 82 Ser. D, June 1960.

[4] R. R. Gatts, "Application of a Cumulative Damage Concept to Fatigue," ASME Paper No. 60-WA-144.

[5] M. A. Miner, "Cumulative Damage in Fatigue," Jour. App. Mech., v. 21, Trans. ASME v. 67, 1947.

Note: For a more complete bibliography on random vibration, see the references at the end of each chapter of Ref. 1. For references on shock, see other Shock, Vibration, and Associated Environments Bulletins.

* * *